Chapter 8

SINGLE-VARIABLE PROBLEMS IN TWO DIMENSIONS

8.1 INTRODUCTION

Finite element analysis of two-dimensional problems involves the same basic steps as those described for one-dimensional problems in Chapters 3–6. The analysis is somewhat complicated by the fact that two-dimensional problems are described by partial differential equations over geometrically complex regions. The boundary Γ of a two-dimensional domain Ω is, in general, a curve. Therefore, finite elements are simple two-dimensional geometric shapes that allow approximations of a given two-dimensional domain as well as the solution over it. Thus, in two-dimensional problems we not only seek an approximate solution to a given problem on a domain, but we also approximate the domain by a suitable finite element mesh. Consequently, we will have approximation errors due to the approximation of the solution as well as discretization errors due to the approximation of the domain in the finite element analysis of two-dimensional problems. The finite element mesh (discretization) consists of simple two-dimensional elements, such as triangles, rectangles, and/or quadrilaterals, that allow unique derivation of the interpolation functions. The elements are connected to each other at nodal points on the boundaries of the elements. The ability to represent domains with irregular geometries by a collection of finite elements makes the method a valuable practical tool for the solution of boundary, initial, and eigenvalue problems arising in various fields of engineering.

The objective of this chapter is to extend the basic steps discussed earlier for one-dimensional problems to two-dimensional boundary value problems involving a single dependent variable. Once again, we describe the basic steps of the finite element analysis with a model second-order partial differential equation governing a single variable. This equation arises in a number of fields including electrostatics, heat transfer, fluid mechanics, and solid mechanics (see Table 8.1.1).

Table 8.1.1 Some examples of the Poisson equation

$$-\nabla \cdot (k\nabla u) = f \text{ in } \Omega$$

Natural boundary condition: $k\dfrac{\partial u}{\partial n} + \beta(u - u_\infty) = q$ on Γ_q

Essential boundary condition: $u = \hat{u}$ on Γ_u

Field of application	Primary variable u	Material constant k	Source variable f	Secondary variables q, $\frac{\partial u}{\partial x}$, $\frac{\partial u}{\partial y}$
Heat transfer	Temperature T	Conductivity k	Heat source g	Heat flow due to conduction $k\frac{\partial T}{\partial n}$ convection $h(T - T_\infty)$
Irrotational flow of an ideal fluid	Stream function ψ	Density ρ	Mass production σ	Velocities $\frac{\partial \psi}{\partial x} = -v$ $\frac{\partial \psi}{\partial y} = u$
	Velocity potential ϕ	Density ρ	Mass production σ	$\frac{\partial \phi}{\partial x} = u$ $\frac{\partial \phi}{\partial y} = v$
Groundwater flow	Piezometric head ϕ	Permeability K	Recharge f (pumping, $-f$)	Seepage $q = k\frac{\partial \phi}{\partial n}$ Velocities $u = -k\frac{\partial \phi}{\partial x}$ $v = -k\frac{\partial \phi}{\partial y}$
Torsion of cylindrical members	Stress function Ψ	$k = 1$ G = shear modulus	$f = 2$ θ = angle of twist per unit length	$G\theta\frac{\partial \Psi}{\partial x} = -\sigma_{yz}$ $G\theta\frac{\partial \Psi}{\partial y} = \sigma_{xz}$
Electrostatics	Scalar potential ϕ	Dielectric constant ϵ	Charge density ρ	Displacement flux density D_n
Magnetostatics	Magnetic potential ϕ	Permeability μ	Charge density ρ	Magnetic flux density B_n
Membranes	Transverse deflection u	Tension in membrane T	Transversely distributed load	Normal force q

8.2 BOUNDARY VALUE PROBLEMS

8.2.1 The Model Equation

Consider the problem of finding the solution $u(x, y)$ of the second-order partial differential equation

$$-\frac{\partial}{\partial x}\left(a_{11}\frac{\partial u}{\partial x} + a_{12}\frac{\partial u}{\partial y}\right) - \frac{\partial}{\partial y}\left(a_{21}\frac{\partial u}{\partial x} + a_{22}\frac{\partial u}{\partial y}\right) + a_{00}u - f = 0 \qquad (8.2.1)$$

for given data a_{ij} $(i, j = 1, 2)$, a_{00} and f, and specified boundary conditions. The form of the boundary conditions will be apparent from the weak formulation. As a special case, we

can obtain the Poisson equation from (8.2.1) by setting $a_{11} = a_{22} = k(x, y)$ and $a_{12} = a_{21} = a_{00} = 0$:

$$-\nabla \cdot (k\nabla u) = f(x, y) \quad \text{in } \Omega \tag{8.2.2}$$

where ∇ is the gradient operator. If $\hat{\mathbf{i}}$ and $\hat{\mathbf{j}}$ denote the unit vectors directed along the x and y axes, respectively, the gradient operator can be expressed as (see Sec. 2.2.3)

$$\nabla = \hat{\mathbf{i}}\frac{\partial}{\partial x} + \hat{\mathbf{j}}\frac{\partial}{\partial y}$$

and (8.2.2) in the Cartesian coordinate system takes the form

$$-\frac{\partial}{\partial x}\left(k\frac{\partial u}{\partial x}\right) - \frac{\partial}{\partial y}\left(k\frac{\partial u}{\partial y}\right) = f(x, y) \tag{8.2.3}$$

In the following, we shall develop the finite element model of (8.2.1). The major steps are as follows:

1. Discretization of the domain into a set of finite elements.
2. Weak (or weighted-integral) formulation of the governing differential equation.
3. Derivation of finite element interpolation functions.
4. Development of the finite element model using the weak form.
5. Assembly of finite elements to obtain the global system of algebraic equations.
6. Imposition of boundary conditions.
7. Solution of equations.
8. Postcomputation of solution and quantities of interest.

Steps 6 and 7 remain unchanged from one-dimensional finite element analysis because at the end of Step 5 we have a set of algebraic equations whose form is independent of the dimension of the domain or nature of the problem. In the following sections, we discuss each step in detail.

8.2.2 Finite Element Discretization

In two dimensions there is more than one simple geometric shape that can be used as a finite element (see Fig. 8.2.1). As we shall see shortly, the interpolation functions depend not only on the number of nodes in the element and the number of unknowns per node, but also on the shape of the element. The shape of the element must be such that its geometry is uniquely defined by a set of points, which serve as the element nodes in the development of the interpolation functions. As will be discussed later in this section, a triangle is the simplest geometric shape, followed by a rectangle.

The representation of a given region by a set of elements (i.e., discretization or *mesh generation*) is an important step in finite element analysis. The choice of element type, number of elements, and density of elements depends on the geometry of the domain, the problem to be analyzed, and the degree of accuracy desired. Of course, there are no specific formulae to obtain this information. In general, the analyst is guided by his or her technical background, insight into the physics of the problem being modeled

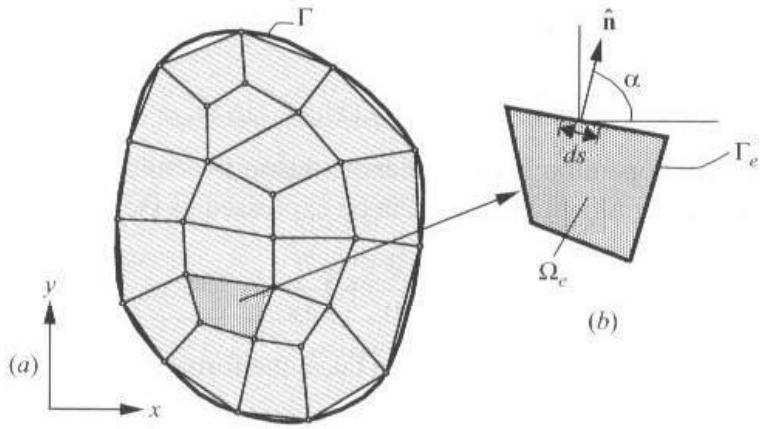

Figure 8.2.1 Finite element discretization of an irregular domain: (*a*) discretization of a domain by quadrilateral elements; and (*b*) a typical quadrilateral element Ω_e (with the unit normal $\hat{\mathbf{n}}$ on the boundary Γ_e of the element).

(e.g., a qualitative understanding of the solution), and experience with finite element modeling. The general rules of mesh generation for finite element formulations include:

1. The elements that are selected should characterize the governing equations of the problem.
2. The number, shape, and type (i.e., linear or quadratic) of elements should be such that the geometry of the domain is represented as accurately as desired.
3. The density of elements should be such that regions of large gradients of the solution are adequately modeled (i.e., use more elements or higher-order elements in regions of large gradients).
4. Mesh refinements should vary gradually from high-density regions to low-density regions. If *transition elements* are used, they should be used away from critical regions (i.e., regions of large gradients). Transition elements are those that connect lower-order elements to higher-order elements (e.g., linear to quadratic).

8.2.3 Weak Form

In the development of the weak form we need only consider a typical element. We assume that Ω_e is a typical element, whether triangular or quadrilateral, of the finite element mesh, and we develop the finite element model of (8.2.1) over Ω_e. Various two-dimensional elements will be discussed in the sequel.

Following the three-step procedure presented in Chapters 2 and 3, we develop the weak form of (8.2.1) over the typical element Ω_e. The first step is to multiply (8.2.1) with a weight function w, which is assumed to be differentiable once with respect to x and y, and then integrate the equation over the element domain Ω_e :

$$0 = \int_{\Omega_e} w\left[-\frac{\partial}{\partial x}(F_1) - \frac{\partial}{\partial y}(F_2) + a_{00}u - f\right]dx\,dy \tag{8.2.4a}$$

where

$$F_1 = a_{11}\frac{\partial u}{\partial x} + a_{12}\frac{\partial u}{\partial y}, \quad F_2 = a_{21}\frac{\partial u}{\partial x} + a_{22}\frac{\partial u}{\partial y} \tag{8.2.4b}$$

In the second step we distribute the differentiation among u and w equally. To achieve this, we integrate the first two terms in (8.2.4a) by parts. First, we note the identities

$$\frac{\partial}{\partial x}(wF_1) = \frac{\partial w}{\partial x}F_1 + w\frac{\partial F_1}{\partial x} \quad \text{or} \quad -w\frac{\partial F_1}{\partial x} = \frac{\partial w}{\partial x}F_1 - \frac{\partial}{\partial x}(wF_1) \tag{8.2.5a}$$

$$\frac{\partial}{\partial y}(wF_2) = \frac{\partial w}{\partial y}F_2 + w\frac{\partial F_2}{\partial y} \quad \text{or} \quad -w\frac{\partial F_2}{\partial y} = \frac{\partial w}{\partial y}F_2 - \frac{\partial}{\partial y}(wF_2) \tag{8.2.5b}$$

Next, we use the component form of the gradient (or divergence) theorem

$$\int_{\Omega_e} \frac{\partial}{\partial x}(wF_1)\,dx\,dy = \oint_{\Gamma_e} wF_1 n_x\,ds \tag{8.2.6a}$$

$$\int_{\Omega_e} \frac{\partial}{\partial y}(wF_2)\,dx\,dy = \oint_{\Gamma_e} wF_2 n_y\,ds \tag{8.2.6b}$$

where n_x and n_y are the components (i.e., the direction cosines) of the unit normal vector

$$\hat{\mathbf{n}} = n_x\hat{\mathbf{i}} + n_y\hat{\mathbf{j}} = \cos\,\alpha\hat{\mathbf{i}} + \sin\,\alpha\hat{\mathbf{j}} \tag{8.2.7}$$

on the boundary Γ_e, and ds is the length of an infinitesimal line element along the boundary (see Fig. 8.2.1b). Using (8.2.5a), (8.2.5b), (8.2.6a), and (8.2.6b) in (8.2.4a), we obtain

$$\begin{aligned} 0 = &\int_{\Omega_e}\left[\frac{\partial w}{\partial x}\left(a_{11}\frac{\partial u}{\partial x} + a_{12}\frac{\partial u}{\partial y}\right) + \frac{\partial w}{\partial y}\left(a_{21}\frac{\partial u}{\partial x} + a_{22}\frac{\partial u}{\partial y}\right) + a_{00}wu - wf\right]dx\,dy \\ &- \oint_{\Gamma_e} w\left[n_x\left(a_{11}\frac{\partial u}{\partial x} + a_{12}\frac{\partial u}{\partial y}\right) + n_y\left(a_{21}\frac{\partial u}{\partial x} + a_{22}\frac{\partial u}{\partial y}\right)\right]ds \end{aligned} \tag{8.2.8}$$

From an inspection of the boundary integral in (8.2.8), we note that the specification of u constitutes the essential boundary condition, and hence u is the primary variable. The specification of the coefficient of the weight function in the boundary expression

$$q_n \equiv n_x\left(a_{11}\frac{\partial u}{\partial x} + a_{12}\frac{\partial u}{\partial y}\right) + n_y\left(a_{21}\frac{\partial u}{\partial x} + a_{22}\frac{\partial u}{\partial y}\right) \tag{8.2.9}$$

constitutes the natural boundary condition; thus, q_n is the secondary variable of the formulation. The function $q_n = q_n(s)$ denotes the projection of the vector $\mathbf{a}\cdot\nabla u$ along the unit normal $\hat{\mathbf{n}}$. By definition, q_n is taken positive outward from the surface as we move counterclockwise along the boundary Γ_e. In most problems, the secondary variable q_n is of physical interest. For example, in the case of heat transfer through an anisotropic medium, a_{ij} are the conductivities of the medium, and q_n is the negative of the heat flux (because of the Fourier heat conduction law) normal to the boundary of the element.

The third and last step of the formulation is to use the definition (8.2.9) in (8.2.8) and write the weak form of (8.2.1) as

$$\begin{aligned} 0 = &\int_{\Omega_e}\left[\frac{\partial w}{\partial x}\left(a_{11}\frac{\partial u}{\partial x} + a_{12}\frac{\partial u}{\partial y}\right) + \frac{\partial w}{\partial y}\left(a_{21}\frac{\partial u}{\partial x} + a_{22}\frac{\partial u}{\partial y}\right) + a_{00}wu - wf\right]dx\,dy \\ &- \oint_{\Gamma_e} wq_n\,ds \end{aligned} \tag{8.2.10}$$

or,

$$B^e(w, u) = l^e(w) \tag{8.2.11a}$$

where the bilinear form $B^e(\cdot, \cdot)$ and linear form $l^e(\cdot)$ are

$$B^e(w, u) = \int_{\Omega_e} \left[\frac{\partial w}{\partial x} \left(a_{11} \frac{\partial u}{\partial x} + a_{12} \frac{\partial u}{\partial y} \right) + \frac{\partial w}{\partial y} \left(a_{21} \frac{\partial u}{\partial x} + a_{22} \frac{\partial u}{\partial y} \right) + a_{00} w u \right] dx\, dy$$

$$l^e(w) = \int_{\Omega_e} w f \, dx\, dy + \oint_{\Gamma_e} w q_n \, ds \tag{8.2.11b}$$

The weak form (or *weighted integral statement*) in (8.2.10) or (8.2.11a) and (8.2.11b) is the basis of the finite element model of (8.2.1).

Whenever $B^e(w, u)$ is symmetric in its arguments w and u [i.e., $B^e(w, u) = B^e(u, w)$], the quadratic functional associated with the variational problem (8.2.11a) can be obtained from [see Eq. (2.4.19)]

$$I^e(w) = \frac{1}{2} B^e(w, w) - l^e(w) \tag{8.2.12a}$$

The bilinear form in (8.2.11b) is symmetric if and only if $a_{12} = a_{21}$. Then the functional is given by

$$I^e(w) = \frac{1}{2} \int_{\Omega_e} \left[a_{11} \left(\frac{\partial u}{\partial x} \right)^2 + 2a_{12} \frac{\partial u}{\partial x} \frac{\partial u}{\partial y} + a_{22} \left(\frac{\partial u}{\partial y} \right)^2 + a_{00} u^2 \right] dx\, dy$$
$$+ \int_{\Omega_e} u f \, dx\, dy + \oint_{\Gamma_e} u q_n \, ds \tag{8.2.12b}$$

Vector Form of the Variational Problem

It is common, especially in structural mechanics literature, to express finite element formulations in vector notation (i.e., in terms of matrices). While the vector/matrix notation is concise, it is not as transparent as the explicit form that has been used throughout the book. However, for the sake of completeness, the vector form of the variational (or weak) problem (8.2.11a) and (8.2.11b) is presented here. We shall use bold face letters for matrices of different order, including the 1×1 matrix and row and column matrices.

We begin with Eq. (8.2.11a), which can be written as

$$B^e(\mathbf{w}, \mathbf{u}) = l^e(\mathbf{w}) \tag{8.2.13}$$

where, in the present case, $\mathbf{w}$ is simply w and $\mathbf{u}$ is u. Next, we express $B^e(\cdot, \cdot)$ and $l^e(\cdot)$ in matrix form. Let

$$\mathbf{C} = \begin{bmatrix} a_{11} & a_{12} & 0 \\ a_{21} & a_{22} & 0 \\ 0 & 0 & a_{00} \end{bmatrix}, \quad \mathbf{D} = \begin{Bmatrix} \dfrac{\partial}{\partial x} \\ \dfrac{\partial}{\partial y} \\ 1 \end{Bmatrix} \tag{8.2.14}$$

Then B^e and l^e of (8.2.11b) can be expressed as

$$B^e(w,u) = \int_{\Omega_e} \begin{Bmatrix} \dfrac{\partial w}{\partial x} \\ \dfrac{\partial w}{\partial y} \\ w \end{Bmatrix}^{\mathrm{T}} \begin{bmatrix} a_{11} & a_{12} & 0 \\ a_{21} & a_{22} & 0 \\ 0 & 0 & a_{00} \end{bmatrix} \begin{Bmatrix} \dfrac{\partial u}{\partial x} \\ \dfrac{\partial u}{\partial y} \\ u \end{Bmatrix} dx\,dy$$

$$l^e(w) = \int_{\Omega_e} \{w\}^{\mathrm{T}}\{f\}\,dx\,dy + \oint_{\Gamma_e} \{w\}^{\mathrm{T}}\{q_n\}\,ds \tag{8.2.15a}$$

or, simply

$$B^e(\mathbf{w},\mathbf{u}) = \int_{\Omega_e} (\mathbf{Dw})^{\mathrm{T}}\mathbf{CDu}\,dx\,dy, \quad l^e(\mathbf{w}) = \int_{\Omega_e} \mathbf{w}^{\mathrm{T}}\mathbf{f}\,dx\,dy + \int_{\Gamma_e} \mathbf{w}^{\mathrm{T}}\mathbf{q}\,ds \tag{8.2.15b}$$

8.2.4 Finite Element Model

The weak form in (8.2.10) requires that the approximation chosen for u should be at least linear in both x and y so that there are no terms in (8.2.10) that are identically zero. Since the primary variable is simply the function itself, the Lagrange family of interpolation functions is admissible.

Suppose that u is approximated over a typical finite element Ω_e by the expression

$$u(x,y) \approx u_h^e(x,y) = \sum_{j=1}^{n} u_j^e \psi_j^e(x,y) \quad \text{or} \quad u_h^e(x,y) = (\Psi^e)^{\mathrm{T}}\mathbf{u}^e \tag{8.2.16a}$$

where $\mathbf{u}^e$ and Ψ^e are $n \times 1$ vectors

$$\mathbf{u}^e = \{u_1^e\ u_2^e\ u_3^e\ \ldots\ u_n^e\}^{\mathrm{T}}, \quad \Psi^e = \{\psi_1^e\ \psi_2^e\ \psi_3^e\ \ldots\ \psi_n^e\}^{\mathrm{T}} \tag{8.2.16b}$$

and u_j^e is the value of u_h^e at the jth node (x_j, y_j) of the element and ψ_j^e are the Lagrange interpolation functions, with the property

$$\psi_i^e(x_j, y_j) = \delta_{ij} \quad (i, j = 1, 2, \ldots, n) \tag{8.2.17}$$

In deriving the finite element equations in algebraic terms, we need not know the shape of the element Ω_e or the form of ψ_i^e. The specific form of ψ_i^e will be developed for triangular and rectangular geometries of the element Ω_e in Section 8.2.5, and higher-order interpolation functions will be presented in Chapter 9.

Substituting the finite element approximation (8.2.16a) for u into the weak form (8.2.10) or (8.2.13), we obtain

$$0 = \int_{\Omega_e} \left[\frac{\partial w}{\partial x}\left(a_{11}\sum_{j=1}^{n} u_j^e \frac{\partial \psi_j^e}{\partial x} + a_{12}\sum_{j=1}^{n} u_j^e \frac{\partial \psi_j^e}{\partial y} \right) + \frac{\partial w}{\partial y}\left(a_{21}\sum_{j=1}^{n} u_j^e \frac{\partial \psi_j^e}{\partial x} \right.\right.$$
$$\left.\left. + a_{22}\sum_{j=1}^{n} u_j^e \frac{\partial \psi_j^e}{\partial y} \right) + a_{00} w \sum_{j=1}^{n} u_j^e \psi_j^e - wf \right] dx\,dy - \oint_{\Gamma_e} w q_n\,ds \tag{8.2.18a}$$

or

$$0 = \int_{\Omega_e} (\mathbf{Dw})^{\mathrm{T}}\mathbf{CD}\left(\Psi^{\mathrm{T}}\mathbf{u}^e\right) dx\,dy - \int_{\Omega_e} \mathbf{w}^{\mathrm{T}}\mathbf{f}\,dx\,dy - \oint_{\Gamma_e} \mathbf{w}^{\mathrm{T}}\mathbf{q}\,ds \tag{8.2.18b}$$

This equation must hold for every admissible choice of weight function w. Since we need n independent algebraic equations to solve for the n unknowns, $u_1^e, u_2^e, \ldots, u_n^e$, we choose n linearly independent functions for w: $w = \psi_1^e, \psi_2^e, \ldots, \psi_n^e$ (or, $\mathbf{w} = \{\psi_1^e \ \psi_2^e \ \ldots \ \psi_n^e\} = \Psi^{\mathrm{T}}$). This particular choice of weight function is a natural one when the weight function is viewed as a virtual variation of the dependent unknown (i.e., $w = \delta u \approx \sum_{i=1}^{n} \delta u_i \psi_i$), and the resulting finite element model is known as the *weak-form finite element model* or *Ritz finite element model*. For each choice of w we obtain an algebraic relation among $(u_1^e, u_2^e, \ldots, u_n^e)$. We label the algebraic equation resulting from substitution of ψ_1^e for w into (8.2.18a) as the first algebraic equation, that resulting from $w = \psi_2^e$ as the second equation, and so on. Thus, the ith algebraic equation is obtained by substituting $w = \psi_i^e$ into (8.2.18a):

$$0 = \sum_{j=1}^{n} \left\{ \int_{\Omega_e} \left[\frac{\partial \psi_i^e}{\partial x} \left(a_{11} \frac{\partial \psi_j^e}{\partial x} + a_{12} \frac{\partial \psi_j^e}{\partial y} \right) + \frac{\partial \psi_i^e}{\partial y} \left(a_{21} \frac{\partial \psi_j^e}{\partial x} + a_{22} \frac{\partial \psi_j^e}{\partial y} \right) + a_{00} \psi_i^e \psi_j^e \right] dx\, dy \right\} u_j - \int_{\Omega_e} f \psi_i^e \, dx\, dy - \oint_{\Gamma_e} \psi_i^e q_n \, ds$$

or

$$\sum_{j=1}^{n} K_{ij}^e u_j^e = f_i^e + Q_i^e \quad (i = 1, 2, \ldots, n) \tag{8.2.19a}$$

where

$$K_{ij}^e = \int_{\Omega_e} \left[\frac{\partial \psi_i^e}{\partial x} \left(a_{11} \frac{\partial \psi_j^e}{\partial x} + a_{12} \frac{\partial \psi_j^e}{\partial y} \right) + \frac{\partial \psi_i^e}{\partial y} \left(a_{21} \frac{\partial \psi_j^e}{\partial x} + a_{22} \frac{\partial \psi_j^e}{\partial y} \right) + a_{00} \psi_i^e \psi_j^e \right] dx\, dy \tag{8.2.19b}$$

$$f_i^e = \int_{\Omega_e} f \psi_i^e \, dx\, dy, \quad Q_i^e = \oint_{\Gamma_e} q_n \psi_i^e \, ds$$

In matrix notation, (8.2.19a) takes the form

$$[K^e]\{u^e\} = \{f^e\} + \{Q^e\} \quad \text{or} \quad \mathbf{K}^e \mathbf{u}^e = \mathbf{f}^e + \mathbf{Q}^e \tag{8.2.20a}$$

where [see Eq. (8.2.18b)]

$$\mathbf{K}^e = \int_{\Omega_e} \mathbf{B}^{\mathrm{T}} \mathbf{C} \mathbf{B} \, dx\, dy, \quad \mathbf{f}^e = \int_{\Omega_e} \Psi \mathbf{f} \, ds, \quad \mathbf{Q}^e = \int_{\Gamma_e} \Psi \mathbf{q} \, ds \tag{8.2.20b}$$

$$\mathbf{B} = \mathbf{D}\Psi^{\mathrm{T}} = \begin{bmatrix} \psi_{1,x}^e & \psi_{2,x}^e & \cdots & \psi_{n,x}^e \\ \psi_{1,y}^e & \psi_{2,y}^e & \cdots & \psi_{n,y}^e \\ \psi_1^e & \psi_2^e & \cdots & \psi_n^e \end{bmatrix}$$

Note that $K_{ij}^e = K_{ji}^e$ (i.e., $[K^e]$ is a symmetric matrix of order $n \times n$) only when $a_{12} = a_{21}$. Equations (8.2.20a) and (8.2.20b) represents the finite element model of (8.2.1). This completes the finite element model development. Before we discuss assembly of element equations, it is informative to consider the derivation of the interpolations ψ_i^e for certain basic elements and the evaluation of the element matrices in Eqs. (8.2.19b).

8.2.5 Derivation of Interpolation Functions

The finite element approximation $u_h^e(x, y)$ over an element Ω_e must satisfy the following conditions in order for the approximate solution to converge to the true solution:

1. u_h^e must be continuous as required in the weak form of the problem (i.e., all terms in the weak form are represented as nonzero values).
2. The polynomials used to represent u_h^e must be complete (i.e., all terms, beginning with a constant term up to the highest-order used in the polynomial, should be included in u_h^e).
3. All terms in the polynomial should be linearly independent.

The number of linearly independent terms in the representation of u_h^e dictates the shape and number of degrees of freedom of the element. Next, we discuss some of the basic polynomials and associated elements for the model problem with a single degree of freedom per node.

Triangular Element

An examination of the weak form (8.2.10) and the finite element matrices in (8.2.19*b*) shows that ψ_i^e should be at least linear functions of x and y. The complete linear polynomial in x and y in Ω_e is of the form

$$u_h^e(x, y) = c_1^e + c_2^e x + c_3^e y \tag{8.2.21}$$

where c_i^e are constants. The set $\{1, x, y\}$ is linearly independent and complete. Equation (8.2.21) defines a unique plane for fixed c_i^e. Thus, if $u(x, y)$ is a curved surface, $u_h^e(x, y)$ approximates the surface by a plane. In particular, $u_h^e(x, y)$ is uniquely defined on a triangle by the three values of $u_h^e(x, y)$ at the vertices of the triangle (see Fig. 8.2.2). Let us denote

$$u_h^e(x_1, y_1) = u_1^e, \quad u_h^e(x_2, y_2) = u_2^e, \quad u_h^e(x_3, y_3) = u_3^e \tag{8.2.22}$$

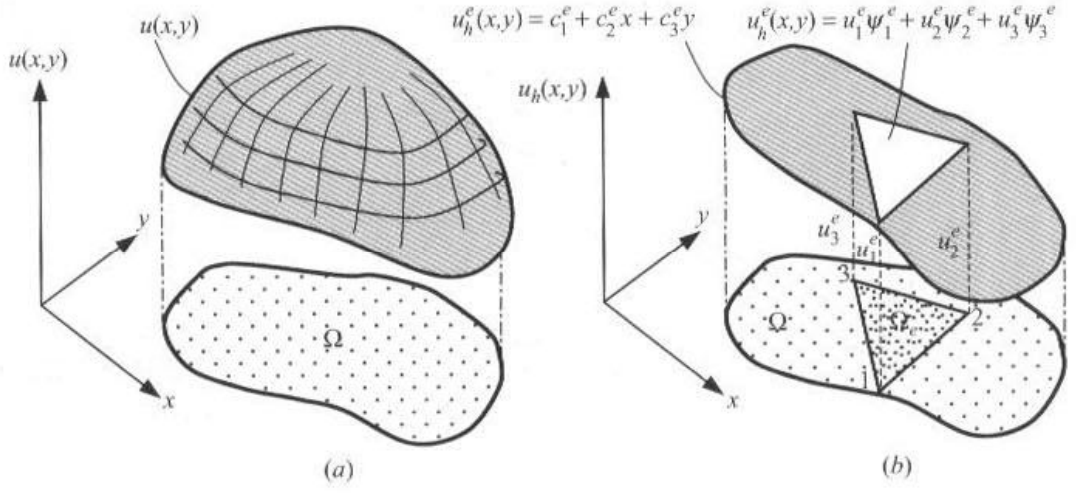

Figure 8.2.2 Approximation of a curved surface over a triangle by a plane.

where (x_i, y_i) denote the coordinates of the ith vertex of the triangle. Note that the triangle is uniquely defined by the three pairs of coordinates (x_i, y_i).

The three constants c_i^e $(i = 1, 2, 3)$ in (8.2.21) can be expressed in terms of three nodal values u_i^e $(i = 1, 2, 3)$. Thus, the polynomial (8.2.21) is associated with a triangular element and there are three nodes identified, namely, the vertices of the triangle. Equations in (8.2.22) have the explicit form

$$\begin{aligned} u_1 &\equiv u_h(x_1, y_1) = c_1 + c_2 x_1 + c_3 y_1 \\ u_2 &\equiv u_h(x_2, y_2) = c_1 + c_2 x_2 + c_3 y_2 \\ u_3 &\equiv u_h(x_3, y_3) = c_1 + c_2 x_3 + c_3 y_3 \end{aligned}$$

where the element label e is omitted for simplicity. Throughout the following discussion, this format will be followed. In matrix form, we have

$$\begin{Bmatrix} u_1 \\ u_2 \\ u_3 \end{Bmatrix} = \begin{bmatrix} 1 & x_1 & y_1 \\ 1 & x_2 & y_2 \\ 1 & x_3 & y_3 \end{bmatrix} \begin{Bmatrix} c_1 \\ c_2 \\ c_3 \end{Bmatrix} \quad \text{or} \quad \mathbf{u} = \mathbf{A}\mathbf{c} \tag{8.2.23}$$

Solution of (8.2.23) for c_i $(i = 1, 2, 3)$ requires the inversion of the coefficient matrix **A** in (8.2.23). The inverse ceases to exist whenever any two rows or columns are the same. Two rows or columns of the coefficient matrix in (8.2.23) will be the same only when all three nodes lie on the same line. Thus, in theory, as long as the three vertices of the triangle are distinct and do not lie on a line, the coefficient matrix is invertible. However, in actual computations, if any two of the three nodes are *very close* to the third node or the three nodes are almost on the same line, the coefficient matrix can be *nearly singular* and numerically noninvertible. Hence, we should avoid elements with narrow geometries (see Fig. 8.2.3) in finite element meshes.

Inverting the coefficient matrix in (8.2.23), we obtain

$$[A]^{-1} = \frac{1}{2A} \begin{bmatrix} \alpha_1 & \alpha_2 & \alpha_3 \\ \beta_1 & \beta_2 & \beta_3 \\ \gamma_1 & \gamma_2 & \gamma_3 \end{bmatrix}, \quad 2A = \alpha_1 + \alpha_2 + \alpha_3$$

where $2A$ is the determinant of the matrix **A**, A being the area of the triangle whose three vertices are at (x_i, y_i) $(i = 1, 2, 3)$. Solving for c_i in terms of u_i (i.e., $\{c\} = [A]^{-1}\{u\}$),

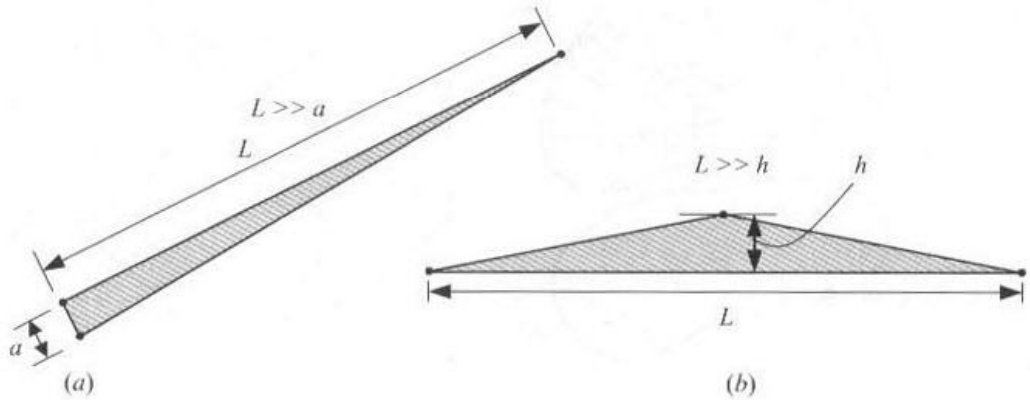

Figure 8.2.3 Triangular geometries that should be avoided in finite element meshes.

we obtain

$$c_1 = \frac{1}{2A}(\alpha_1 u_1 + \alpha_2 u_2 + \alpha_3 u_3)$$
$$c_2 = \frac{1}{2A}(\beta_1 u_1 + \beta_2 u_2 + \beta_3 u_3) \tag{8.2.24a}$$
$$c_3 = \frac{1}{2A}(\gamma_1 u_1 + \gamma_2 u_2 + \gamma_3 u_3)$$

where α_i, β_i, and γ_i are constants that depend only on the global coordinates of element nodes (x_i, y_i)

$$\left.\begin{aligned} \alpha_i &= x_j y_k - x_k y_j \\ \beta_i &= y_j - y_k \\ \gamma_i &= -(x_j - x_k) \end{aligned}\right\} \quad (i \neq j \neq k;\ i,\ j, \text{ and } k \text{ permute in a natural order}) \tag{8.2.24b}$$

Substituting for c_i from (8.2.24a) into (8.2.21), we obtain

$$\begin{aligned} u_h^e(x, y) &= \frac{1}{2A}[(u_1\alpha_1 + u_2\alpha_2 + u_3\alpha_3) + (u_1\beta_1 + u_2\beta_2 + u_3\beta_3)x \\ &\quad + (\gamma_1 u_1 + \gamma_2 u_2 + \gamma_3 u_3)y] \\ &= \sum_{i=1}^{3} u_i^e \psi_i^e(x, y) \end{aligned} \tag{8.2.25a}$$

where ψ_i^e are the linear interpolation functions for the triangular element

$$\psi_i^e = \frac{1}{2A_e}\left(\alpha_i^e + \beta_i^e x + \gamma_i^e y\right) \quad (i = 1, 2, 3) \tag{8.2.25b}$$

and α_i^e, β_i^e, and γ_i^e are the constants defined in (8.2.24b). The linear interpolation functions ψ_i^e are shown in Fig. 8.2.4.

The interpolation functions ψ_i^e have the properties

$$\psi_i^e\left(x_j^e, y_j^e\right) = \delta_{ij} \quad (i, j = 1, 2, 3) \tag{8.2.26a}$$

$$\sum_{i=1}^{3} \psi_i^e = 1, \quad \sum_{i=1}^{3} \frac{\partial \psi_i^e}{\partial x} = 0, \quad \sum_{i=1}^{3} \frac{\partial \psi_i^e}{\partial y} = 0 \tag{8.2.26b}$$

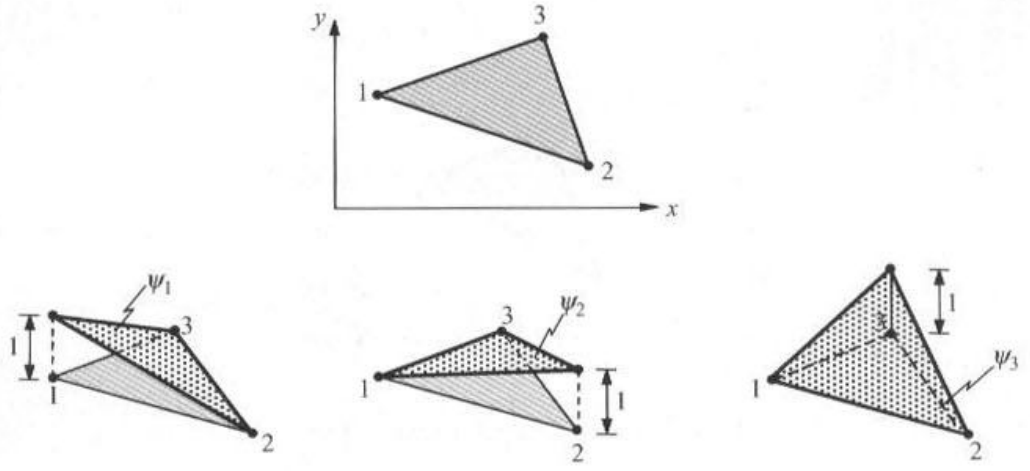

Figure 8.2.4 Interpolation functions for the three-node triangle.

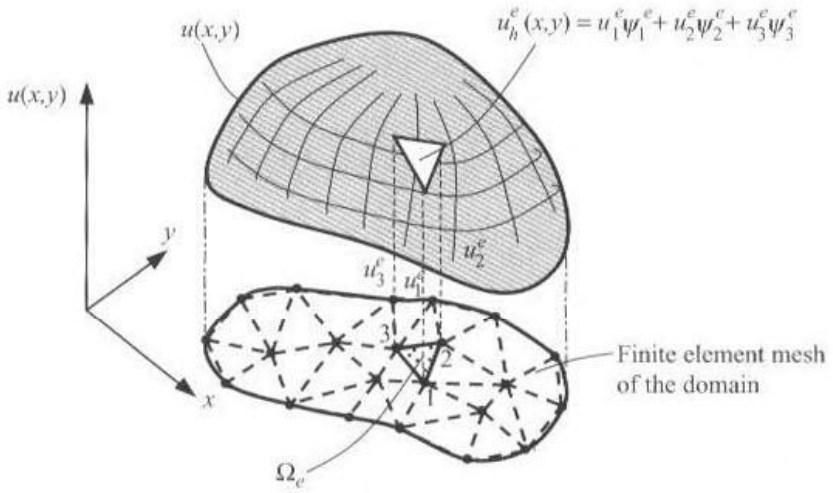

Figure 8.2.5 Representation of a continuous function $u(x, y)$ by linear interpolation functions of three-node triangular elements.

Note that (8.2.24*a*) determines a plane surface passing through u_1, u_2, and u_3. Hence, use of the linear interpolation functions ψ_i^e of a triangle will result in the approximation of the curved surface $u(x, y)$ by a planar function $u_h^e = \sum_{i=1}^{3} u_i^e \psi_i^e$ as shown in Fig. 8.2.5. We consider an example of computing ψ_i^e.

Example 8.2.1

Consider the triangular element shown in Fig. 8.2.6. Let

$$u_h(x, y) = c_1 + c_2 x + c_3 y = [1 \; x \; y] \begin{Bmatrix} c_1 \\ c_2 \\ c_3 \end{Bmatrix}$$

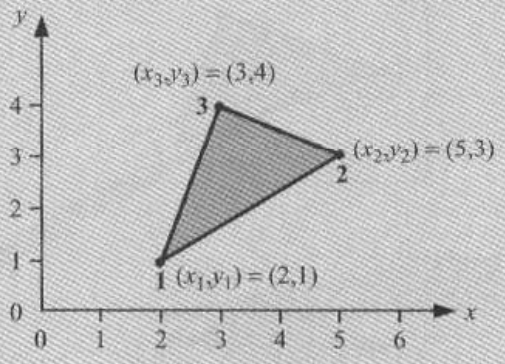

Figure 8.2.6 The triangular element of Example 8.2.1.

Evaluating this polynomial at nodes 1, 2, and 3, we obtain the equations

$$\begin{Bmatrix} u_1 \\ u_2 \\ u_3 \end{Bmatrix} = \begin{bmatrix} 1 & 2 & 1 \\ 1 & 5 & 3 \\ 1 & 3 & 4 \end{bmatrix} \begin{Bmatrix} c_1 \\ c_2 \\ c_3 \end{Bmatrix}, \quad \begin{Bmatrix} c_1 \\ c_2 \\ c_3 \end{Bmatrix} = [A]^{-1} \begin{Bmatrix} u_1 \\ u_2 \\ u_3 \end{Bmatrix}$$

where

$$[A]^{-1} = \begin{bmatrix} 1 & 2 & 1 \\ 1 & 5 & 3 \\ 1 & 3 & 4 \end{bmatrix}^{-1} = \frac{1}{7} \begin{bmatrix} 11 & -5 & 1 \\ -1 & 3 & -2 \\ -2 & -1 & 3 \end{bmatrix}$$

Substituting the last expression into u_h, we obtain

$$u_h(x, y) = \{1 \quad x \quad y\}[A]^{-1} \begin{Bmatrix} u_1 \\ u_2 \\ u_3 \end{Bmatrix} = \frac{1}{7}\{11 - x - 2y, \quad -5 + 3x - y, \quad 1 - 2x + 3y\} \begin{Bmatrix} u_1 \\ u_2 \\ u_3 \end{Bmatrix}$$

$$\equiv \{\psi_1^e \quad \psi_2^e \quad \psi_3^e\} \begin{Bmatrix} u_1 \\ u_2 \\ u_3 \end{Bmatrix} = \sum_{i=1}^{3} \psi_i^e u_i^e$$

where

$$\psi_1^e = \frac{1}{7}(11 - x - 2y), \quad \psi_2^e = \frac{1}{7}(-5 + 3x - y), \quad \psi_3^e = \frac{1}{7}(1 - 2x + 3y)$$

Alternatively, from definitions (8.2.24*b*), we have

$$\alpha_1 = 5 \times 4 - 3 \times 3 = 11, \quad \alpha_2 = 3 \times 1 - 2 \times 4 = -5, \quad \alpha_3 = 2 \times 3 - 5 \times 1 = 1$$

$$\beta_1 = 3 - 4 = -1, \quad \beta_2 = 4 - 1 = 3, \quad \beta_3 = 1 - 3 = -2$$

$$\gamma_1 = -(5 - 3) = -2, \quad \gamma_2 = -(3 - 2) = -1, \quad \gamma_3 = -(2 - 5) = 3$$

$$2A = \alpha_1 + \alpha_2 + \alpha_3 = 7$$

The interpolation functions are

$$\psi_1^e = \frac{1}{7}(11 - x - 2y), \quad \psi_2^e = \frac{1}{7}(-5 + 3x - y), \quad \psi_3^e = \frac{1}{7}(1 - 2x + 3y)$$

which are the same as those obtained earlier.

Linear Rectangular Element

Next, consider the complete polynomial

$$u_h^e(x, y) = c_1^e + c_2^e x + c_3^e y + c_4^e xy \tag{8.2.27}$$

which contains four linearly independent terms and is linear in x and y, with a bilinear term in x and y. This polynomial requires an element with four nodes. There are two possible geometric shapes: a triangle with the fourth node at the center (or centroid) of the triangle or

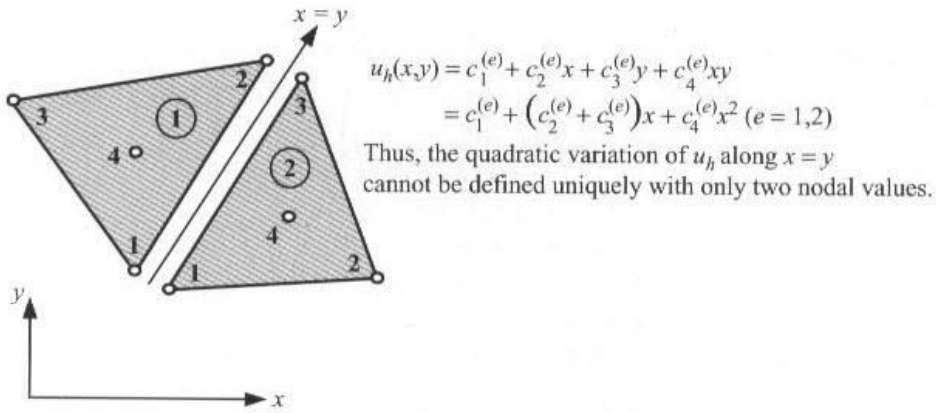

$$u_h(x,y) = c_1^{(e)} + c_2^{(e)}x + c_3^{(e)}y + c_4^{(e)}xy$$
$$= c_1^{(e)} + \left(c_2^{(e)} + c_3^{(e)}\right)x + c_4^{(e)}x^2 \quad (e = 1,2)$$

Thus, the quadratic variation of u_h along $x = y$ cannot be defined uniquely with only two nodal values.

Figure 8.2.7 Incompatible four-node triangular elements.

a rectangle with the nodes at the vertices. A triangle with a fourth node at the center does not provide a single-valued variation of u at interelement boundaries, resulting in *incompatible* variation of u at interelement boundaries and is therefore not admissible (see Fig. 8.2.7). The linear rectangular element is a compatible element because on any side u_h^e varies only linearly and there are two nodes to uniquely define it.

Here we consider an approximation of the form (8.2.27) and use a rectangular element with sides a and b [see Fig. 8.2.8(*a*)]. For the sake of convenience, we choose a local coordinate system $(\bar{x}, \bar{y})$ to derive the interpolation functions. We assume that (the element label is omitted)

$$u_h(\bar{x}, \bar{y}) = c_1 + c_2\bar{x} + c_3\bar{y} + c_4\bar{x}\bar{y} \tag{8.2.28}$$

and require

$$\begin{aligned} u_1 &= u_h(0,0) = c_1 \\ u_2 &= u_h(a,0) = c_1 + c_2 a \\ u_3 &= u_h(a,b) = c_1 + c_2 a + c_3 b + c_4 ab \\ u_4 &= u_h(0,b) = c_1 + c_3 b \end{aligned} \tag{8.2.29}$$

Solving for c_i $(i = 1, \ldots, 4)$, we obtain

$$\begin{aligned} c_1 &= u_1, & c_2 &= \frac{u_2 - u_1}{a} \\ c_3 &= \frac{u_4 - u_1}{b}, & c_4 &= \frac{u_3 - u_4 + u_1 - u_2}{ab} \end{aligned} \tag{8.2.30}$$

Substituting (8.2.30) into (8.2.28), we obtain

$$u_h(\bar{x}, \bar{y}) = u_1\left(1 - \frac{\bar{x}}{a} - \frac{\bar{y}}{b} + \frac{\bar{x}}{a}\frac{\bar{y}}{b}\right) + u_2\left(\frac{\bar{x}}{a} - \frac{\bar{x}}{a}\frac{\bar{y}}{b}\right) + u_3\frac{\bar{x}}{a}\frac{\bar{y}}{b} + u_4\left(\frac{\bar{y}}{b} - \frac{\bar{x}}{a}\frac{\bar{y}}{b}\right)$$

$$= u_1^e\psi_1^e + u_2^e\psi_2^e + u_3^e\psi_3^e + u_4^e\psi_4^e = \sum_{i=1}^{4} u_i^e\psi_i^e \tag{8.2.31}$$

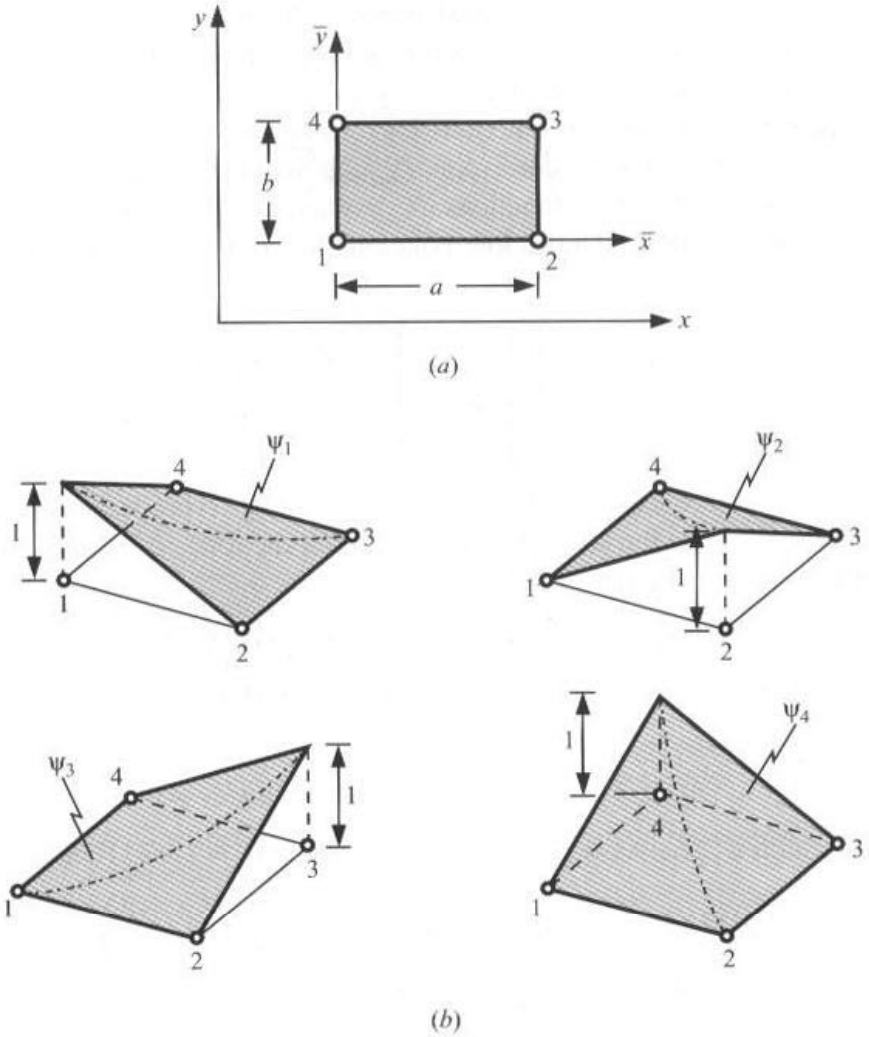

Figure 8.2.8 Linear rectangular element and its interpolation functions.

where

$$\psi_1^e = \left(1 - \frac{\bar{x}}{a}\right)\left(1 - \frac{\bar{y}}{b}\right), \quad \psi_2^e = \frac{\bar{x}}{a}\left(1 - \frac{\bar{y}}{b}\right)$$
$$\psi_3^e = \frac{\bar{x}}{a}\frac{\bar{y}}{b}, \quad \psi_4^e = \left(1 - \frac{\bar{x}}{a}\right)\frac{\bar{y}}{b} \tag{8.2.32a}$$

or, in concise form,

$$\psi_i^e(\bar{x}, \bar{y}) = (-1)^{i+1}\left(1 - \frac{\bar{x} + \bar{x}_i}{a}\right)\left(1 - \frac{\bar{y} + \bar{y}_i}{b}\right) \tag{8.2.32b}$$

where $(\bar{x}_i, \bar{y}_i)$ are the $(\bar{x}, \bar{y})$ coordinates of node i. The interpolation functions are shown in Fig. 8.2.8(b). Once again, we have

$$\psi_i^e(\bar{x}_j, \bar{y}_j) = \delta_{ij} \quad (i, j = 1, \ldots, 4), \quad \sum_{i=1}^{4} \psi_i^e = 1 \tag{8.2.33}$$

The procedure given above for the construction of the interpolation functions involves the inversion of an $n \times n$ matrix, where n is the number of nodes in the element. When n is large, the inversion becomes very tedious.

Alternatively, the interpolation functions for rectangular element can also be obtained by taking the tensor product of the corresponding one-dimensional interpolation functions. To obtain the linear interpolation functions of a rectangular element, we take the "tensor product" of the one-dimensional linear interpolation functions (3.2.19) associated with sides 1–2 and 1–3:

$$\begin{Bmatrix} 1-\dfrac{\bar{x}}{a} \\ \dfrac{\bar{x}}{a} \end{Bmatrix} \begin{Bmatrix} 1-\dfrac{\bar{y}}{b} \\ \dfrac{\bar{y}}{b} \end{Bmatrix}^{\mathrm{T}} = \begin{bmatrix} \psi_1 & \psi_4 \\ \psi_2 & \psi_3 \end{bmatrix} \tag{8.2.34}$$

The alternative procedure that makes use of the interpolation properties (8.2.33) can also be used. Here we illustrate the alternative procedure for the four-node rectangular element. Equation (8.2.26a) requires that

$$\psi_1^e(\bar{x}_i, \bar{y}_i) = 0 \quad (i = 2, 3, 4), \qquad \psi_1^e(\bar{x}_1, \bar{y}_1) = 1$$

That is, ψ_1^e is identically zero on lines $\bar{x} = a$ and $\bar{y} = b$. Hence, $\psi_1^e(\bar{x}, \bar{y})$ must be of the form

$$\psi_1^e(\bar{x}, \bar{y}) = c_1(a - \bar{x})(b - \bar{y}) \quad \text{for any } c_1 \neq 0$$

Using the condition $\psi_1^e(\bar{x}_1, \bar{y}_1) = \psi_1^e(0, 0) = 1$, we obtain $c_1 = 1/ab$. Hence,

$$\psi_1^e(\bar{x}, \bar{y}) = \frac{1}{ab}(a - \bar{x})(b - \bar{y}) = \left(1 - \frac{\bar{x}}{a}\right)\left(1 - \frac{\bar{y}}{b}\right)$$

Likewise, we can obtain the remaining three interpolation functions.

Quadratic Elements

A quadratic triangular element must have three nodes per side in order to define a unique quadratic variation along that side. Thus, there are a total of six nodes in a quadratic triangular element [see Fig. 8.2.9(a)]. A six-term complete polynomial that includes both x and y is

$$u_h^e(x, y) = c_1 + c_2 x + c_3 y + c_4 xy + c_5 x^2 + c_6 y^2 \tag{8.2.35}$$

The constants may be expressed in terms of the six nodal values by the procedure outlined for the three-node triangular element and four-node rectangular element. However, in practice the interpolation functions of higher-order elements are derived using the alternative procedure (i.e., use the interpolation properties).

Similarly, a quadratic rectangular element has three nodes per side, resulting in an eight-node rectangular element [see Fig. 8.2.9(b)]. The eight-term polynomial is

$$u_h^e(x, y) = c_1 + c_2 x + c_3 y + c_4 xy + c_5 x^2 + c_6 y^2 + c_7 xy^2 + c_8 yx^2 \tag{8.2.36}$$

The interpolation functions of this element cannot be generated by the tensor product of one-dimensional quadratic functions (3.2.27). Indeed, the two-dimensional interpolation functions associated with the tensor product of one-dimensional quadratic functions correspond to the nine-node rectangular element [see Fig. 8.2.9(c)]. The nine-term polynomial

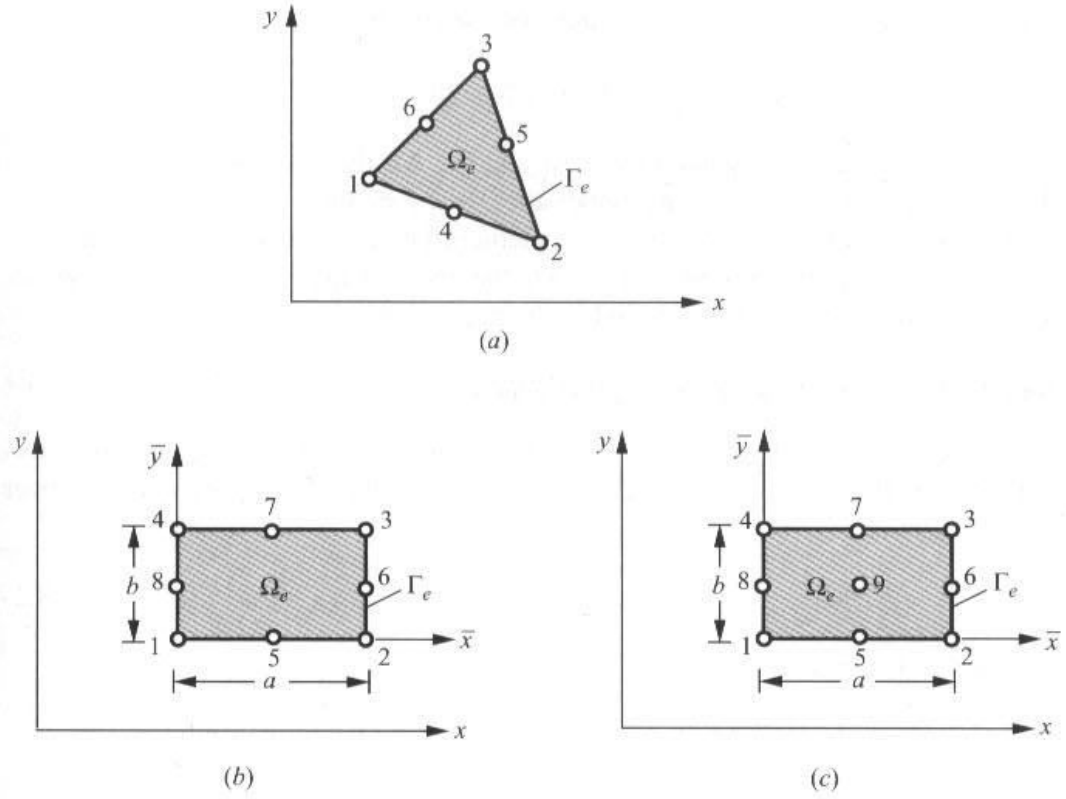

Figure 8.2.9 (*a*) Quadratic triangular element. (*b*) Eight-node quadratic rectangular element. (*c*) Nine-node quadratic rectangular element.

is given by

$$u_h^e(x, y) = c_1 + c_2x + c_3y + c_4xy + c_5x^2 + c_6y^2 + c_7xy^2 + c_8yx^2 + c_9x^2y^2 \quad (8.2.37)$$

Additional discussion on the derivation of element interpolation functions is presented in Chapter 9.

8.2.6 Evaluation of Element Matrices and Vectors

The exact evaluation of the element matrices $[K^e]$ and $\{f^e\}$ in (8.2.19*b*) is, in general, not easy. In general, they are evaluated using numerical integration techniques described in Section 9.3. However, when a_{ij}, a_{00}, and f are elementwise constant, it is possible to evaluate the integrals exactly over the linear triangular and rectangular elements discussed in the previous section. The boundary integral in $\{Q^e\}$ of (8.2.19*b*) can be evaluated whenever q_n is known. For an interior element (i.e., an element that does not have any of its sides on the boundary of the problem), the contribution from the boundary integral cancels with similar contributions from adjoining elements of the mesh (analogous to the Q_i^e in the one-dimensional problems). A more detailed discussion is given below.

For the sake of brevity, we rewrite $[K^e]$ in (8.2.19*b*) as the sum of five basic matrices $[S^{\alpha\beta}](\alpha, \beta = 0, 1, 2)$

$$[K^e] = a_{00}[S^{00}] + a_{11}[S^{11}] + a_{12}[S^{12}] + a_{21}[S^{12}]^T + a_{22}[S^{22}] \quad (8.2.38)$$

where $[\cdot]^{\mathrm{T}}$ denotes the transpose of the enclosed matrix, and

$$S_{ij}^{\alpha\beta} = \int_{\Omega_e} \psi_{i,\alpha}\psi_{j,\beta}\, dx\, dy \tag{8.2.39}$$

with $\psi_{i,\alpha} \equiv \partial\psi_i/\partial x_\alpha$, $x_1 = x$, and $x_2 = y$; $\psi_{i,0} = \psi_i$. All the matrices in (8.2.38) and interpolation functions in (8.2.39) are understood to be defined over an element, i.e., all expressions and quantities should have the element label e, but these are omitted in the interest of brevity. We now proceed to compute the matrices in (8.2.39) and (8.2.19*b*) using the linear interpolation functions derived in the previous section.

Element Matrices of a Linear Triangular Element

First, we note that integrals of polynomials over arbitrary shaped triangular domains can be evaluated exactly. To this end, let I_{mn} denote the integral of the expression $x^m y^n$ over an arbitrary triangle Δ

$$I_{mn} \equiv \int_\Delta x^m y^n\, dx\, dy \tag{8.2.40}$$

Then, it can be shown that

$$\begin{aligned}
I_{00} &= \int_\Delta x^0 y^0\, dx\, dy = \int_\Delta 1 \cdot dx\, dy = A \quad \text{area of the triangle} \\
I_{10} &= \int_\Delta x^1 y^0\, dx\, dy = \int_\Delta x\, dx\, dy = A\hat{x}, \quad \hat{x} = \frac{1}{3}\sum_{i=1}^{3} x_i \\
I_{01} &= \int_\Delta x^0 y^1\, dx\, dy = \int_\Delta y\, dx\, dy = A\hat{y}, \quad \hat{y} = \frac{1}{3}\sum_{i=1}^{3} y_i \\
I_{11} &= \int_\Delta xy\, dx\, dy = \frac{A}{12}\left(\sum_{i=1}^{3} x_i y_i + 9\hat{x}\hat{y}\right) \\
I_{20} &= \int_\Delta x^2\, dx\, dy = \frac{A}{12}\left(\sum_{i=1}^{3} x_i^2 + 9\hat{x}^2\right) \\
I_{02} &= \int_\Delta y^2\, dx\, dy = \frac{A}{12}\left(\sum_{i=1}^{3} y_i^2 + 9\hat{y}^2\right)
\end{aligned} \tag{8.2.41}$$

where (x_i, y_i) are the coordinates of the vertices of the triangle. We can use the above results to evaluate integrals defined over triangular elements.

Next, we evaluate $[K^e]$ and $\{f^e\}$ for linear triangular element under the assumption that a_{ij} and f are elementwise constant. Also, note that (see Problem 8.1)

$$\sum_{i=1}^{3} \alpha_i^e = 2A_e, \quad \sum_{i=1}^{3} \beta_i^e = 0, \quad \sum_{i=1}^{3} \gamma_i^e = 0 \tag{8.2.42a}$$

$$\alpha_i^e + \beta_i^e \hat{x}_e + \gamma_i^e \hat{y}_e = \frac{2}{3}A_e \tag{8.2.42b}$$

$$\frac{\partial\psi_i}{\partial x} = \frac{\beta_i^e}{2A_e}, \quad \frac{\partial\psi_i}{\partial y} = \frac{\gamma_i^e}{2A_e} \tag{8.2.43}$$

we obtain

$$S_{ij}^{11} = \frac{1}{4A}\beta_i\beta_j, \quad S_{ij}^{12} = \frac{1}{4A}\beta_i\gamma_j, \quad S_{ij}^{22} = \frac{1}{4A}\gamma_i\gamma_j$$

$$S_{ij}^{00} = \frac{1}{4A}\left\{[\alpha_i\alpha_j + (\alpha_i\beta_j + \alpha_j\beta_i)\hat{x} + (\alpha_i\gamma_j + \alpha_j\gamma_i)\hat{y}]\right. \tag{8.2.44}$$

$$\left. + \frac{1}{A}[I_{20}\beta_i\beta_j + I_{11}(\gamma_i\beta_j + \gamma_j\beta_i) + I_{02}\gamma_i\gamma_j]\right\}$$

In view of the identity (8.2.42*b*) and for an elementwise constant value of $f = f_e$, we have

$$\begin{aligned} f_i^e &= \int_{\Delta_e} f_e\psi_i^e(x, y)\,dx\,dy = \frac{f_e}{2A_e}\int_{\Delta_e}\left(\alpha_i^e + \beta_i^e x + \gamma_i^e y\right)dx\,dy \\ &= \frac{f_e}{2A_e}\left(\alpha_i^e I_{00} + \beta_i^e I_{10} + \gamma_i^e I_{01}\right) \\ &= \frac{f_e}{2A_e}\left(\alpha_i^e A_e + \beta_i^e A_e\hat{x}_e + \gamma_i^e A_e\hat{y}_e\right) \\ &= \frac{1}{2}f_e\left(\alpha_i^e + \beta_i^e\hat{x}_e + \gamma_i^e\hat{y}_e\right) = \frac{1}{3}f_eA_e \end{aligned} \tag{8.2.45}$$

The result in (8.2.45) should be obvious because for a constant source f_e the total magnitude of the source (say, heat) on the element is equal to f_eA_e, which is then distributed equally among the three nodes, giving a nodal value of $f_eA_e/3$.

Once the coordinates of the element nodes are known, we can compute α_i^e, β_i^e, and γ_i^e from (8.2.24*b*) and substitute into (8.2.44) to obtain the element matrices, which in turn can be used in (8.2.38) to obtain the element matrix $[K^e]$. In particular, when a_{12}, a_{21}, and a_{00} are zero and a_{11} and a_{22} are elementwise constant, Eq. (8.2.1) becomes

$$-\left(a_{11}\frac{\partial^2 u}{\partial x^2} + a_{22}\frac{\partial^2 u}{\partial y^2}\right) - f = 0 \text{ in } \Omega_e \tag{8.2.46}$$

and the associated element coefficient matrix for a linear triangular element is

$$K_{ij}^e = \frac{1}{4A_e}\left(a_{11}^e\beta_i^e\beta_j^e + a_{22}^e\gamma_i^e\gamma_j^e\right) \tag{8.2.47}$$

Example 8.2.2

Consider the right-angle triangle shown in Fig. 8.2.10(*a*). We wish to determine the element coefficient matrix $[K^e]$ of (8.2.47) and source vector $\{f^e\}$ associated with the Poisson equation (8.2.46). We note that the element calculations do not depend on the global coordinate system (x, y). Therefore, we choose the local coordinate system $(\bar{x}, \bar{y})$ to compute A, α, β, and γ for

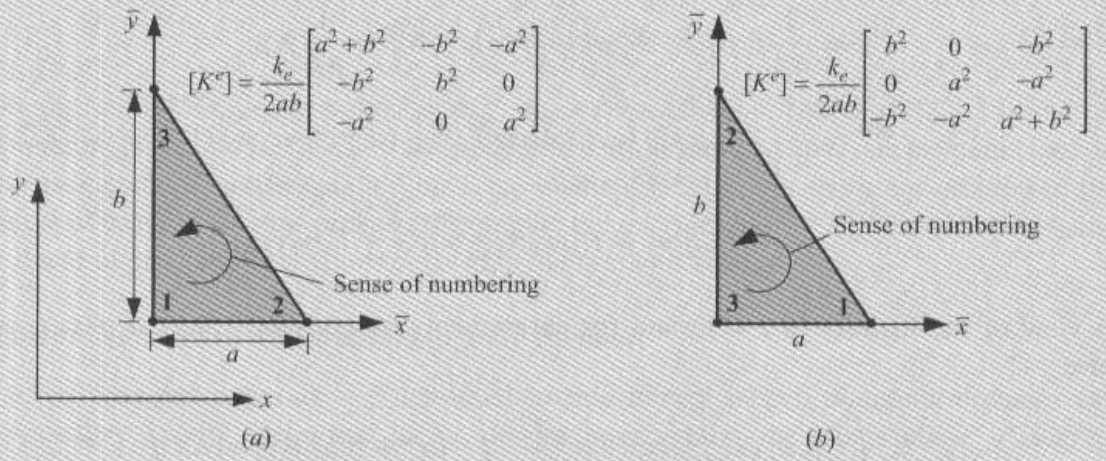

Figure 8.2.10 The right-angle linear triangular element of Example 8.2.2.

the element. We have

$$2A = ab, \quad \alpha_1 = ab, \quad \alpha_2 = 0, \quad \alpha_3 = 0, \quad \beta_1 = -b, \quad \beta_2 = b, \quad \beta_3 = 0, \quad \gamma_1 = -a, \quad \gamma_2 = 0, \quad \gamma_3 = a$$

$$\psi_1 = 1 - \frac{\bar{x}}{a} - \frac{\bar{y}}{b}, \quad \psi_2 = \frac{\bar{x}}{a}, \quad \psi_3 = \frac{\bar{y}}{b}$$

and

$$[K^e] = \frac{a_{11}^e}{2ab}\begin{bmatrix} b^2 & -b^2 & 0 \\ -b^2 & b^2 & 0 \\ 0 & 0 & 0 \end{bmatrix} + \frac{a_{22}^e}{2ab}\begin{bmatrix} a^2 & 0 & -a^2 \\ 0 & 0 & 0 \\ -a^2 & 0 & a^2 \end{bmatrix}, \quad \{f^e\} = \frac{f_e ab}{6}\begin{Bmatrix} 1 \\ 1 \\ 1 \end{Bmatrix} \tag{8.2.48}$$

If $a_{11}^e = a_{22}^e = k_e$, for the numbering system shown in Fig. 8.2.10(a), we have

$$[K^e] = \frac{k_e}{2ab}\begin{bmatrix} b^2+a^2 & -b^2 & -a^2 \\ -b^2 & b^2 & 0 \\ -a^2 & 0 & a^2 \end{bmatrix}, \quad \{f^e\} = \frac{f_e ab}{6}\begin{Bmatrix} 1 \\ 1 \\ 1 \end{Bmatrix} \tag{8.2.49}$$

In addition, if $a = b$, we have

$$[K^e] = \frac{k_e}{2}\begin{bmatrix} 2 & -1 & -1 \\ -1 & 1 & 0 \\ -1 & 0 & 1 \end{bmatrix}, \quad \{f^e\} = \frac{f_e a^2}{6}\begin{Bmatrix} 1 \\ 1 \\ 1 \end{Bmatrix} \tag{8.2.50}$$

We note that contents of $[K^e]$ depend, even for the same geometry, on the node numbering scheme, as shown in Figs. 8.2.10(a) and 8.2.10(b). For the same element, if the node numbering is changed, the element coefficients will change accordingly. For example, if we renumber the element nodes of the element in Fig. 8.2.10(a) to be those in Fig. 8.2.10(b), then $[K^e]$ for the element in Fig. 8.2.10(b) is obtained from (8.2.49) [which corresponds to the element numbering in Fig. 8.2.10(a)] by moving rows and columns $1 \to 3$, $3 \to 2$, and $2 \to 1$ (if the first row and column are moved after the third row and column, the last two

moves are automatic):

$$\frac{k_e}{2ab}\begin{bmatrix} b^2+a^2 & -b^2 & -a^2 \\ -b^2 & b^2 & 0 \\ -a^2 & 0 & a^2 \end{bmatrix} \to \frac{k_e}{2ab}\begin{bmatrix} -b^2 & -a^2 & b^2+a^2 \\ b^2 & 0 & -b^2 \\ 0 & a^2 & -a^2 \end{bmatrix} \to \frac{k_e}{2ab}\begin{bmatrix} b^2 & 0 & -b^2 \\ 0 & a^2 & -a^2 \\ -b^2 & -a^2 & b^2+a^2 \end{bmatrix}$$

In addition, all elements with the same geometry and node numbering, irrespective of their orientation (i.e., rigid body rotation about an axis perpendicular to the plane of the element), have the same coefficient matrix. Elements with the same coefficient matrix are listed in Fig. 8.2.11. For uniformity, we fix the sign convention and use counterclockwise numbering scheme for the element nodes.

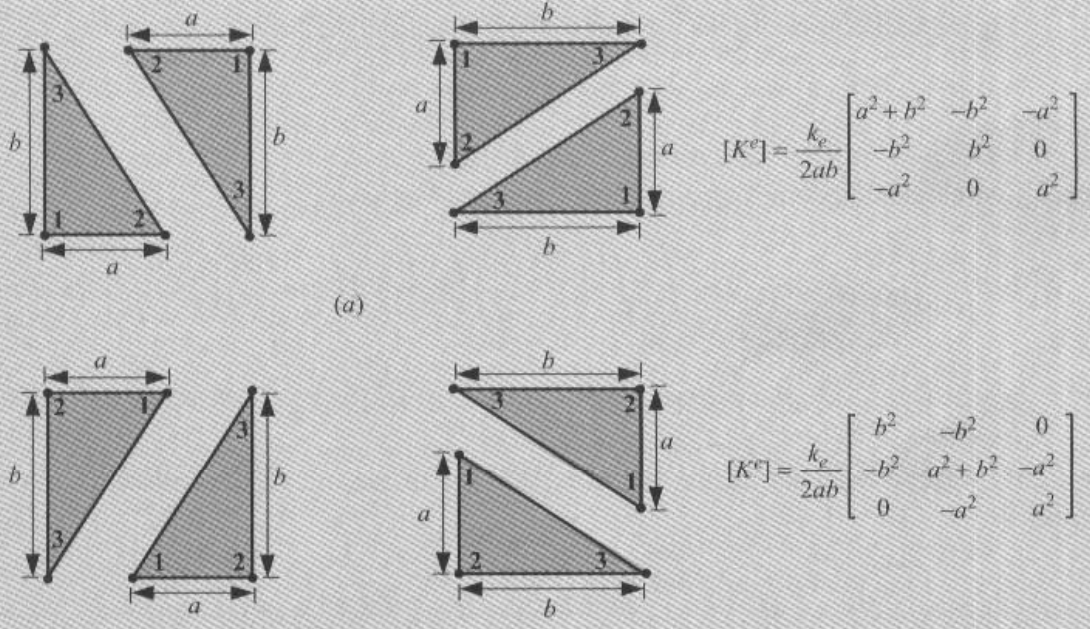

Figure 8.2.11 Coefficient matrices associated with Eq. (8.2.46) with $a_{11}^e = a_{22}^e = k_e$ for two different element node numbers of linear right-angle triangular elements.

Element Matrices of a Linear Rectangular Element

When the data a_{ij} $(i, j = 0, 1, 2)$ and f of the problem is not a function of x and y, we can use the interpolation functions in (8.2.32a), expressed in the local coordinates $(\bar{x}, \bar{y})$ that are mere translation of (x, y) (see Fig. 8.2.12), to compute the element coefficients $S_{ij}^{\alpha\beta}$ $(\alpha, \beta = 1, 2)$ of Eq. (8.2.39). For example, we have

$$S_{ij}^{00} = \int_{\Omega_e} \psi_i(x, y)\psi_j(x, y)\, dx\, dy = \int_0^a \int_0^b \psi_i \psi_j\, d\bar{x}\, d\bar{y}$$

where a and b are the lengths along the $\bar{x}$ and $\bar{y}$ axes of the element. Since the integration with respect to $\bar{x}$ and $\bar{y}$ can be carried out independent of each other, integration over a

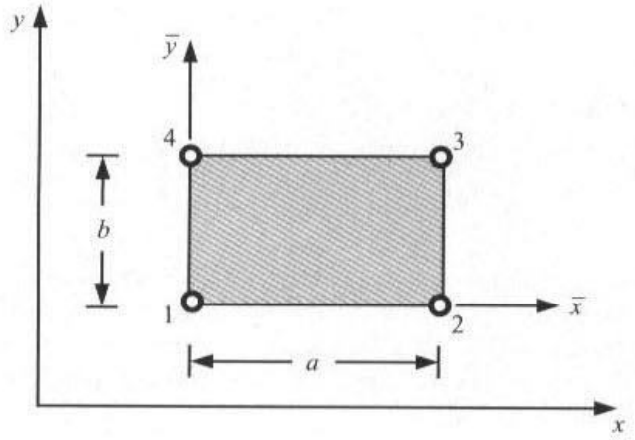

Figure 8.2.12 A rectangular element with the global and local coordinate systems.

rectangular element becomes a pair of line integrals. We have

$$S_{11}^{00} = \int_0^a \int_0^b \psi_1 \psi_1 \, d\bar{x} \, d\bar{y} = \int_0^a \int_0^b \left(1 - \frac{\bar{x}}{a}\right)\left(1 - \frac{\bar{y}}{b}\right)\left(1 - \frac{\bar{x}}{a}\right)\left(1 - \frac{\bar{y}}{b}\right) d\bar{x} \, d\bar{y}$$

$$= \int_0^a \left(1 - \frac{\bar{x}}{a}\right)^2 d\bar{x} \int_0^b \left(1 - \frac{\bar{y}}{b}\right)^2 d\bar{y} = \frac{a}{3}\frac{b}{3} = \frac{ab}{9}$$

Similarly, we can evaluate all the matrices $[S^{\alpha\beta}]$ with the aid of the following integral identities:

$$\int_0^a \left(1 - \frac{s}{a}\right) ds = \frac{a}{2}, \quad \int_0^a \frac{s}{a} \, ds = \frac{a}{2}$$

$$\int_0^a \left(1 - \frac{s}{a}\right)^2 ds = \frac{a}{3}, \quad \int_0^a \frac{s}{a}\left(1 - \frac{s}{a}\right) ds = \frac{a}{6}, \quad \int_0^a \left(\frac{s}{a}\right)^2 ds = \frac{a}{3} \tag{8.2.51}$$

In summary, the element matrices $[S^{\alpha\beta}]$ for a rectangular element are

$$[S^{11}] = \frac{b}{6a}\begin{bmatrix} 2 & -2 & -1 & 1 \\ -2 & 2 & 1 & -1 \\ -1 & 1 & 2 & -2 \\ 1 & -1 & -2 & 2 \end{bmatrix}, \quad [S^{12}] = \frac{1}{4}\begin{bmatrix} 1 & 1 & -1 & -1 \\ -1 & -1 & 1 & 1 \\ -1 & -1 & 1 & 1 \\ 1 & 1 & -1 & -1 \end{bmatrix}$$

$$[S^{22}] = \frac{a}{6b}\begin{bmatrix} 2 & 1 & -1 & -2 \\ 1 & 2 & -2 & -1 \\ -1 & -2 & 2 & 1 \\ -2 & -1 & 1 & 2 \end{bmatrix}, \quad [S^{00}] = \frac{ab}{36}\begin{bmatrix} 4 & 2 & 1 & 2 \\ 2 & 4 & 2 & 1 \\ 1 & 2 & 4 & 2 \\ 2 & 1 & 2 & 4 \end{bmatrix} \tag{8.2.52}$$

$$\{f\} = \frac{1}{4} f_e ab \{1 \quad 1 \quad 1 \quad 1\}^{\mathrm{T}}$$

Example 8.2.3

Here, we wish to determine the element coefficient matrix $[K^e]$ associated with the Poisson equation (8.2.46) over a linear rectangular element. We have

$$[K^e] = a_{11}^e [S^{11}] + a_{22}^e [S^{22}]$$

or

$$[K^e] = \frac{a_{11}^e b}{6a} \begin{bmatrix} 2 & -2 & -1 & 1 \\ -2 & 2 & 1 & -1 \\ -1 & 1 & 2 & -2 \\ 1 & -1 & -2 & 2 \end{bmatrix} + \frac{a_{22}^e a}{6b} \begin{bmatrix} 2 & 1 & -1 & -2 \\ 1 & 2 & -2 & -1 \\ -1 & -2 & 2 & 1 \\ -2 & -1 & 1 & 2 \end{bmatrix} \tag{8.2.53}$$

Note that the coefficient matrix is a function of both element aspect ratios a/b and b/a. Therefore, elements with very large aspect ratios should not be used as they will result in an ill-conditioned matrix (i.e., very large numbers are added to very small numbers), where either $[S^{11}]$ or $[S^{22}]$ will dominate the element matrix.

For $a_{11}^e = a_{22}^e = k_e$, the element coefficient matrix becomes

$$[K^e] = \frac{k_e}{6ab} \begin{bmatrix} 2(a^2+b^2) & a^2-2b^2 & -(a^2+b^2) & b^2-2a^2 \\ a^2-2b^2 & 2(a^2+b^2) & b^2-2a^2 & -(a^2+b^2) \\ -(a^2+b^2) & b^2-2a^2 & 2(a^2+b^2) & a^2-2b^2 \\ b^2-2a^2 & -(a^2+b^2) & a^2-2b^2 & 2(a^2+b^2) \end{bmatrix} \tag{8.2.54}$$

When the element aspect ratio is $a/b = 1$, the coefficient matrix in Eq. (8.2.54) becomes

$$[K^e] = \frac{k_e}{6} \begin{bmatrix} 4 & -1 & -2 & -1 \\ -1 & 4 & -1 & -2 \\ -2 & -1 & 4 & -1 \\ -1 & -2 & -1 & 4 \end{bmatrix} \tag{8.2.55}$$

Evaluation of Boundary Integrals

Here, we consider the evaluation of boundary integrals of the type [see Eq. (8.2.19*b*)]

$$Q_i^e = \oint_{\Gamma_e} q_n^e \psi_i^e(s)\, ds \tag{8.2.56}$$

where q_n^e is a known function of the distance s along the boundary Γ_e. It is not necessary to compute such integrals when a portion of Γ_e does not coincide with the boundary Γ of the total domain Ω [see Fig. 8.2.13(*a*)]. On portions of Γ_e that are in the interior of the domain Ω, q_n^e on side (i, j) of element Ω_e cancels with q_n^f on side (p, q) of element Ω_f when sides (i, j) of element Ω_e and (p, q) of element Ω_f are the same (i.e., at the interface of elements Ω_e and Ω_f). This can be viewed as the equilibrium of the internal "flux" [see Fig. 8.2.13(*b*)]. When Γ_e falls on the boundary of the domain Ω, q_n is either known as a function of s [see Fig. 8.2.13(*c*)] or to be determined in the postcomputation. The primary variable must be specified on the portion of the boundary where q_n is not specified.

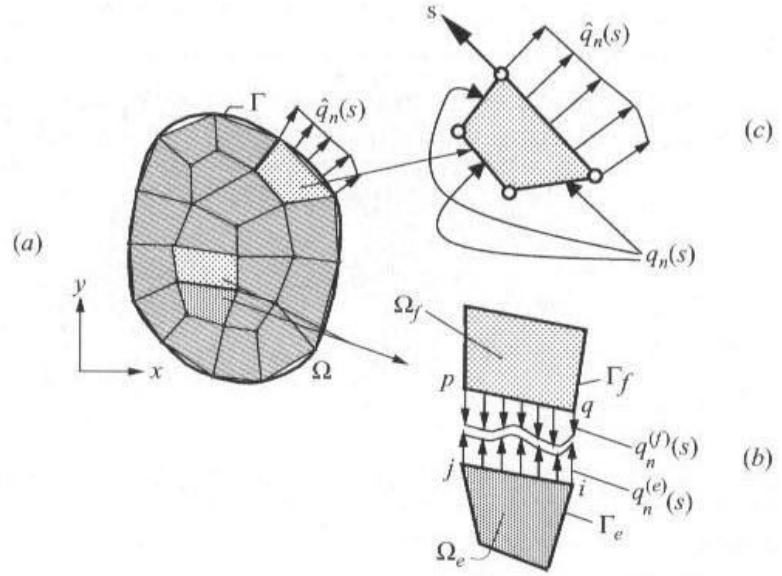

Figure 8.2.13 (*a*) Finite element discretization. (*b*) Equilibrium of fluxes at element interfaces. (*c*) Computation of forces on the boundary of the total domain.

The boundary Γ_e of a two-dimensional element consist of line segments, which can be viewed as one-dimensional elements. Thus, the evaluation of the boundary integrals on two-dimensional problems amounts to evaluating line integrals. It should not be surprising that when two-dimensional interpolation functions are evaluated on the boundary of an element, we obtain the corresponding one-dimensional interpolation functions.

For example, consider a linear triangular element shown in Fig. 8.2.14. The linear interpolation functions for this element are given by (8.2.25*b*). Now let us choose a coordinate system (s, t) with its origin at node 1 and the coordinate s parallel to the side connecting nodes 1 and 2. The two coordinate systems (x, y) and (s, t) are related as follows:

$$x = a_1 + b_1 s + c_1 t$$
$$y = a_2 + b_2 s + c_2 t$$

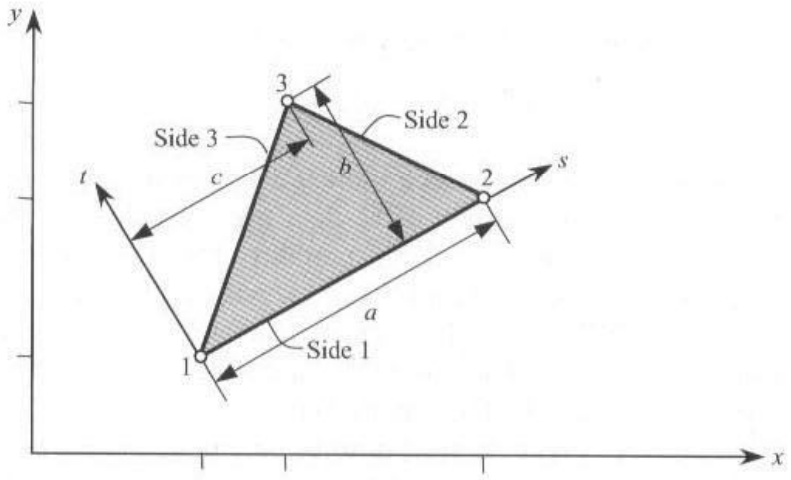

Figure 8.2.14 The linear triangular element in the global (x, y) and local (s, t) coordinate systems.

The constants a_1, b_1, c_1, a_2, b_2, and c_2 can be determined with the following conditions:

$$\begin{aligned} &\text{when } s=0,\ t=0, \quad x=x_1,\ y=y_1 \\ &\text{when } s=a,\ t=0, \quad x=x_2,\ y=y_2 \\ &\text{when } s=c,\ t=b, \quad x=x_3,\ y=y_3 \end{aligned}$$

We obtain

$$\begin{aligned} x(s,t) &= x_1 + (x_2 - x_1)\frac{s}{a} + \left[\left(\frac{c}{a} - 1\right)x_1 - \frac{c}{a}x_2 + x_3\right]\frac{t}{b} \\ y(s,t) &= y_1 + (y_2 - y_1)\frac{s}{a} + \left[\left(\frac{c}{a} - 1\right)y_1 - \frac{c}{a}y_2 + y_3\right]\frac{t}{b} \end{aligned} \tag{8.2.57}$$

Equations (8.2.57) allow us to express $\psi_i(x, y)$ as $\psi_i(s, t)$, which can be evaluated on the side connecting nodes 1 and 2 by setting $t = 0$ in $\psi_i(s, t)$:

$$\psi_i(s) \equiv \psi_i(s,0) = \psi_i(x(s,0), y(s,0))$$

$$x(s) = x_1 + (x_2 - x_1)\frac{s}{a}, \quad y(s) = y_1 + (y_2 - y_1)\frac{s}{a}$$

For instance, we have

$$\begin{aligned} \psi_1(s) &= \frac{1}{2A}\left\{\alpha_1 + \beta_1\left[\left(1 - \frac{s}{a}\right)x_1 + \frac{s}{a}x_2\right] + \gamma_1\left[\left(1 - \frac{s}{a}\right)y_1 + \frac{s}{a}y_2\right]\right\} \\ &= \frac{1}{2A}(\alpha_1 + \alpha_2 + \alpha_3)\left(1 - \frac{s}{a}\right) = 1 - \frac{s}{a} \end{aligned}$$

where the definitions of α_1, β_1, and γ_1 are used to rewrite the entire expression. Similarly, we have

$$\psi_2(s) = \frac{s}{a}, \quad \psi_3(s) = 0$$

where $a = h_{12}$ is the length of side 1–2. We note that $\psi_1(s)$ and $\psi_2(s)$ are precisely the linear, one-dimensional, interpolation functions associated with the line element connecting nodes 1 and 2.

Similarly, when $\psi_i(x, y)$ are evaluated on side 3–1 of the element, we obtain

$$\psi_1(s) = \frac{s}{h_{13}}, \quad \psi_2 = 0, \quad \psi_3(s) = 1 - \frac{s}{h_{13}}$$

where the s coordinate is taken along the side 3–1, with origin at node 3, and h_{13} is the length of side 1–3. Thus, evaluation of Q_i^e involves the use of appropriate one-dimensional interpolation functions and the known variation of q_n on the boundary.

In general, the integral (8.2.56) over the boundary of a linear triangular element can be expressed as

$$\begin{aligned} Q_i^e &= \int_{1-2} \psi_i(s) q_n(s)\, ds + \int_{2-3} \psi_i(s) q_n(s)\, ds + \int_{3-1} \psi_i(s) q_n(s)\, ds \\ &\equiv Q_{i1}^e + Q_{i2}^e + Q_{i3}^e \end{aligned} \tag{8.2.58a}$$

where $\int_{i-j}$ denotes integral over the line connecting node i to node j, the s coordinate is taken from node i to node j, with the origin at node i (see Fig. 8.2.15), and Q_{iJ}^e is defined

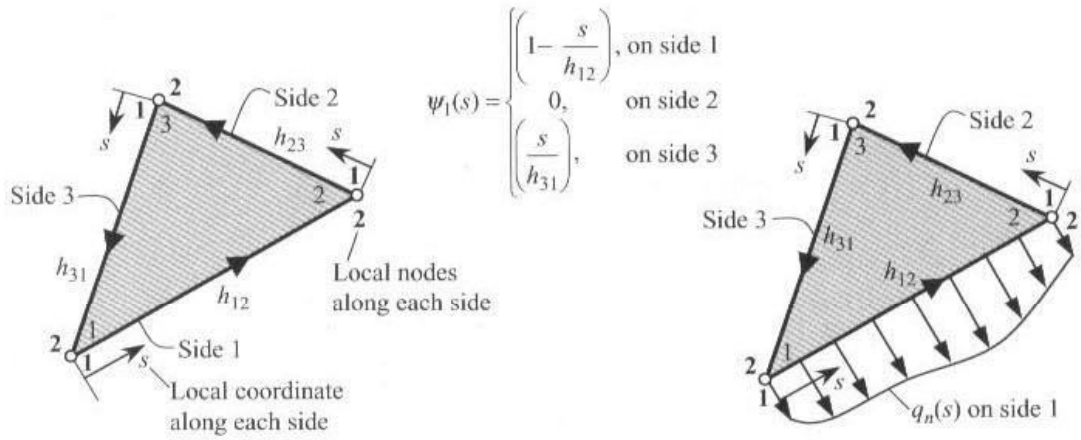

Figure 8.2.15 Computation of the boundary integral (8.2.56) over a linear triangular element.

to be the contribution of q_n on side J of element Ω_e to Q_i^e:

$$Q_{iJ}^e = \int_{\text{side } J} \psi_i q_n \, ds \tag{8.2.58b}$$

where i refers to the ith node of the element and J refers to the Jth side of the element. For example, we have

$$Q_1^e = \oint_{\Gamma_e} q_n \psi_1(s) \, ds = \int_{1-2} (q_n)_{1-2} \psi_1 \, ds + 0 + \int_{3-1} (q_n)_{3-1} \psi_1 \, ds$$

The contribution from side 2–3 is zero because ψ_1 is zero on side 2–3 of a triangular element. For a rectangular element, Q_1^e has four parts but only contributions from sides 1–2 and 4–1 are nonzero because ψ_1 is zero on sides 2–3 and 3–4.

Example 8.2.4

We wish to evaluate the boundary integral Q_i^e in (8.2.56) for the four cases of $q(s)$ and finite element meshes shown in Fig. 8.2.16. For each case we must use the $q(s)$ and the interpolation functions associated with the type of boundary element (i.e., linear or quadratic). On element sides on which q_n is not shown, assume that it is zero.

Case 1. $q(s) = q_0 =$ constant, linear element. Clearly, q_0 will contribute to the nodal values at element nodes 1 and 2. The contribution to node 3 is zero ($Q_3^e = 0$) as there is no specified flux on sides 2–3 and 3–1. We have

$$Q_1^e = \oint_{\Gamma_e} q_n(s)\psi_1(s) \, ds = \int_0^{h_{12}} q_0 (\psi_1)_{1-2} \, ds + \int_0^{h_{31}} (0)(\psi_1)_{3-1} \, ds = Q_{11}^e = \frac{1}{2} q_0 h_{12}$$

$$Q_2^e = \oint_{\Gamma_e} q_n(s)\psi_2(s) \, ds = \int_0^{h_{12}} q_0 (\psi_2)_{1-2} \, ds + \int_0^{h_{23}} (0)(\psi_2)_{2-3} \, ds = Q_{21}^e = \frac{1}{2} q_0 h_{12}$$

where

$$(\psi_1)_{1-2} = 1 - \frac{s}{h_{12}}, \quad (\psi_2)_{1-2} = \frac{s}{h_{12}}$$

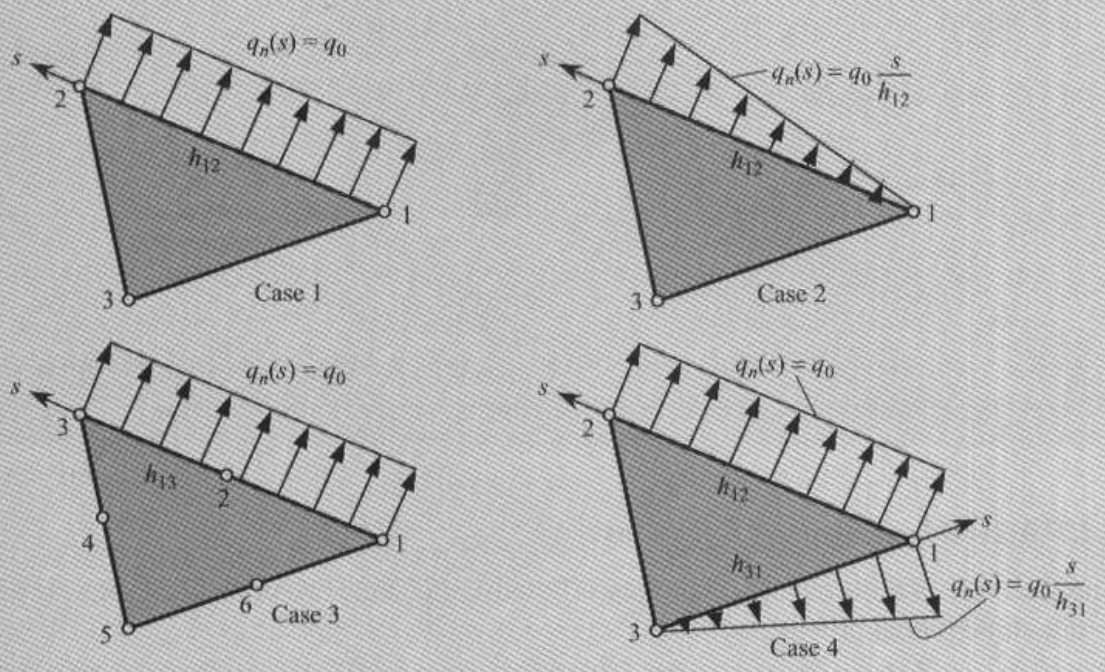

Figure 8.2.16 Evaluation of boundary integrals in the finite element analysis (Example 8.2.4).

Case 2. $q(s) = q_0 s/h_{12}$ (linear variation), linear element. The equations are the same as above except that the flux is linear. We have

$$Q_1^e = \oint_{\Gamma_e} q_n(s)\psi_1(s)\,ds = \int_0^{h_{12}} \left(q_0 \frac{s}{h_{12}}\right)(\psi_1)_{1-2}\,ds + \int_0^{h_{31}} (0)(\psi_1)_{3-1}\,ds = Q_{11}^e = \frac{1}{6}q_0 h_{12}$$

$$Q_2^e = \oint_{\Gamma_e} q_n(s)\psi_2(s)\,ds = \int_0^{h_{12}} \left(q_0 \frac{s}{h_{12}}\right)(\psi_2)_{1-2}\,ds + \int_0^{h_{23}} (0)(\psi_2)_{2-3}\,ds = Q_{21}^e = \frac{1}{3}q_0 h_{12}$$

Case 3. $q(s) = q_0 =$ constant, quadratic triangular element. In this case, quadratic interpolation functions must be used. We have ($Q_4^e = Q_5^e = Q_6^e = 0$)

$$Q_1^e = \oint_{\Gamma_e} q_n(s)\psi_1(s)\,ds = \int_0^{h_{13}} q_0(\psi_1)_{1-2-3}\,ds = Q_{11}^e = \frac{1}{6}q_0 h_{13}$$

$$Q_2^e = \oint_{\Gamma_e} q_n(s)\psi_2(s)\,ds = \int_0^{h_{13}} q_0(\psi_2)_{1-2-3}\,ds = Q_{21}^e = \frac{4}{6}q_0 h_{13}$$

$$Q_3^e = \oint_{\Gamma_e} q_n(s)\psi_3(s)\,ds = \int_0^{h_{13}} q_0(\psi_3)_{1-2-3}\,ds = Q_{31}^e = \frac{1}{6}q_0 h_{13}$$

where

$$(\psi_1)_{1-2-3} = \left(1 - \frac{s}{h_{13}}\right)\left(1 - \frac{2s}{h_{13}}\right), \quad (\psi_2)_{1-2-3} = 4\frac{s}{h_{13}}\left(1 - \frac{s}{h_{13}}\right)$$

$$(\psi_3)_{1-2-3} = -\frac{s}{h_{13}}\left(1 - \frac{2s}{h_{13}}\right)$$

Case 4. Two sides have nonzero $q(s)$, as shown in Fig. 8.2.16, on a linear element. In this case, all three nodes will have nonzero contributions. We have

$$Q_1^e = \oint_{\Gamma_e} q_n(s)\psi_1(s)\,ds = \int_0^{h_{12}} q_0(\psi_1)_{1-2}\,ds + \int_0^{h_{31}} \left(q_0 \frac{s}{h_{31}}\right)(\psi_1)_{3-1}\,ds$$

$$= Q_{11}^e + Q_{13}^e = q_0\left(\frac{h_{12}}{2} + \frac{h_{31}}{3}\right)$$

$$Q_2^e = \oint_{\Gamma_e} q_n(s)\psi_2(s)\,ds = \int_0^{h_{12}} q_0(\psi_2)_{1-2}\,ds + \int_0^{h_{31}} \left(q_0 \frac{s}{h_{31}}\right)(0)\,ds = Q_{21}^e = \frac{1}{2}q_0 h_{12}$$

$$Q_3^e = \oint_{\Gamma_e} q_n(s)\psi_3(s)\,ds = \int_0^{h_{12}} q_0(0)\,ds + \int_0^{h_{31}} \left(q_0 \frac{s}{h_{31}}\right)(\psi_3)_{3-1}\,ds = Q_{33}^e = \frac{1}{6}q_0 h_{31}$$

8.2.7 Assembly of Element Equations

The assembly of finite element equations is based on the same two principles that were used in one-dimensional problems:

1. Continuity of primary variables
2. "Equilibrium" (or "balance") of secondary variables

We illustrate the procedure by considering a finite element mesh consisting of a triangular element and a quadrilateral element [see Fig. 8.2.17(*a*)]. Let K_{ij}^1 $(i, j = 1, 2, 3)$ denote the coefficient matrix corresponding to the triangular element, and let K_{ij}^2 $(i, j = 1, \ldots, 4)$ denote the coefficient matrix corresponding to the quadrilateral element. From the finite element mesh shown in Fig. 8.2.17(*a*), we note the following correspondence (i.e., connectivity relations) between the global and element nodes:

$$[B] = \begin{bmatrix} 1 & 2 & 3 & \times \\ 2 & 4 & 5 & 3 \end{bmatrix} \tag{8.2.59}$$

where $\times$ indicates that there is no entry. The correspondence between the local and global nodal values is [see Fig. 8.2.17(*a*)]

$$u_1^1 = U_1, \quad u_2^1 = u_1^2 = U_2, \quad u_3^1 = u_4^2 = U_3, \quad u_2^2 = U_4, \quad u_3^2 = U_5 \tag{8.2.60}$$

which amounts to imposing the continuity of the primary variables at the nodes common to elements 1 and 2.

Note that the continuity of the primary variables at the interelement nodes guarantees the continuity of the primary variable along the entire interelement boundary. For the case in Fig. 8.2.17(*a*), the requirement $u_2^1 = u_1^2$ and $u_3^1 = u_4^2$ guarantees $u_h^1(s) = u_h^2(s)$ on the side connecting global nodes 2 and 3. This can be shown as follows. The solution $u_h^1(s)$ along the line connecting global nodes 2 and 3 is linear, and it is given by

$$u_h^1(s) = u_2^1\left(1 - \frac{s}{h}\right) + u_3^1 \frac{s}{h}$$

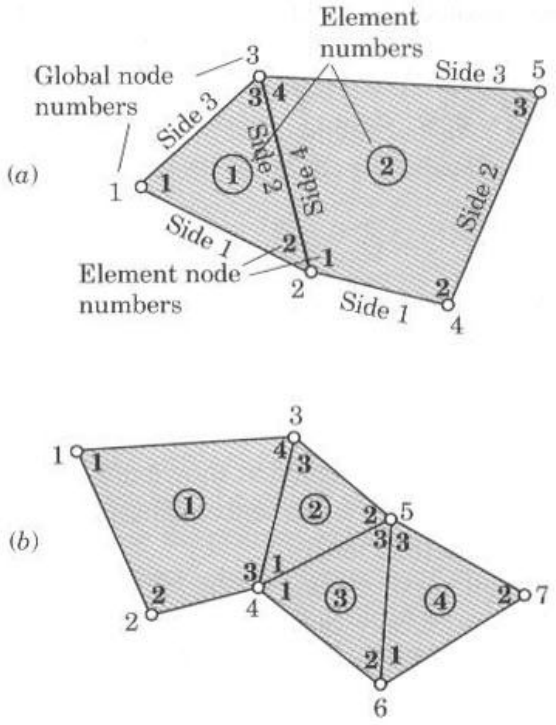

Global	⇒	Local (element)
K_{11}		K^1_{11}
K_{12}		K^1_{12}
K_{13}		K^1_{13}
K_{22}		$K^1_{22} + K^2_{11}$
K_{23}		$K^1_{23} + K^2_{14}$
K_{14}		0
K_{15}		0
K_{14}		K^1_{13}
K_{23}		K^1_{24}
K_{44}		$K^1_{33} + K^2_{11} + K^3_{11}$
K_{45}		$K^2_{12} + K^3_{13}$
K_{25}		0
K_{47}		0

Figure 8.2.17 Assembly of finite element coefficient matrices using the correspondence between global and element nodes (one unknown per node): (*a*) assembly of two elements; and (*b*) assembly of several elements. Single primary degree of freedom per node is assumed.

where s is the local coordinate with its origin at global node 2 and h is the length of the side 2–3 (or side 2). Similarly, the finite element solution along the same line but from element 2 is

$$u_h^2(s) = u_1^2\left(1 - \frac{s}{h}\right) + u_4^2\frac{s}{h}$$

Since $u_1^2 = u_2^1$ and $u_4^2 = u_3^1$, it follows that $u_h^1(s) = u_h^2(s)$ for every value of s along the interface of the two elements.

Next we use the balance of secondary variables. At the interface between the two elements, the flux from the two elements should be equal in magnitude and opposite in sign. For the two elements in Fig. 8.2.17(*a*), the interface is along the side connecting global nodes 2 and 3. Hence, the internal flux q_n^1 on side 2–3 of element 1 should balance the flux q_n^2 on side 4–1 of element 2 (recall the sign convention on q_n^e):

$$\left(q_n^1\right)_{2-3} = \left(q_n^2\right)_{4-1} \text{ or } \left(q_n^1\right)_{2-3} = \left(-q_n^2\right)_{1-4} \tag{8.2.61}$$

In the finite element method we impose the above relation in a weighted integral sense:

$$\int_{h_{23}^1} q_n^1 \psi_2^1 \, ds = -\int_{h_{14}^2} q_n^2 \psi_1^2 \, ds, \quad \int_{h_{23}^1} q_n^1 \psi_3^1 \, ds = -\int_{h_{14}^2} q_n^2 \psi_4^2 \, ds \tag{8.2.62a}$$

where h^e_{pq} denotes length of the side connecting node p to node q of element Ω_e. The above equations can be written in the form,

$$\int_{h^1_{23}} q^1_n \psi^1_2 \, ds + \int_{h^2_{14}} q^2_n \psi^2_1 \, ds = 0, \quad \int_{h^1_{23}} q^1_n \psi^1_3 \, ds + \int_{h^2_{14}} q^2_n \psi^2_4 \, ds = 0 \tag{8.2.62b}$$

or

$$Q^1_{22} + Q^2_{14} = 0, \quad Q^1_{32} + Q^2_{44} = 0 \tag{8.2.62c}$$

where Q^e_{iJ} denotes the part of Q^e_i that comes from side J of element e:

$$Q^e_{iJ} = \int_{\text{side } J} q^e_n \psi^e_i \, ds$$

The sides of triangular and quadrilateral elements are numbered as shown in Fig. 8.2.17(a). These balance relations must be imposed in assembling the element equations. We note that Q^e_{iJ} is only a portion of Q^e_i [see Eqs. (8.2.56) and (8.2.58b)].

The element equations of the two-element mesh shown in Fig. 8.2.17(a) are written first. For the model problem at hand, there is only one primary degree of freedom (NDF = 1) per node. For the triangular element, the element equations are of the form

$$\begin{aligned} K^1_{11}u^1_1 + K^1_{12}u^1_2 + K^1_{13}u^1_3 &= f^1_1 + Q^1_1 \\ K^1_{21}u^1_1 + K^1_{22}u^1_2 + K^1_{23}u^1_3 &= f^1_2 + Q^1_2 \\ K^1_{31}u^1_1 + K^1_{32}u^1_2 + K^1_{33}u^1_3 &= f^1_3 + Q^1_3 \end{aligned} \tag{8.2.63a}$$

For the quadrilateral element, the element equations are given by

$$\begin{aligned} K^2_{11}u^2_1 + K^2_{12}u^2_2 + K^2_{13}u^2_3 + K^2_{14}u^2_4 &= f^2_1 + Q^2_1 \\ K^2_{21}u^2_1 + K^2_{22}u^2_2 + K^2_{23}u^2_3 + K^2_{24}u^2_4 &= f^2_2 + Q^2_2 \\ K^2_{31}u^2_1 + K^2_{32}u^2_2 + K^2_{33}u^2_3 + K^2_{34}u^2_4 &= f^2_3 + Q^2_3 \\ K^2_{41}u^2_1 + K^2_{42}u^2_2 + K^2_{43}u^2_3 + K^2_{44}u^2_4 &= f^2_4 + Q^2_4 \end{aligned} \tag{8.2.63b}$$

In order to impose the balance of secondary variables in (8.2.62c), it is required that we add the second equation of element 1 to the first equation of element 2, and also add the third equation of element 1 to the fourth equation of element 2:

$$\begin{aligned} &\left(K^1_{21}u^1_1 + K^1_{22}u^1_2 + K^1_{23}u^1_3\right) + \left(K^2_{11}u^2_1 + K^2_{12}u^2_2 + K^2_{13}u^2_3 + K^2_{14}u^2_4\right) \\ &\quad = \left(f^1_2 + Q^1_2\right) + \left(f^2_1 + Q^2_1\right) \\ &\left(K^1_{31}u^1_1 + K^1_{32}u^1_2 + K^1_{33}u^1_3\right) + \left(K^2_{41}u^2_1 + K^2_{42}u^2_2 + K^2_{43}u^2_3 + K^2_{44}u^2_4\right) \\ &\quad = \left(f^1_3 + Q^1_3\right) + \left(f^2_4 + Q^2_4\right) \end{aligned}$$

Using the global-variable notation in (8.2.60), we can rewrite the above equations as [which amounts to imposing continuity of the primary variables in (8.2.60)]:

$$\begin{aligned} &K^1_{21}U_1 + \left(K^1_{22} + K^2_{11}\right)U_2 + \left(K^1_{23} + K^2_{14}\right)U_3 + K^2_{12}U_4 + K^2_{13}U_5 \\ &\quad = f^1_2 + f^2_1 + \left(Q^1_2 + Q^2_1\right) \end{aligned}$$

$$K_{31}^1 U_1 + \left(K_{32}^1 + K_{41}^2\right) U_2 + \left(K_{33}^1 + K_{44}^2\right) U_3 + K_{42}^2 U_4 + K_{43}^2 U_5$$
$$= f_3^1 + f_4^2 + \left(Q_3^1 + Q_4^2\right)$$

Now we can impose the conditions in (8.2.62*c*) by setting appropriate portions of the expressions in parenthesis on the right-hand side of the above equations to zero:

$$Q_2^1 + Q_1^2 = \left(Q_{21}^1 + Q_{22}^1 + Q_{23}^1\right) + \left(Q_{11}^2 + Q_{12}^2 + Q_{13}^2 + Q_{14}^2\right)$$
$$= Q_{21}^1 + Q_{23}^1 + \underline{\left(Q_{22}^1 + Q_{14}^2\right)} + Q_{11}^2 + Q_{12}^2 + Q_{13}^2$$
$$Q_3^1 + Q_4^2 = \left(Q_{31}^1 + Q_{32}^1 + Q_{33}^1\right) + \left(Q_{41}^2 + Q_{42}^2 + Q_{43}^2 + Q_{44}^2\right)$$
$$= Q_{31}^1 + Q_{33}^1 + \underline{\left(Q_{32}^1 + Q_{44}^2\right)} + Q_{41}^2 + Q_{42}^2 + Q_{43}^2$$

The underlined terms are zero by the balance requirement (8.2.62*c*). The remaining terms of each equation will be either known because q_n is known on the boundary or remain unknown because the primary variable is specified on the boundary.

In general, when several elements are connected, the assembly of the elements is carried out by putting element coefficients K_{ij}^e, f_i^e, and Q_i^e into proper locations of the global coefficient matrix and right-hand column vectors. This is done by means of the connectivity relations, i.e., correspondence of the local node number to the global node number. For example, if global node number 3 corresponds to node 3 of element 1 and node 4 of element 2, then we have

$$F_3 = F_3^1 + F_4^2 \equiv f_3^1 + f_4^2 + Q_3^1 + Q_4^2, \quad K_{33} = K_{33}^1 + K_{44}^2$$

If global node numbers 2 and 3 correspond, respectively, to nodes 2 and 3 of element 1 and nodes 1 and 4 of element 2, then global coefficients K_{22}, K_{23}, and K_{33} are given by

$$K_{22} = K_{22}^1 + K_{11}^2, \quad K_{23} = K_{23}^1 + K_{14}^2, \quad K_{33} = K_{33}^1 + K_{44}^2$$

Similarly, the source components of global nodes 2 and 3 are added:

$$F_2 = F_2^1 + F_1^2, \quad F_3 = F_3^1 + F_4^2$$

For the two-element mesh shown in Fig. 8.2.17(*a*), the assembled equations are given by

$$\begin{bmatrix} K_{11}^1 & K_{12}^1 & K_{13}^1 & 0 & 0 \\ K_{21}^1 & K_{22}^1 + K_{11}^2 & K_{23}^1 + K_{14}^2 & K_{12}^2 & K_{13}^2 \\ K_{31}^1 & K_{32}^1 + K_{41}^2 & K_{33}^1 + K_{44}^2 & K_{42}^2 & K_{43}^2 \\ 0 & K_{21}^2 & K_{24}^2 & K_{22}^2 & K_{23}^2 \\ 0 & K_{31}^2 & K_{34}^2 & K_{32}^2 & K_{33}^2 \end{bmatrix} \begin{Bmatrix} U_1 \\ U_2 \\ U_3 \\ U_4 \\ U_5 \end{Bmatrix} = \begin{Bmatrix} F_1^1 \\ F_2^1 + F_1^2 \\ F_3^1 + F_4^2 \\ F_2^2 \\ F_3^2 \end{Bmatrix} \tag{8.2.64}$$

The assembly procedure described above can be used to assemble elements of any shape and type. The procedure can be implemented in a computer, as described for one-dimensional problems, with the help of the array $[B]$ (program variable is NOD). For hand calculations, the readers are required to use the procedure described above. For example, consider the finite element mesh shown in Fig. 8.2.17(*b*). The location (4,4) of the global coefficient matrix contains $K_{33}^1 + K_{11}^2 + K_{11}^3$. The location 4 in the assembled column vector contains $F_3^1 + F_1^2 + F_1^3$. Locations (1,5), (1,6), (1,7), (2,5), (2,6), (2,7), (3,6), (3,7), and (4,7) of the

global matrix contain zeros because $K_{IJ} = 0$ when global nodes I and J do not correspond to nodes of the same element in the mesh.

This completes the first five steps in the finite element modeling of the model equation (8.2.1). The next two steps of the analysis, namely, the imposition of boundary conditions and solution of equations will remain the same as for one-dimensional problems. The postprocessing of the solution for two-dimensional problems is discussed next.

8.2.8 Postcomputations

The finite element solution at any point (x, y) in an element Ω_e is given by

$$u_h^e(x, y) = \sum_{j=1}^{n} u_j^e \psi_j^e(x, y) \tag{8.2.65}$$

and its derivatives are computed from (8.2.65) as

$$\frac{\partial u_h^e}{\partial x} = \sum_{j=1}^{n} u_j^e \frac{\partial \psi_j^e}{\partial x}, \quad \frac{\partial u_h^e}{\partial y} = \sum_{j=1}^{n} u_j^e \frac{\partial \psi_j^e}{\partial y} \tag{8.2.66}$$

Equations (8.2.65) and (8.2.66) can be used to compute the solution and its derivatives at any point (x, y) in the element. It is useful to generate, by the interpolation of (8.2.65), information needed to plot contours of u_h^e and its gradient.

The derivatives of u_h^e will not be continuous at interelement boundaries because continuity of the derivatives is not imposed during the assembly procedure. The weak form of the equations suggests that the primary variable is u, which is to be carried as the nodal variable. If additional variables, such as higher-order derivatives of the dependent unknown, are carried as nodal variables in the interest of making them continuous across interelement boundaries, the degree of interpolation (or order of the element) increases. In addition, the continuity of higher-order derivatives that are not identified as the primary variables may violate the physical principles of the problem. For example, making $\partial u/\partial x$ continuous will violate the requirement that q_x $(= a_{11}\, \partial u/\partial x)$ be continuous at the interface of two dissimilar materials because a_{11} is different for the two materials at the interface.

For the linear triangular element, the derivatives are constants within each element:

$$\begin{gathered} \psi_j^e = \frac{1}{2A_e}(\alpha_j + \beta_j x + \gamma_j y), \quad \frac{\partial \psi_j^e}{\partial x} = \frac{1}{2A_e}\beta_j, \quad \frac{\partial \psi_j^e}{\partial y} = \frac{1}{2A_e}\gamma_j \\ \frac{\partial u_h^e}{\partial x} = \sum_{j=1}^{n} \frac{u_j^e \beta_j}{2A_e}, \qquad \frac{\partial u_h^e}{\partial y} = \sum_{j=1}^{n} \frac{u_j^e \gamma_j}{2A_e} \end{gathered} \tag{8.2.67}$$

For linear rectangular elements, $\partial U^e/\partial \bar{x}$ is linear in $\bar{y}$ and $\partial u_h^e/\partial \bar{y}$ is linear in $\bar{x}$ [see (8.2.32*b*)]:

$$\begin{gathered} \frac{\partial \psi_j^e}{\partial \bar{x}} = -\frac{1}{a}\left(1 - \frac{\bar{y} + \bar{y}_j}{b}\right), \quad \frac{\partial \psi_j^e}{\partial \bar{y}} = -\frac{1}{b}\left(1 - \frac{\bar{x} + \bar{x}_j}{a}\right) \\ \frac{\partial u_h^e}{\partial \bar{x}} = \frac{1}{a}\sum_{j=1}^{n}(-1)^{j+2} u_j^e \left(1 - \frac{\bar{y} + \bar{y}_j}{b}\right), \quad \frac{\partial u_h^e}{\partial \bar{y}} = \frac{1}{b}\sum_{j=1}^{n}(-1)^{j+2} u_j^e \left(1 - \frac{\bar{x} + \bar{x}_j}{a}\right) \end{gathered} \tag{8.2.68}$$

where $\bar{x}$ and $\bar{y}$ are the local coordinates [see Fig. 8.2.8(*a*)]. Although $\partial u_h^e/\partial \bar{x}$ and $\partial u_h^e/\partial \bar{y}$ are linear functions of y and x, respectively, in each element, they are discontinuous at interelement boundaries. Consequently, quantities computed using derivatives of the finite element solution u_h^e are discontinuous at interelement boundaries. For example, if we compute $q_x^e = a_{11}^e \partial u_h^e/\partial x$ at a node shared by three different elements, three different values of q_x^e are expected. The difference between the three values will diminish as the mesh is refined. Some commercial finite element software give a single value of q_x at the node by averaging the values obtained from various elements connected at the node.

8.2.9 Axisymmetric Problems

In studying problems involving cylindrical geometries, it is convenient to use the cylindrical coordinate system (r, θ, z) to formulate the problem. If the geometry, boundary conditions, and loading (or source) of the problem are independent of the angular coordinate θ, the problem solution will also be independent of θ. Consequently, a three-dimensional problem is reduced to a two-dimensional one in (r, z) coordinates (see Fig. 3.4.1). Here we consider a model axisymmetric problem, develop its weak form, and formulate the finite element model.

Model Equation

Consider the partial differential equation,

$$-\frac{1}{r}\frac{\partial}{\partial r}\left(r\hat{a}_{11}\frac{\partial u}{\partial r}\right) - \frac{\partial}{\partial z}\left(\hat{a}_{22}\frac{\partial u}{\partial z}\right) + \hat{a}_{00}u = \hat{f}(r, z) \tag{8.2.69}$$

where $\hat{a}_{00}$, $\hat{a}_{11}$, $\hat{a}_{22}$, and $\hat{f}$ are given functions of r and z. The equation arises in the study of heat transfer in cylindrical geometries, as well as in other fields of engineering and applied science. Our objective is to develop the finite element model of the equation based on the weak formulation of (8.2.69).

Weak Form

Following the three-step procedure, we write the weak form of (8.2.69):

$$\text{(i)}\quad 0 = \int_{\Omega_e} w\left[-\frac{1}{r}\frac{\partial}{\partial r}\left(r\hat{a}_{11}\frac{\partial u}{\partial r}\right) - \frac{\partial}{\partial z}\left(\hat{a}_{22}\frac{\partial u}{\partial z}\right) + \hat{a}_{00}u - \hat{f}\right] r\,dr\,dz$$

$$\text{(ii)}\quad 0 = \int_{\Omega_e}\left(\frac{\partial w}{\partial r}\hat{a}_{11}\frac{\partial u}{\partial r} + \frac{\partial w}{\partial z}\hat{a}_{22}\frac{\partial u}{\partial z} + w\hat{a}_{00}u - w\hat{f}\right) r\,dr\,dz - \oint_{\Gamma_e} w\left(\hat{a}_{11}\frac{\partial u}{\partial r}n_r + \hat{a}_{22}\frac{\partial u}{\partial z}n_z\right) ds$$

$$\text{(iii)}\quad 0 = \int_{\Omega_e}\left(\hat{a}_{11}\frac{\partial w}{\partial r}\frac{\partial u}{\partial r} + \hat{a}_{22}\frac{\partial w}{\partial z}\frac{\partial u}{\partial z} + \hat{a}_{00}wu - w\hat{f}\right) r\,dr\,dz - \oint_{\Gamma_e} wq_n\,ds \tag{8.2.70}$$

where w is the weight function and q_n is the normal flux

$$q_n = \left(\hat{a}_{11} \frac{\partial u}{\partial r} n_r + \hat{a}_{22} \frac{\partial u}{\partial z} n_z \right) \tag{8.2.71}$$

Note that the weak form (8.2.70) does not differ significantly from that developed for model (8.2.1) when $a_{12} = a_{21} = 0$. The only difference is the presence of r in the integrand. Consequently, (8.2.70) can be obtained as a special case of (8.2.10) for $a_{00} = \hat{a}_{00} x$, $a_{11} = \hat{a}_{11} x$, $a_{22} = \hat{a}_{22} x$, and $f = \hat{f} x$; the coordinates r and z are treated like x and y, respectively.

Finite Element Model

Let us assume that $u(r, z)$ is approximated by the finite element interpolation u_h^e over the element Ω_e

$$u \approx u_h^e(r, z) = \sum_{j=1}^{n} u_j^e \psi_j^e(r, z) \tag{8.2.72}$$

The interpolation functions $\psi_j^e(r, z)$ are the same as those developed in (8.2.25a) and (8.2.32a) for linear triangular and rectangular elements, with $x = r$ and $y = z$. Substitution of (8.2.72) for u and ψ_i^e for w into the weak form gives the ith equation of the finite element model

$$\begin{aligned} 0 = \sum_{j=1}^{n} \left[\int_{\Omega_e} \left(\hat{a}_{11} \frac{\partial \psi_i^e}{\partial r} \frac{\partial \psi_j^e}{\partial r} + \hat{a}_{22} \frac{\partial \psi_i^e}{\partial z} \frac{\partial \psi_j^e}{\partial z} + \hat{a}_{00} \psi_i^e \psi_j^e \right) r \, dr \, dz \right] u_j^e \\ - \int_{\Omega_e} \psi_i^e \hat{f} \, r \, dr \, dz - \oint_{\Gamma_e} \psi_i^e q_n \, ds \end{aligned} \tag{8.2.73}$$

or

$$0 = \sum_{j=1}^{n} K_{ij}^e u_j^e - f_i^e - Q_i^e \tag{8.2.74a}$$

where

$$\begin{aligned} K_{ij}^e &= \int_{\Omega_e} \left(\hat{a}_{11} \frac{\partial \psi_i^e}{\partial r} \frac{\partial \psi_j^e}{\partial r} + \hat{a}_{22} \frac{\partial \psi_i^e}{\partial z} \frac{\partial \psi_j^e}{\partial z} + a_{00} \psi_i^e \psi_j^e \right) r \, dr \, dz \\ f_i^e &= \int_{\Omega_e} \psi_i^e \hat{f} \, r \, dr \, dz, \quad Q_i^e = \oint_{\Gamma_e} \psi_i^e q_n \, ds \end{aligned} \tag{8.2.74b}$$

The evaluation of the integrals in K_{ij}^e and f_i^e for polynomial forms of $\hat{a}_{ij}$ and $\hat{f}$ is possible. However, we evaluate them numerically using the numerical integration methods discussed in Chapter 7 for one-dimensional cases (see Section 7.1.5) and reviewed in Chapter 9 for two-dimensional problems. This completes the development of finite element model of an axisymmetric problem.

8.3 A NUMERICAL EXAMPLE

The model equation in (8.2.1) arises in many fields of engineering and applied sciences, and some examples are given in Table 8.1.1. The application of the finite element model developed in Sections 8.2.2–8.2.8 to problems governed by the Poisson equations is discussed here. This example is designed to illustrate selection of the computational domain, choice of elements and mesh, assembly of element equations, imposition of boundary conditions,

and postprocessing. The physical background of the problem is not discussed here but Table 8.1.1 provides the background.

Example 8.3.1

Consider a problem described by the Poisson equation

$$-\nabla^2 u = f_0 \quad \text{or} \quad -\left(\frac{\partial^2 u}{\partial x^2} + \frac{\partial^2 u}{\partial y^2}\right) = f_0 \quad \text{in } \Omega \tag{8.3.1}$$

in a square region [see Fig. 8.3.1(*a*)]

$$\Omega = \{(x, y) : -A < x < A,\ -A < y < A\}$$

where $u(x, y)$ is the dependent unknown and f_0 is the uniformly distributed source. We shall consider the following boundary conditions for the problem:

$$u = 0 \text{ on the entire boundary } \Gamma \tag{8.3.2}$$

We wish to use the finite element method to determine $u(x, y)$ everywhere in Ω.

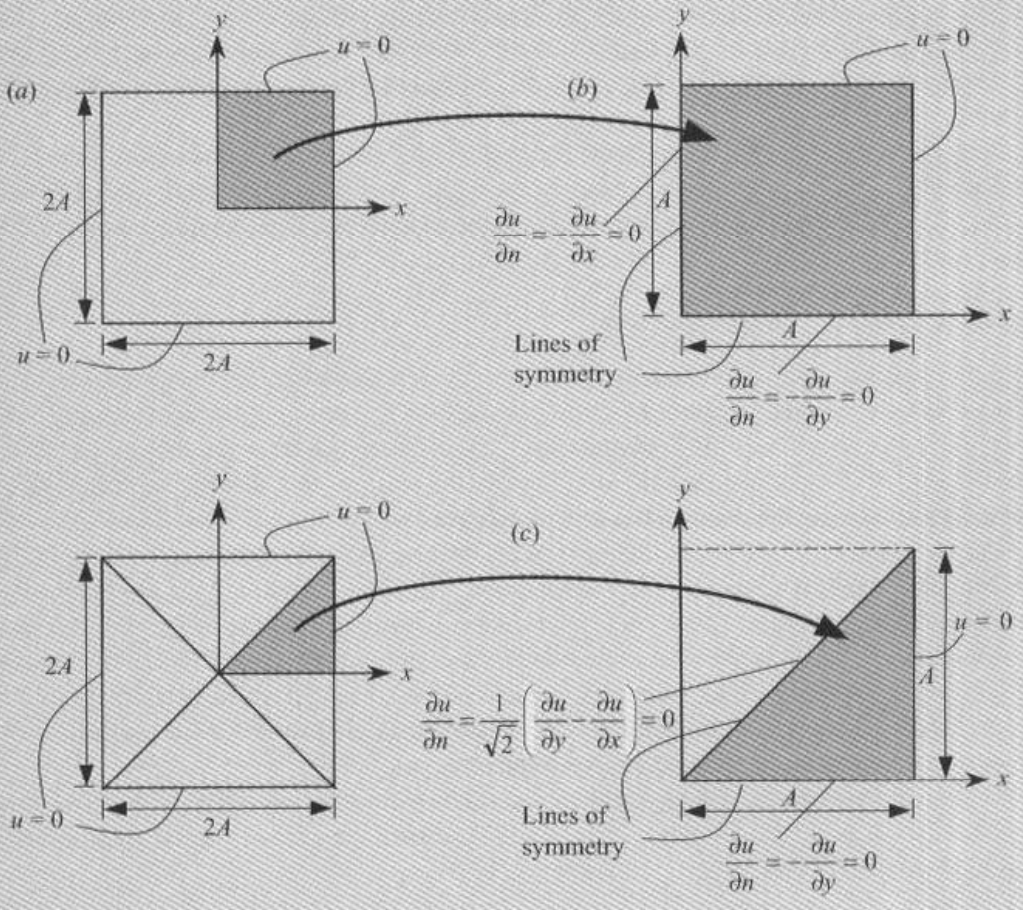

Figure 8.3.1 Finite element analysis of the Poisson equation in a square region: (*a*) Geometry of the actual domain with boundary conditions. (*b*) Computational domain based on biaxial symmetry. (*c*) Computational domain based on biaxial as well as diagonal symmetry.

Selection of the Computational Domain

When the given domain Ω exhibits solution symmetries, it is sufficient to solve the problem on a portion of Ω that provides the solution on the entire domain. A problem possesses symmetry of the solution about a line only when symmetry of the (*a*) geometry, (*b*) material properties, (*c*) source variation, and (*d*) boundary conditions exist about the line. Whenever a portion of the domain is modeled to exploit symmetries available in the problem, the lines of symmetries become a portion of the boundary of the computational domain. On lines of symmetry, the normal derivative of the solution (i.e., derivative of the solution with respect to the coordinate normal to the line of symmetry) is zero:

$$q_n = \frac{\partial u}{\partial n} = \frac{\partial u}{\partial x} n_x + \frac{\partial u}{\partial y} n_y = 0 \tag{8.3.2}$$

The problem at hand has the geometric symmetry about the $x = 0$ and $y = 0$ axes; since the coefficients describing the material behavior, a_{ij}, are either zero or unity, material symmetry about the $x = 0$ and $y = 0$ axes is automatically met. The symmetry of source variation is dictated by f. Since it is uniform, i.e., $f = f_0$, constant, the data is symmetric with respect to the $x = 0$ and $y = 0$ axes. Lastly, the boundary conditions are symmetric with respect to the $x = 0$ and $y = 0$ axes. Thus, the solution is symmetric about the $x = 0$ and $y = 0$ axes, and hence, a quadrant of the domain can be used as the computational domain [see Fig. 8.3.1(*b*)]. The solution is also symmetric about the diagonal lines, and an octant can be used as the computational domain [see Fig. 8.3.1(*c*)]. In the latter case, a mesh of only rectangular elements cannot be used.

While it is possible to mix triangular and rectangular elements to represent the computational domain as well as the solution, in much of this book we shall use only one type of element at a time. Two different finite element meshes for the triangular and rectangular computational domains are shown in Figs. 8.3.2 and 8.3.3, respectively.

Solution by Linear Triangular Elements

Due to the symmetry along the diagonal $x = y$, we model the triangular domain shown in Fig. 8.3.1(*c*). As a first choice we use a uniform mesh of four linear triangular elements, as shown in Fig. 8.3.2(*a*), to represent the domain (mesh T1), and then use the refined mesh (mesh T2) shown in Fig. 8.3.2(*b*) to compare the solutions. In the present case, there is no discretization error involved because the geometry is exactly represented.

The elements 1, 3, and 4 are identical in orientation as well as geometry. Element 2 is geometrically identical to element 1, except that it is oriented differently. If we number the local nodes of element 2 to match those of element 1, then all four elements have the same element matrices, and it is necessary to compute them only for element 1. When the element matrices are computed on a computer, such considerations are not taken into account. In solving the problem by hand, we use the similarity between a master element (element 1) and the other elements in the mesh to avoid unnecessary computations.

We consider element 1 as the typical element. The element is exactly the same as the one shown in Fig. 8.2.11(*b*). Hence, the element coefficient matrix and source vector are (the reader should independently verify this)

$$[K^1] = \frac{1}{2ab} \begin{bmatrix} b^2 & -b^2 & 0 \\ -b^2 & a^2+b^2 & -a^2 \\ 0 & -a^2 & a^2 \end{bmatrix}, \quad \{f^1\} = \frac{f_0 ab}{6} \begin{Bmatrix} 1 \\ 1 \\ 1 \end{Bmatrix} \tag{8.3.4}$$

where in the present case $a = b = A/2 = 0.5$.

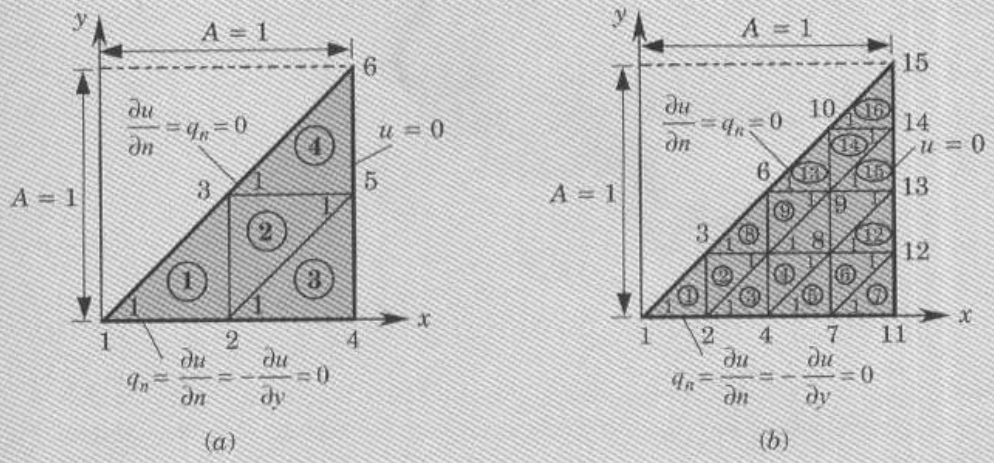

Figure 8.3.2 (*a*) Mesh T1 of triangular elements. (*b*) Mesh T2 of triangular elements.

The element matrix in (8.3.4) is valid for the Laplace operator $-\nabla^2$ on any right-angle triangle with sides a and b in which the right angle is at node 2, and the diagonal line of the triangle connects node 3 to node 1. Note that the off-diagonal coefficient associated with the nodes on the diagonal line is zero for a right-angled triangle.

In summary, for the mesh shown in Fig. 8.3.2(*a*), we have

$$[K^1]=[K^2]=[K^3]=[K^4], \quad \{f^1\}=\{f^2\}=\{f^3\}=\{f^4\}$$

with

$$[K^e]=\frac{1}{2}\begin{bmatrix} 1 & -1 & 0 \\ -1 & 2 & -1 \\ 0 & -1 & 1 \end{bmatrix}, \quad \{f^e\}=\frac{f_0}{24}\begin{Bmatrix} 1 \\ 1 \\ 1 \end{Bmatrix} \tag{8.3.5}$$

The assembled coefficient matrix for the finite element mesh is 6×6, because there are six global nodes with one unknown per node. The assembled matrix can be obtained directly by using the correspondence between the global nodes and the local nodes, expressed through the connectivity matrix,

$$[B]=\begin{bmatrix} 1 & 2 & 3 \\ 5 & 3 & 2 \\ 2 & 4 & 5 \\ 3 & 5 & 6 \end{bmatrix} \tag{8.3.6}$$

A few representative global coefficients are given below in terms of the element coefficients.

$$K_{11}=K_{11}^1=\frac{1}{2}, \quad K_{12}=K_{12}^1=-\frac{1}{2}, \quad K_{22}=K_{22}^1+K_{33}^2+K_{11}^3=\frac{2}{2}+\frac{1}{2}+\frac{1}{2}$$

$$K_{13}=K_{13}^1=0, \quad K_{14}=0, \quad K_{15}=0, \quad K_{16}=0, \quad K_{23}=K_{23}^1+K_{32}^2=-\frac{1}{2}-\frac{1}{2}$$

$$K_{33}=K_{33}^1+K_{22}^2+K_{11}^4=\frac{1}{2}+\frac{2}{2}+\frac{1}{2}, \quad F_1=F_1^1=Q_1^1+f_1^1 \tag{8.3.7}$$

$$F_2=(Q_2^1+Q_3^2+Q_1^3)+(f_2^1+f_3^2+f_1^3), \quad F_3=(Q_3^1+Q_2^2+Q_1^4)+(f_3^1+f_2^2+f_1^4)$$

$$F_4=F_2^3=Q_2^3+f_2^3, \quad F_5=(Q_1^2+Q_3^3+Q_2^4)+(f_1^2+f_3^3+f_2^4), \quad F_6=F_3^4=Q_3^4+f_3^4$$

The assembled system of equations associated with mesh T1 are

$$\frac{1}{2}\begin{bmatrix} 1 & -1 & 0 & 0 & 0 & 0 \\ -1 & 4 & -2 & -1 & 0 & 0 \\ 0 & -2 & 4 & 0 & -2 & 0 \\ 0 & -1 & 0 & 2 & -1 & 0 \\ 0 & 0 & -2 & -1 & 4 & -1 \\ 0 & 0 & 0 & 0 & -1 & 1 \end{bmatrix} \begin{Bmatrix} U_1 \\ U_2 \\ U_3 \\ U_4 \\ U_5 \\ U_6 \end{Bmatrix} = \frac{f_0}{24} \begin{Bmatrix} 1 \\ 3 \\ 3 \\ 1 \\ 3 \\ 1 \end{Bmatrix} + \begin{Bmatrix} Q_1^1 \\ Q_2^1 + Q_3^2 + Q_1^3 \\ Q_3^1 + Q_2^2 + Q_1^4 \\ Q_2^3 \\ Q_1^2 + Q_3^3 + Q_2^4 \\ Q_3^4 \end{Bmatrix} \tag{8.3.8}$$

Note that at nodes 4 and 6, both u and q_n are specified (a type of singularity in the specified data). However, we shall give priority to the primary variable over the secondary variable. Thus, we assume that

$$U_4 = U_5 = U_6 = 0 \tag{8.3.9}$$

and Q_4, Q_5, and Q_6, assumed to be unknown, are determined in the postcomputation. The specified secondary degrees of freedom are (all due to symmetry)

$$Q_1 = Q_1^1 = 0, \quad Q_2 = Q_2^1 + Q_3^2 + Q_1^3 = 0, \quad Q_3 = Q_3^1 + Q_2^2 + Q_1^4 = 0 \tag{8.3.10}$$

For example, consider the sum

$$\begin{aligned} Q_2^1 + Q_3^2 + Q_1^3 &= (Q_{21}^1 + Q_{22}^1) + (Q_{32}^2 + Q_{33}^2) + (Q_{11}^3 + Q_{13}^3) \\ &= Q_{21}^1 + (Q_{22}^1 + Q_{32}^2) + (Q_{33}^2 + Q_{13}^3) + Q_{11}^3 = 0 + 0 + 0 + 0 \end{aligned}$$

where Q_{21}^1 and Q_{11}^3 are zero because of $q_n = 0$ and $Q_{22}^1 + Q_{32}^2$ and $Q_{33}^2 + Q_{13}^3$ are zero because of the balance of fluxes between neighboring elements.

Since the only unknown primary variables for mesh T1 are U_1, U_2, and U_3, the condensed equations for the primary unknowns can be obtained by deleting rows and columns 4, 5, and 6 from the system (8.3.8). In retrospect, it would have been sufficient to write the finite element equations associated with the global nodes 1, 2, and 3:

$$\begin{aligned} K_{11}U_1 + K_{12}U_2 + K_{13}U_3 &= F_1 \\ K_{21}U_1 + K_{22}U_2 + K_{23}U_3 + K_{24}U_4 + K_{25}U_5 &= F_2 \\ K_{31}U_1 + K_{32}U_2 + K_{33}U_3 + K_{35}U_5 + K_{36}U_6 &= F_3 \end{aligned}$$

Noting that $U_4 = U_5 = U_6 = 0$, we can write the above equations in terms of the element coefficients:

$$\begin{bmatrix} K_{11}^1 & K_{12}^1 & K_{13}^1 \\ K_{21}^1 & K_{22}^1 + K_{33}^2 + K_{11}^3 & K_{23}^1 + K_{32}^2 \\ K_{31}^1 & K_{32}^1 + K_{23}^2 & K_{33}^1 + K_{22}^2 + K_{11}^4 \end{bmatrix} \begin{Bmatrix} U_1 \\ U_2 \\ U_3 \end{Bmatrix} = \begin{Bmatrix} f_1^1 \\ f_2^1 + f_3^2 + f_1^3 \\ f_3^1 + f_2^2 + f_1^4 \end{Bmatrix} \tag{8.3.11}$$

The unknown secondary variables Q_4, Q_5, and Q_6 can be computed from the element equations

$$\begin{Bmatrix} Q_4 \\ Q_5 \\ Q_6 \end{Bmatrix} = -\begin{Bmatrix} f_2^3 \\ f_1^2 + f_3^3 + f_2^4 \\ f_3^4 \end{Bmatrix} + \begin{bmatrix} 0 & K_{21}^3 & 0 \\ 0 & K_{13}^2 + K_{31}^3 & K_{12}^2 + K_{21}^4 \\ 0 & 0 & K_{31}^4 \end{bmatrix} \begin{Bmatrix} U_1 \\ U_2 \\ U_3 \end{Bmatrix} \tag{8.3.12}$$

For example, we have

$$\begin{aligned} Q_4 = Q_2^3 &= Q_{21}^3 + Q_{22}^3 + Q_{23}^3 \\ &= \int_{1-2} q_n^3 \psi_2^3 \, dx + \int_{2-3} q_n^3 \psi_2^3 \, dy + \int_{3-1} q_n^3 \psi_2^3 \, ds \end{aligned} \tag{8.3.13a}$$

where

$$\begin{aligned} (q_n^3)_{1-2} &= \left(\frac{\partial u}{\partial x} n_x + \frac{\partial u}{\partial y} n_y \right)_{1-2} = 0 \quad \left(n_x = 0, \quad \frac{\partial u}{\partial y} = 0 \right) \\ (q_n^3)_{2-3} &= \left(\frac{\partial u}{\partial x} n_x + \frac{\partial u}{\partial y} n_y \right)_{2-3} = \frac{\partial u}{\partial x} \quad (n_x = 1, \quad n_y = 0) \\ (\psi_2^3)_{2-3} &= 1 - \frac{y}{h_{23}}, \quad (\psi_2^3)_{3-1} = 0 \end{aligned} \tag{8.3.13b}$$

Thus, we have

$$Q_4 = Q_{22}^3 = \int_0^{h_{23}} \frac{\partial u}{\partial x} \left(1 - \frac{y}{h_{23}} \right) dy$$

where $\partial u / \partial x$ is calculated using $\partial u_h / \partial x$ from the finite element interpolation

$$\frac{\partial u_h}{\partial x} = \sum_{j=1}^{3} u_j^3 \frac{\beta_j^3}{2A_3}$$

We obtain ($h_{23} = a = 0.5$, $\beta_1^3 = -a = -0.5$, $2A_3 = a^2 = 0.25$, $U_4 = U_5 = 0$),

$$Q_4 = \frac{h_{23}}{4A_3} \sum_{j=1}^{3} u_j^3 \beta_j^3 = \frac{h_{23}}{4A_3} (\beta_1^3 U_2 + \beta_2^3 U_4 + \beta_3^3 U_5) = -0.5 U_2 \tag{8.3.14}$$

Using the numerical values of the coefficients K_{ij}^e and f_i^e, (with $f_0 = 1$), we write the condensed equations for U_1, U_2, and U_3 as

$$\begin{bmatrix} 0.5 & -0.5 & 0.0 \\ -0.5 & 2.0 & -1.0 \\ 0.0 & -1.0 & 2.0 \end{bmatrix} \begin{Bmatrix} U_1 \\ U_2 \\ U_3 \end{Bmatrix} = \frac{1}{24} \begin{Bmatrix} 1 \\ 3 \\ 3 \end{Bmatrix} \tag{8.3.15}$$

Solving (8.3.15) for U_i ($i = 1, 2, 3$), we obtain

$$\begin{Bmatrix} U_1 \\ U_2 \\ U_3 \end{Bmatrix} = \frac{1}{24} \begin{bmatrix} 3 & 1 & 0.5 \\ 1 & 1 & 0.5 \\ 0.5 & 0.5 & 0.75 \end{bmatrix} \begin{Bmatrix} 1 \\ 3 \\ 3 \end{Bmatrix} = \frac{1}{24} \begin{Bmatrix} 7.5 \\ 5.5 \\ 4.25 \end{Bmatrix} = \begin{Bmatrix} 0.31250 \\ 0.22917 \\ 0.17708 \end{Bmatrix} \tag{8.3.16}$$

and, from (8.3.12), we have

$$\begin{Bmatrix} Q_{22}^3 \\ Q_{32}^3 + Q_{22}^4 \\ Q_{32}^4 \end{Bmatrix} = -\frac{1}{24}\begin{Bmatrix} 1 \\ 3 \\ 1 \end{Bmatrix} + \begin{bmatrix} 0 & -0.5 & 0 \\ 0 & 0 & -1 \\ 0 & 0 & 0 \end{bmatrix}\begin{Bmatrix} U_1 \\ U_2 \\ U_3 \end{Bmatrix} = \begin{Bmatrix} -0.197917 \\ -0.302083 \\ -0.041667 \end{Bmatrix} \tag{8.3.17}$$

By interpolation, Q_4 is equal to $-0.5U_2$, and it differs from Q_{22}^3 computed from equilibrium by the amount f_2^3 $(= \frac{1}{24})$.

Solution by Linear Rectangular Elements

We use a 2×2 (2 elements in the x direction and 2 elements in the y direction) uniform mesh (mesh R1) of four linear rectangular elements [see Fig. 8.3.3(a)] to discretize a quadrant of the domain. The 4×4 mesh (mesh R2) [see Fig. 8.3.3(b)] will be used for comparison. Once again, no discretization error is introduced in the present case.

Since all the elements in the mesh are identical, we need to compute the element coefficient matrices for only one element, say element 1. The element coefficient matrix is available from Example 8.2.3 with $a = b$. We have

$$[K^e] = \frac{1}{6}\begin{bmatrix} 4 & -1 & -2 & -1 \\ -1 & 4 & -1 & -2 \\ -2 & -1 & 4 & -1 \\ -1 & -2 & -1 & 4 \end{bmatrix}, \quad \{f^e\} = \frac{f_0 a^2}{4}\begin{Bmatrix} 1 \\ 1 \\ 1 \\ 1 \end{Bmatrix} \tag{8.3.18}$$

The coefficient matrix of the condensed equations for the primary unknowns in mesh R1 can be directly assembled. There are four unknowns (at nodes 1, 2, 4, and 5). The finite element equations associated with the four unknowns are (noting that $U_3 = U_6 = U_7 = U_8 = U_9 = 0$)

$$\begin{aligned} K_{11}U_1 + K_{12}U_2 + K_{14}U_4 + K_{15}U_5 &= F_1 \\ K_{21}U_1 + K_{22}U_2 + K_{24}U_4 + K_{25}U_5 &= F_2 \\ K_{41}U_1 + K_{42}U_2 + K_{44}U_4 + K_{45}U_5 &= F_4 \\ K_{51}U_1 + K_{52}U_2 + K_{54}U_4 + K_{55}U_5 &= F_5 \end{aligned} \tag{8.3.19a}$$

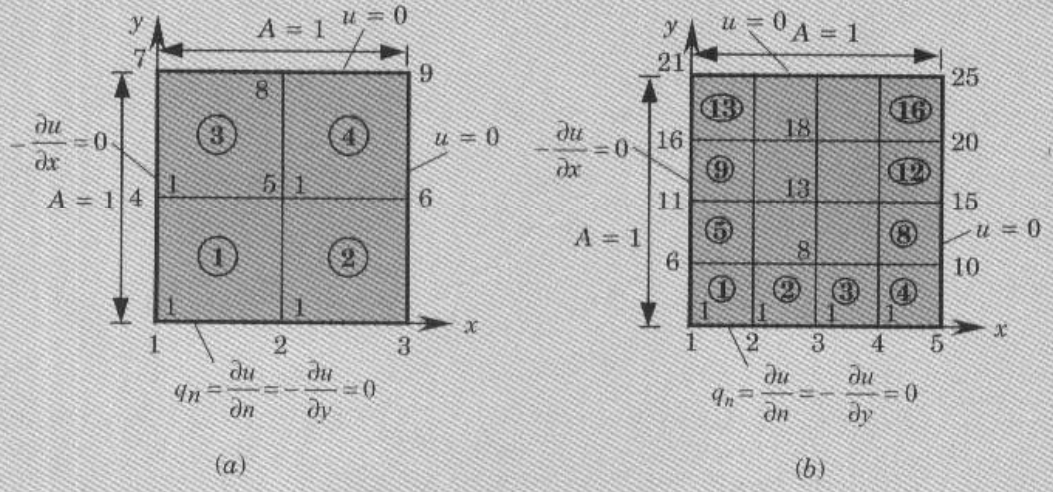

Figure 8.3.3 (a) Mesh R1 (2×2) of rectangular elements. (b) Mesh R2 (4×4) of rectangular elements.

where K_{IJ} and F_I are the global coefficients, which can be written in terms of the element coefficients as

$$\begin{aligned}
&K_{11}=K^1_{11}, \quad K_{12}=K^1_{12}, \quad K_{14}=K^1_{14}, \quad K_{15}=K^1_{13}\\
&K_{22}=K^1_{22}+K^2_{11}, \quad K_{24}=K^1_{24}, \quad K_{25}=K^1_{23}+K^2_{14}\\
&K_{44}=K^1_{44}+K^3_{11}, \quad K_{45}=K^1_{43}+K^3_{12}, \quad K_{55}=K^1_{33}+K^2_{44}+K^4_{11}+K^3_{22} \qquad (8.3.19b)\\
&F_1=f^1_1+Q^1_1, \quad F_2=f^1_2+f^2_1+Q^1_2+Q^2_1, \quad F_4=f^1_4+f^3_1+Q^1_4+Q^3_1\\
&F_5=f^1_3+f^2_4+f^4_1+f^3_2+Q^1_3+Q^2_4+Q^4_1+Q^3_2
\end{aligned}$$

The boundary conditions on the secondary variables are

$$Q^1_1=0, \quad Q^1_2+Q^2_1=0, \quad Q^1_4+Q^3_1=0 \qquad (8.3.20a)$$

and the balance of secondary variables at global node 5 requires

$$Q^1_3+Q^2_4+Q^3_2+Q^4_1=0 \qquad (8.3.20b)$$

Thus, the condensed equations for the primary unknowns are (for $f_0=1$ and $a=0.5$)

$$\frac{1}{6}\begin{bmatrix} 4 & -1 & -1 & -2\\ -1 & 8 & -2 & -2\\ -1 & -2 & 8 & -2\\ -2 & -2 & -2 & 16 \end{bmatrix}\begin{Bmatrix} U_1\\ U_2\\ U_4\\ U_5 \end{Bmatrix}=\frac{1}{16}\begin{Bmatrix} 1\\ 2\\ 2\\ 4 \end{Bmatrix} \qquad (8.3.21)$$

The solution of these equations is

$$U_1=0.31071, \quad U_2=0.24107, \quad U_4=0.24107, \quad U_5=0.19286 \qquad (8.3.22)$$

The secondary variables $Q_3=Q_7$, $Q_6=Q_8$, and Q_9 at nodes 3 (7), 6 (8), and 9, respectively (by symmetry), can be computed from the equations ($Q_3=Q^2_2$, $Q_6=Q^2_3+Q^4_2$, and $Q_9=Q^4_3$)

$$\begin{Bmatrix} Q_3\\ Q_6\\ Q_9 \end{Bmatrix}=-\begin{Bmatrix} f^2_2\\ f^2_3+f^4_2\\ f^4_3 \end{Bmatrix}+\begin{bmatrix} K_{31} & K_{32} & K_{34} & K_{35}\\ K_{61} & K_{62} & K_{64} & K_{65}\\ K_{91} & K_{92} & K_{94} & K_{95} \end{bmatrix}\begin{Bmatrix} U_1\\ U_2\\ U_4\\ U_5 \end{Bmatrix} \qquad (8.3.23a)$$

where

$$\begin{aligned}
&K_{31}=0, \quad K_{32}=K^2_{21}, \quad K_{34}=0, \quad K_{35}=K^2_{24}\\
&K_{61}=0, \quad K_{62}=K^2_{31}, \quad K_{64}=0, \quad K_{65}=K^2_{34}+K^4_{21} \qquad (8.3.23b)\\
&K_{91}=0, \quad K_{92}=0, \quad K_{94}=0, \quad K_{95}=K^4_{31}
\end{aligned}$$

Substituting the numerical values, we obtain

$$\begin{Bmatrix} Q_3\\ Q_6\\ Q_9 \end{Bmatrix}=-\frac{1}{16}\begin{Bmatrix} 1\\ 2\\ 1 \end{Bmatrix}+\frac{1}{6}\begin{bmatrix} 0 & -1 & 0 & -2\\ 0 & -2 & 0 & -2\\ 0 & 0 & 0 & -2 \end{bmatrix}\begin{Bmatrix} U_1\\ U_2\\ U_4\\ U_5 \end{Bmatrix}=-\begin{Bmatrix} 0.16697\\ 0.26964\\ 0.12679 \end{Bmatrix} \qquad (8.3.24)$$

Table 8.3.1 Comparison of the finite element solutions $u(0, y)$ with the series solution and the Ritz solution of (8.3.1).

	Triangular elem.		Rectangular elem.		Ritz solution	Series solution
y	Mesh T1	Mesh T2	Mesh R1	Mesh R2	(2.5.39)	(2.5.40)
0.00	0.3125	0.3013	0.3107	0.2984	0.3125	0.2947
0.25	0.2708†	0.2805	0.2759†	0.2824	0.2930	0.2789
0.50	0.2292	0.2292	0.2411	0.2322	0.2344	0.2293
0.75	0.1146†	0.1393	0.1205†	0.1414	0.1367	0.1397
1.00	0.0000	0.0000	0.0000	0.0000	0.0000	0.0000

†Interpolated values

The finite element solutions obtained by two different meshes of triangular elements and two different meshes of rectangular elements are compared in Table 8.3.1 with the 50-term series solution (at $x = 0$ for varying y) in (2.5.40) (set $k = 1$, $g_0 = f_0 = 1$) and the one-parameter Ritz solution in (2.5.39); see also Fig. 8.3.4. The finite element solution obtained by 16 triangular elements (in an octant) is the most accurate when compared to the series solution. The accuracy of the triangular element mesh is due to the large number of elements it has compared to the number of elements in the rectangular element mesh for the same size of the domain.

The solution u and components of flux (q_x, q_y) can be computed at any interior point of the domain. For a point (x, y) in element Ω_e, we have $(k = 1)$

$$u_h^e(x, y) = \sum_{j=1}^{n} u_j^e \psi_j^e(x, y) \tag{8.3.25a}$$

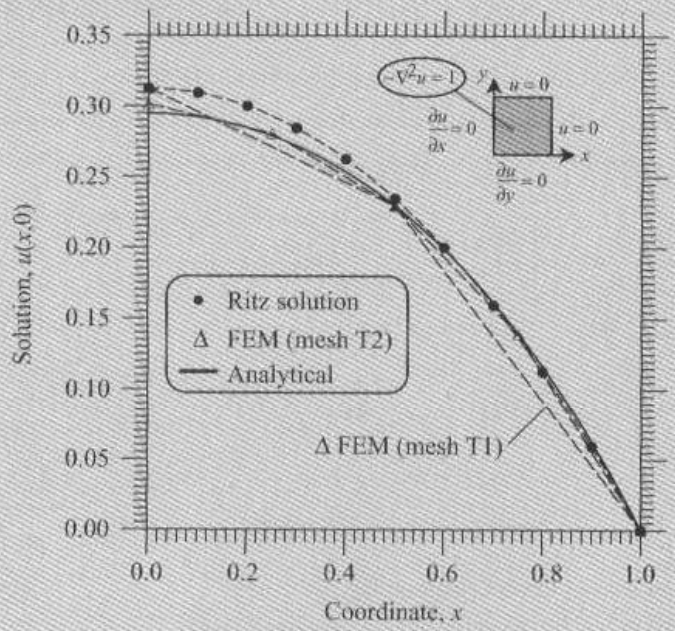

Figure 8.3.4 Comparison of the finite element solution with the two-parameter Ritz solution and the analytical (series) solution.

$$q_y^e(x,y) = -k\frac{\partial u_h^e}{\partial y} = -\sum_{i=1}^{n} u_i^e \frac{\partial \psi_i^e}{\partial y}, \quad q_x^e(x,y) = -k\frac{\partial u_h^e}{\partial x} = -\sum_{i=1}^{n} u_i^e \frac{\partial \psi_i^e}{\partial x} \tag{8.3.25b}$$

The negative sign in the definition of fluxes is dictated by the physics of the problem. Here we interpreted the problem at hand to be one of heat transfer. Note that for a linear triangular element, q_x and q_y are constants over an entire element, whereas q_x is linear in y and q_y is linear in x for a linear rectangular element. For example, consider element 1 of mesh T1 of triangular elements

$$\begin{aligned} q_x^1(x,y) &= -\frac{k}{2A_1}\sum_{i=1}^{3} u_i^1 \beta_i^1 = -2(U_2 - U_1) = 0.16667 \\ q_y^1(x,y) &= -\frac{k}{2A_1}\sum_{i=1}^{3} u_i^1 \gamma_i^1 = -2(U_3 - U_2) = 0.10417 \end{aligned} \tag{8.3.26a}$$

Clearly, the gradients (and hence the components of flux) are constant. For element 1 of mesh R1 rectangular element (four elements) we have

$$\begin{aligned} q_x^1(x,y) &= -k\sum_{i=1}^{4} u_i^1 \frac{\partial \psi_i^1}{\partial x} = 2U_1(1-2y) - 2U_2(1-2y) - 4yU_5 + 4yU_4 \\ q_x^1(0.25, 0.25) &= 0.11785 \\ q_y^1(x,y) &= -k\sum_{i=1}^{4} u_i^1 \frac{\partial \psi_i^1}{\partial y} = 2U_1(1-2x) - 2U_2(1-2x) - 4xU_5 + 4xU_4 \\ q_y^1(0.25, 0.25) &= 0.11785 \end{aligned} \tag{8.3.26b}$$

Plots of q_x, obtained by mesh T1 (8 elements) and mesh T2 (16 elements) of linear triangular elements as a function of x (for $y = 0.0$) are shown in Fig. 8.3.5.

The computation of *isolines*, i.e., lines of constant u, for linear finite elements is straightforward. Suppose that we wish to find $u = u_0$ (constant) isoline. On a side of a linear triangle or rectangular element, the solution u varies according to the equation

$$u_h^e(s) = u_1^e + \frac{u_2^e - u_1^e}{h}s$$

where s is the local coordinate with its origin at node 1 of the side, (u_1^e, u_2^e) are the nodal values (see Fig. 8.3.6), and h is the length of the side. Then, if $u \equiv u_0$ lies on the line (i.e., $u_1^e < u_0 < u_2^e$ or $u_2^e < u_0 < u_1^e$), the point s_0 at which $U^e(s_0) = u_0$ is given by

$$s_0 = \frac{(u_0 - u_1^e)h}{(u_2^e - u_1^e)} \tag{8.3.27}$$

Similar equations apply for other sides of the element. Since the solution varies linearly between any two points of linear elements, the isoline is determined by joining two points on any two sides of the element for which (8.3.27) gives a positive value (and $s_0 < h$).

For quadratic elements, isolines are determined by finding three points s_i in the element at which $u_h^e(s_i) = u_0$ ($i = 1$, 2, and 3):

$$\frac{s_0}{h} = \frac{-b \pm \sqrt{b^2 - 4ac}}{2a} > 0 \tag{8.3.28a}$$

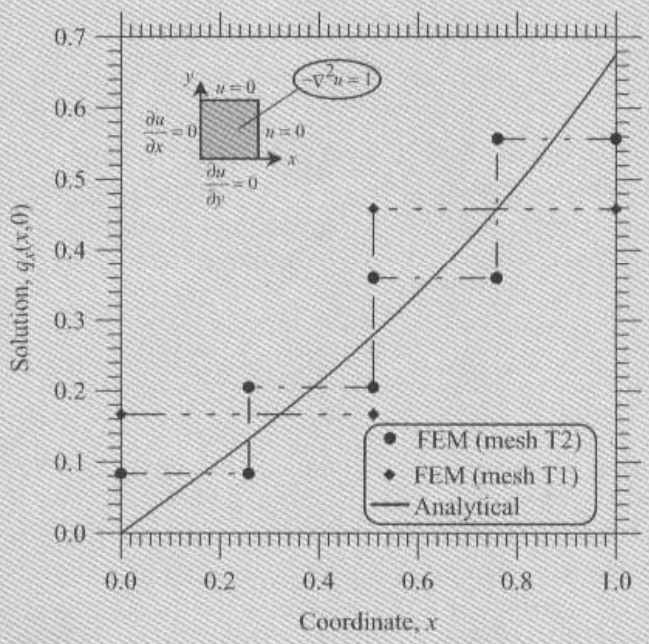

Figure 8.3.5 Comparison of the finite element solution with the analytical (series) solution of $q_x(x, 0)$.

where

$$c = u_1^e - u_0, \quad b = -3u_1^e + 4u_2^e - u_3^e, \quad a = 2\left(u_1^e - 2u_2^e + u_3^e\right) \tag{8.3.28b}$$

Equation (8.3.28*a*) is to be applied on any three lines in the element until three different values $h > s_0 > 0$ are found.

The problem considered here has several physical interpretations (see Table 8.1.1). The problem can be viewed as one of finding the temperature u in a unit square with uniform internal heat generation, where the sides $x = 0$ and $y = 0$ are insulated and the other two sides are subjected to zero temperature (see Section 8.5.1). Another interpretation of the equation is that it defines the torsion of a 2-inch-square cross-sectional cylindrical bar (see Section 8.5.3). In this case, u denotes the stress function Ψ, and the components of the gradient of the solution

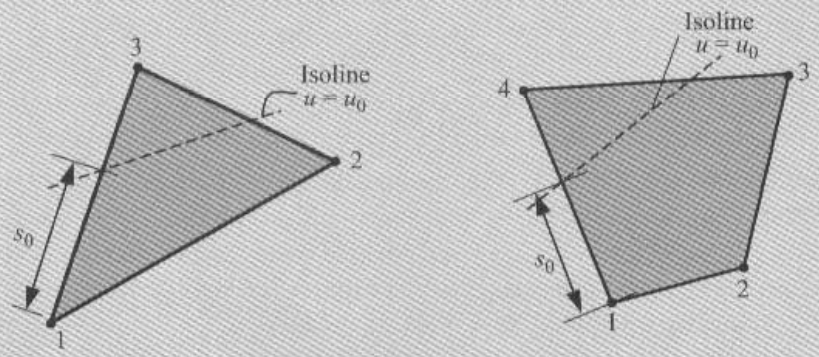

Figure 8.3.6 Isolines for linear triangular and quadrilateral elements.

are the stresses (which are of primary interest):

$$\sigma_{xz} = G\theta \frac{\partial \Psi}{\partial y}, \quad \sigma_{yz} = -G\theta \frac{\partial \Psi}{\partial x}$$

where G is the shear modulus and θ is the angle of twist per unit length of the bar.

A third interpretation of (8.3.1) is provided by groundwater (seepage) and potential flow problems. In this case, u denotes the piezometric head ϕ, stream function ψ, or velocity potential ϕ (see Section 8.5.2). The x and y components of the velocity for the groundwater flow are defined as

$$u_1 = -a_{11} \frac{\partial \phi}{\partial x}, \quad u_2 = -a_{22} \frac{\partial \phi}{\partial y}$$

where a_{11} and a_{22} are the permeabilities of the soil along the x and y directions, respectively. Examples of each of these field problems will be considered in Section 8.5.

8.4 SOME COMMENTS ON MESH GENERATION AND IMPOSITION OF BOUNDARY CONDITIONS

8.4.1 Discretization of a Domain

The representation of a given domain by a collection of finite elements requires engineering judgement on the part of the finite element practitioner. The number, type (e.g., linear or quadratic), shape (e.g., triangular or rectangular), and density (i.e., mesh refinement) of elements used in a given problem depend on a number of considerations. The first consideration is to discretize the domain as closely as possible with elements that are admissible. As we shall see later, we can use one set of elements for the approximation of a domain and another set for the solution. In discretizing a domain, consideration must be given to an accurate representation of the domain, point sources, distributed sources with discontinuities (i.e., sudden change in the intensity of the source), and material and geometric discontinuities, including a reentrant corner. The discretization should include, for example, nodes at point sources (so that the point source is accurately lumped at the node), reentrant corners, and element interfaces where abrupt changes in geometry and material properties occur.

A second consideration, which requires some engineering judgement, is to discretize the body or portions of the body into sufficiently small elements so that steep gradients of the solution are accurately calculated. The engineering judgement should come from both a qualitative understanding of the behavior of the solution and an estimate of the computational costs involved in the mesh refinement (i.e., reducing the size of the elements). For example, consider the inviscid flow around a cylinder in a channel. The flow entering the channel at the left goes around the cylinder and exits the channel at the right [see Fig. 8.4.1(a)]. Since the section at the cylinder is smaller than the inlet section, it is expected that the flow accelerates in the vicinity of the cylinder. On the other hand, the velocity field far from the cylinder (e.g., at the inlet) is essentially uniform. Such knowledge of the qualitative behavior of the flow allows us to employ a coarse mesh (i.e., elements that are relatively

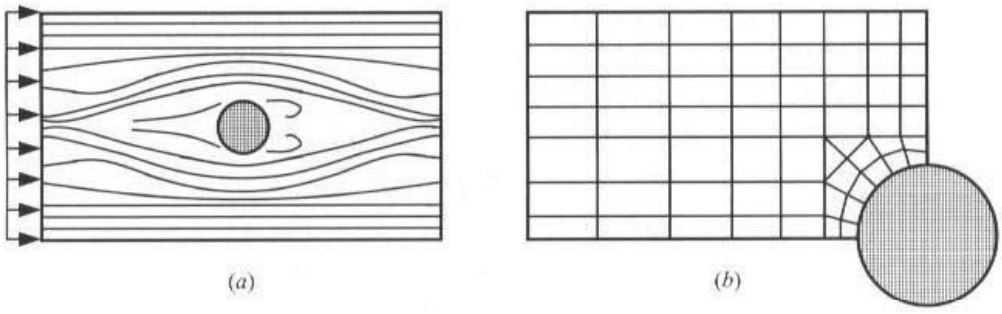

Figure 8.4.1 (*a*) Flow of an inviscid fluid around a cylinder (streamlines). (*b*) A typical mesh for a quadrant of the domain.

large in size) at sites sufficiently far from the cylinder, and a fine one at closer distances to the cylinder [see Fig. 8.4.1(*b*)]. Another reason for using a refined mesh near the cylinder is to accurately represent the curved boundary of the domain there. In general, a refined mesh is required in places where acute changes in geometry, boundary conditions, loading, material properties, or solution occur.

A mesh refinement should meet three conditions: (1) All the previous meshes should be contained in the current refined mesh; (2) every point in the body can be included within an arbitrarily small element at any stage of the mesh refinement; and (3) the same order of approximation for the solution should be retained through all stages of the refinement process. The last requirement eliminates comparison of two different approximations in two different meshes.

When a mesh is refined, care should be taken to avoid elements with very large aspect ratios (i.e., the ratio of one side of an element to the other) or small angles. Recall from the element matrices in Eqs. (8.2.48) and (8.2.53) that the coefficient matrices depend on the ratios of a to b and b to a, where a and b are the lengths of elements in the x and y directions, respectively. If the value of a/b or b/a is very large, the resulting coefficient matrices are ill-conditioned (i.e., numerically not invertible). Although the safe lower and upper limits on b/a are believed to be 0.1 and 10, respectively, the actual values are much more extreme and they depend on the nature of physical phenomenon being modeled. For example, in the inviscid flow problem discussed above, large aspect ratios are allowed at the entrance of the channel.

The words "coarse" and "fine" are relative. In any given problem, we begin with a finite element mesh that is believed to be adequate (based on experience and engineering judgement) to solve the problem at hand. Then, as a second choice, we select a mesh that consists of a larger number of elements (and includes the first one as a subset) to solve the problem once again. If there is a significant difference between the two solutions, we see the benefit of mesh refinement and further mesh refinement may be warranted. If the difference is negligibly small, further mesh refinements are not necessary. Such numerical experiments with mesh refinements are not always feasible in practice, mostly due to the computational costs involved.

In cases where computational cost is the prime concern, we must depend on our judgement concerning what is a reasonably good mesh, which is often dictated by the geometry and qualitative understanding of the variations of the solution and its gradient. Since most

practical problems are approximated in their engineering formulations, we should not be overly concerned with the numerical accuracy of the solution. A feel for the relative proportions and directions of various errors introduced into the analysis helps the finite element practitioner to make a decision on when to stop refining a mesh. In summary, engineering knowledge and experience with a given class of problems are essential to a suitable numerical study.

8.4.2 Generation of Finite Element Data

An important part of finite element modeling is the mesh generation, which involves numbering the nodes and elements, and the generation of nodal coordinates and the connectivity matrix. While the task of generating such data is not difficult, the type of the data has an effect on the computational efficiency as well as on accuracy. More specifically, the numbering of the nodes directly affects the bandwidth of the final assembled equations, which in turn increases the storage requirement and computational cost if equation solvers with the Gauss elimination procedure are used. The elements can be numbered arbitrarily because it has no effect on the half-bandwidth. In a general-purpose program with a preprocessor, options to minimize the bandwidth are included. The saving of computational cost due to a smaller bandwidth in the solution of equations can be substantial, especially in problems where a large number of nodes and degrees of freedom per node are involved. While element numbering does not affect the half-bandwidth, it may affect the computer time required to assemble the global coefficient matrix (usually, a very small percentage of the time required to solve the equations).

The accuracy of the finite element solution can also depend on the choice of the finite element mesh. For instance, if the mesh selected violates the symmetry present in the problem, the resulting solution will be less accurate than one obtained using a mesh that agrees with the physical symmetry present in the problem. Geometrically, a triangular element has fewer (or no) lines of symmetry when compared to a rectangular element, and therefore meshes of triangular elements should be used with care (e.g., select a mesh that does not contradict the mathematical symmetry present in the problem).

The effect of the finite element meshes shown in Fig. 8.4.2 on the solution of the Poisson equation in Example 8.3.1 is investigated. The finite element solutions obtained by the three meshes are compared with the series solution in Table 8.4.1. Clearly, the solution obtained using mesh 3 is less accurate. This is expected because mesh 3 is symmetric about the diagonal line connecting node 3 to node 7, whereas the mathematical symmetry is about the diagonal line connecting node 1 to node 9 (see Fig. 8.4.2). Mesh 1 is the most desirable of the three because it does not contradict the mathematical symmetry of the problem.

Next, the effect of mesh refinement with rectangular elements is investigated. Four different meshes of rectangular elements are shown in Fig. 8.4.3. Each of the meshes contains the previous mesh as a subset. The mesh shown in Fig. 8.4.3(*c*) is nonuniform; it is obtained by subdividing the first two rows and columns of elements of the mesh shown in Fig. 8.4.3(*b*). The finite element solutions obtained by these meshes are compared in Table 8.4.2. The numerical convergence of the finite element solution of the refined meshes to the series solution is apparent from the results presented.

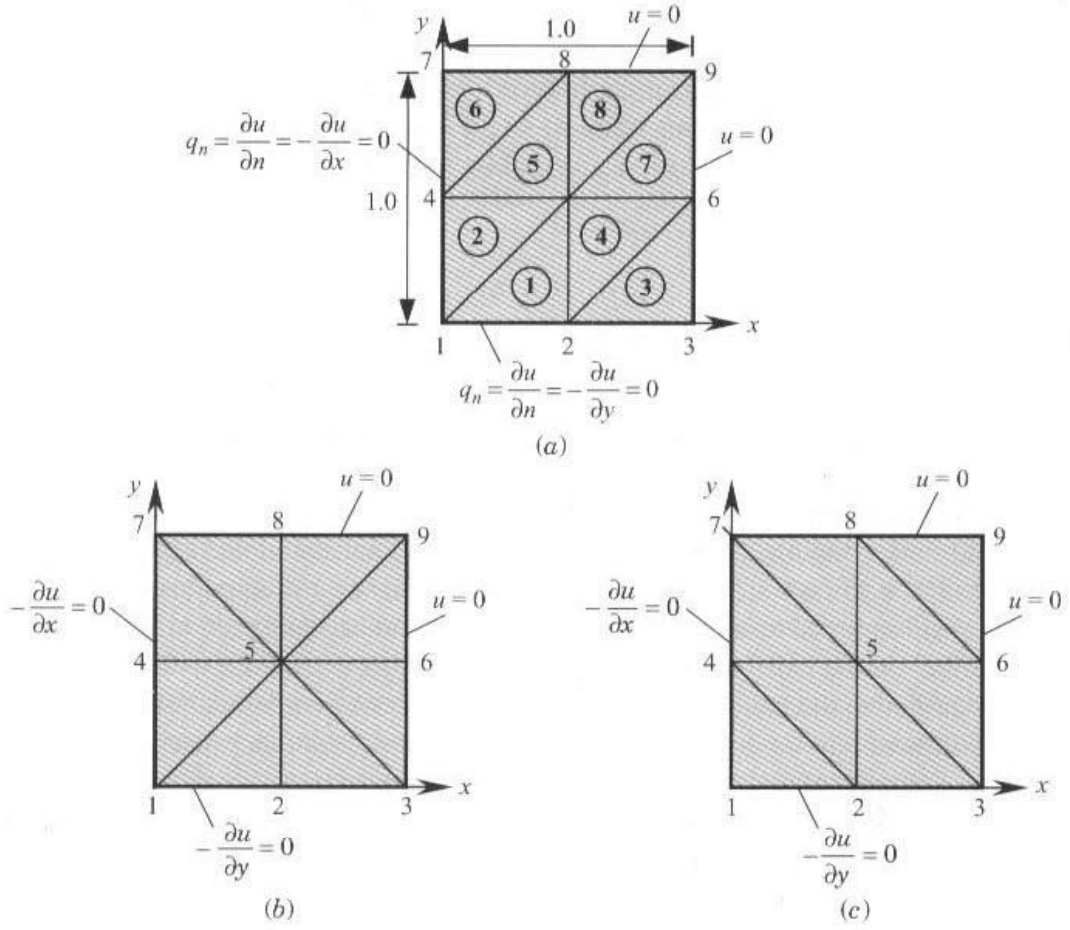

Figure 8.4.2 Various types of triangular-element meshes for the domain of Example 8.3.1: (*a*) mesh 1; (*b*) mesh 2; and (*c*) mesh 3.

8.4.3 Imposition of Boundary Conditions

In some problems of interest we encounter situations where at a point of the boundary both primary and secondary degrees of freedom are specified at the same point. Such points are called *singular points*. In this case we impose the boundary condition on the primary variable and let the secondary variable take its value (calculated in the postcomputation).

Table 8.4.1 Comparison of the finite element solutions obtained using various linear triangular-element meshes† with the series solution of the problem in Example 8.3.1.

	Finite element solution			
Node	Mesh 1	Mesh 2	Mesh 3	Series solution
1	0.31250	0.29167	0.25000	0.29469
2	0.22917	0.20833	0.20833	0.22934
3	0.22917	0.20833	0.20833	0.22934
4	0.17708	0.18750	0.16667	0.18114

†See Fig. 8.4.2 for the finite element meshes.

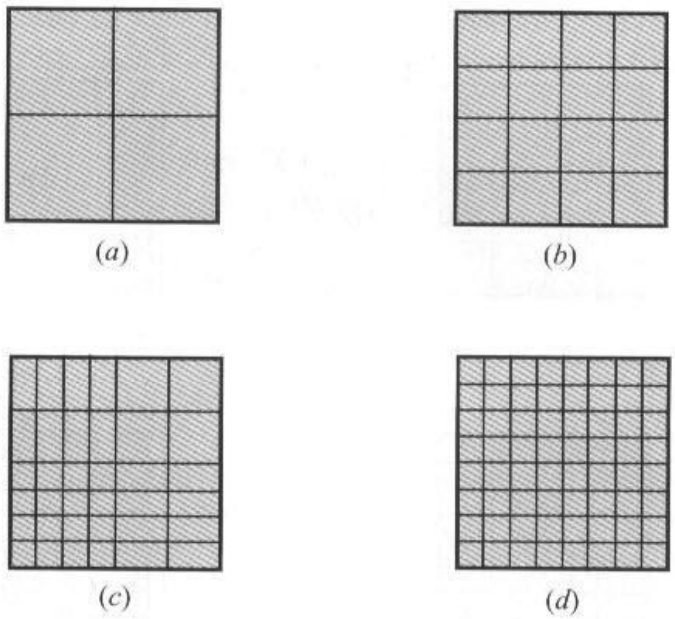

Figure 8.4.3 Mesh refinement; the meshes in (*a*), (*b*), and (*d*) are uniform; the mesh in (*c*) is nonuniform: (*a*) 2 × 2 mesh; (*b*) 4 × 4 mesh; (*c*) 6 × 6 mesh; and (*d*) 8 × 8 mesh.

This is because the boundary conditions on the primary variables are often maintained more strictly than those on the secondary variables. Of course, if the problem is such that the essential boundary conditions are a result of the natural boundary conditions, then we must impose the natural boundary conditions.

Another type of singularity we encounter in the solution of boundary value problems is the specification of two different values of a primary variable at the same point.

Table 8.4.2 Convergence of the finite element solution (with mesh refinement)† of the problem in Example 8.3.1.

Location		Finite element solution				
x	y	2 × 2	4 × 4	6 × 6	8 × 8	Series solution
0.000	0.0	0.31071	0.29839	0.29641	0.29560	0.29469
0.125	0.0	—	—	0.29248	0.29167	0.29077
0.250	0.0	—	0.28239	0.28055	0.27975	0.27888
0.375	0.0	—	—	0.26022	0.24943	0.25863
0.500	0.0	0.24107	0.23220	0.23081	0.23005	0.22934
0.625	0.0	—	—	—	0.19067	0.19009
0.750	0.0	—	0.14137	0.14064	0.14014	0.13973
0.875	0.0	—	—	—	0.07709	0.07687
0.125	0.125	—	—	0.28862	0.28781	0.28692
0.250	0.250	—	0.26752	0.26580	0.26498	0.26415
0.375	0.375	—	—	0.22960	0.22873	0.22799
0.500	0.50	0.19286	0.18381	0.18282	0.18179	0.18114
0.625	0.625	—	—	—	0.12813	0.12757
0.750	0.750	—	0.07506	0.07481	0.07332	0.07282
0.875	0.875	—	—	—	0.02561	0.02510

†See Fig. 8.4.3 for the finite element meshes.

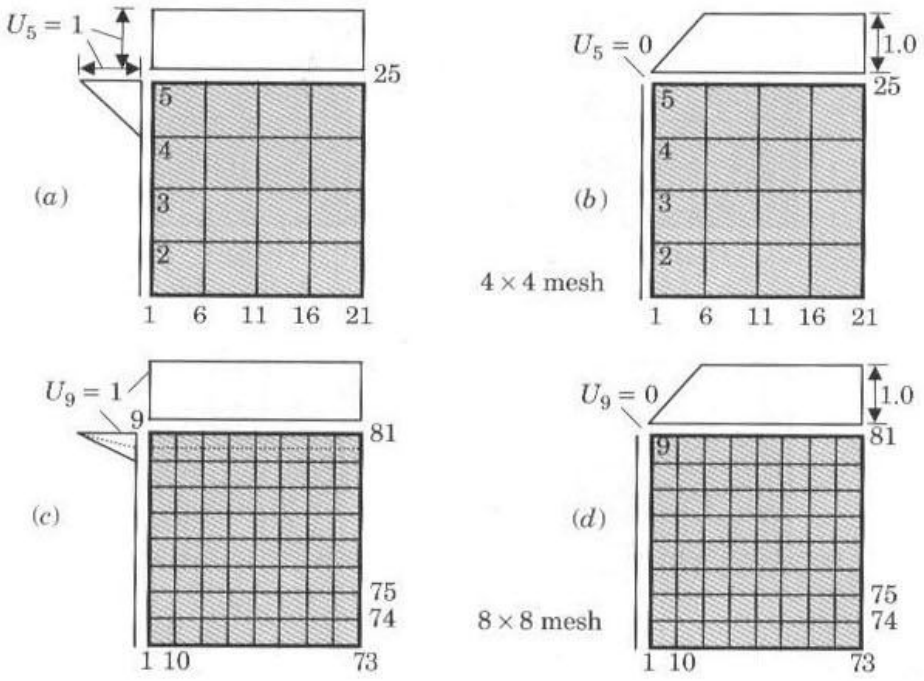

Figure 8.4.4 Effect of specifying two values of a primary variable at a node [node 5 in (*a*) and (*b*) and node 9 in (*c*) and (*d*)].

An example of such cases is provided by the problem in Fig. 8.4.4, where u is specified to be zero on the boundary defined by the line $x = 0$ and is specified to be unity on the boundary defined by the line $y = 1$. Consequently, at $x = 0$ and $y = 1$, u has two different values. The analyst must make a choice between the two values. In either case, the true boundary condition is replaced by an approximate condition. Often, the larger value is used to obtain a conservative design. The closeness of the approximate boundary condition to the true one depends on the size of the element containing the point (see Fig. 8.4.3). A mesh refinement in the vicinity of the singular point often yields an acceptable solution.

Additional comments on the choice of element geometry, meshes, and load-representation in finite element analysis are presented in Section 9.4.

8.5 APPLICATIONS

8.5.1 Conduction and Convection Heat Transfer

In Section 4.3, heat transfer (by conduction and convection) in one-dimensional (axial and radially symmetric) systems was considered. Here we consider heat transfer in two-dimensional plane and axisymmetric systems. The derivation of two-dimensional heat transfer equations in plane and axisymmetric geometries follows the same procedure as in one dimension but the heat transfer is in two directions. Details of such derivations can be found in textbooks on heat transfer [e.g., Holman (1986) and Özisik (1985)]. Here we record the governing equations for various cases, construct their finite element models, and present typical applications.

For heat conduction in plane or axisymmetric geometries, the finite element models developed in Sections 8.2 and 8.3 are immediately applicable with the following interpretation of the variables:

$$\begin{aligned} u &= T \equiv \text{temperature } (^\circ\text{C}) \\ q_n &\equiv \text{negative of heat flux } [\text{W}/(\text{m}^2 \cdot {}^\circ\text{C})] \\ a_{11}, a_{22} &\equiv \text{conductivities } [\text{W}/(\text{m} \cdot {}^\circ\text{C})] \text{ of an orthotropic medium} \\ &\quad \text{whose principal material axes coincide with the } (x, y) \text{ axes} \\ f &\equiv \text{internal heat generation } (\text{W}/\text{m}^3) \\ a_{00} &= 0 \end{aligned} \tag{8.5.1}$$

For convection heat transfer, i.e., when heat is transferred from one medium to the surrounding medium (often, a fluid) by convection, the finite element model developed earlier requires some modification. The reason for this modification is that in two-dimensional problems, the convective boundary is a curve as opposed to a point in one-dimensional problems. Therefore, the contribution of the convection (or Newton's type) boundary condition to the coefficient matrix and source vector are to be computed by evaluating boundary integrals involving the interpolation functions of elements with convection boundaries. The model to be presented allows the computation of the additional contributions to the coefficient matrix and source vector whenever the element has the convection boundary condition.

Plane Systems

The governing equation for steady-state heat transfer in plane systems is a special case of (8.2.1) and is given by

$$-\frac{\partial}{\partial x}\left(k_x \frac{\partial T}{\partial x}\right) - \frac{\partial}{\partial y}\left(k_y \frac{\partial T}{\partial y}\right) = f(x, y) \tag{8.5.2}$$

where T is the temperature (in °C), k_x and k_y are the thermal conductivities [in W/(m · °C)] along the x and y directions, respectively, and f is the internal heat generation per unit volume (in W/m^3). For a convection boundary, the natural boundary condition is a balance of energy transfer across the boundary due to conduction *and/or* convection (i.e., Newton's law of cooling):

$$k_x \frac{\partial T}{\partial x} n_x + k_y \frac{\partial T}{\partial y} n_y + \beta(T - T_\infty) = \hat{q}_n \tag{8.5.3}$$

where β is the convective conductance (or the convective heat transfer coefficient) [in W/(m^2 · °C)], T_∞ is the (ambient) temperature of the surrounding fluid medium, and $\hat{q}_n$ is the specified heat flux. The first term accounts for heat transfer by conduction, the second by convection, and the third accounts for the specified heat flux, if any. It is the presence of the term $\beta(T - T_\infty)$ that requires some modification of (8.2.10).

The weak form of (8.5.2) can be obtained from (8.2.8). The boundary integral should be modified to account for the convection heat transfer boundary condition in (8.5.3).

The coefficient of w, $k_x(\partial T/\partial x)n_x + k_y(\partial T/\partial y)n_y$, in the boundary integral is replaced with $q_n - \beta(T - T_\infty)$:

$$
\begin{aligned}
0 &= \int_{\Omega_e} \left(k_x \frac{\partial w}{\partial x}\frac{\partial T}{\partial x} + k_y \frac{\partial w}{\partial y}\frac{\partial T}{\partial y} - wf \right) dx\, dy - \oint_{\Gamma_e} w \left(k_x \frac{\partial T}{\partial x} n_x + k_y \frac{\partial T}{\partial y} n_y \right) ds \\
&= \int_{\Omega_e} \left(k_x \frac{\partial w}{\partial x}\frac{\partial T}{\partial x} + k_y \frac{\partial w}{\partial y}\frac{\partial T}{\partial y} - wf \right) dx\, dy - \oint_{\Gamma_e} w\, [\hat{q}_n - \beta(T - T_\infty)]\, ds \\
&= B(w, T) - l(T)
\end{aligned}
\tag{8.5.4a}
$$

where w is the test function and $B(\cdot, \cdot)$ and $l(\cdot)$ are the bilinear and linear forms, respectively,

$$
\begin{aligned}
B(w, T) &= \int_{\Omega_e} \left(k_x \frac{\partial w}{\partial x}\frac{\partial T}{\partial x} + k_y \frac{\partial w}{\partial y}\frac{\partial T}{\partial y} \right) dx\, dy + \oint_{\Gamma_e} \beta w T\, ds \\
l(T) &= \int_{\Omega_e} wf\, dx\, dy + \oint_{\Gamma_e} \beta w T_\infty\, ds + \oint_{\Gamma_e} w \hat{q}_n\, ds
\end{aligned}
\tag{8.5.4b}
$$

The finite element model of (8.5.4a) and (8.5.4b) is obtained by substituting the finite element approximation of the form,

$$
T = \sum_{j=1}^{n} T_j^e \psi_j^e(x, y) \tag{8.5.5}
$$

for T and ψ_i^e for w into (8.5.4a):

$$
\sum_{j=1}^{n} (K_{ij}^e + H_{ij}^e) T_j^e = F_i^e + P_i^e \tag{8.5.6a}
$$

where

$$
\begin{aligned}
K_{ij}^e &= \int_{\Omega_e} \left(k_x \frac{\partial \psi_i^e}{\partial x}\frac{\partial \psi_j^e}{\partial x} + k_y \frac{\partial \psi_i^e}{\partial y}\frac{\partial \psi_j^e}{\partial y} \right) dx\, dy \\
F_i^e &= \int_{\Omega_e} f \psi_i^e\, dx\, dy + \oint_{\Gamma_e} \hat{q}_n^e \psi_i^e\, ds \equiv f_i^e + Q_i^e \\
H_{ij}^e &= \beta^e \oint_{\Gamma_e} \psi_i^e \psi_j^e\, ds, \qquad P_i^e = \beta^e \oint_{\Gamma_e} \psi_i^e T_\infty\, ds
\end{aligned}
\tag{8.5.6b}
$$

Note that by setting the heat transfer coefficient β to zero, we obtain the heat conduction model that accounts for no convection.

The additional coefficients H_{ij}^e and P_i^e due to the convection boundary conditions can be computed by evaluating boundary integrals. These coefficients must be computed only for those elements and boundaries that are subjected to a convection boundary condition. The computation of the coefficients for the linear triangular and rectangular elements is presented in the following paragraphs. The coefficients H_{ij}^e and P_i^e for a linear triangular

element are defined by

$$
\begin{aligned}
H_{ij}^e &= \beta_{12}^e \int_0^{h_{12}^e} \psi_i^e \psi_j^e \, ds + \beta_{23}^e \int_0^{h_{23}^e} \psi_i^e \psi_j^e \, ds + \beta_{31}^e \int_0^{h_{31}^e} \psi_i^e \psi_j^e \, ds \\
P_i^e &= \beta_{12}^e T_\infty^{12} \int_0^{h_{12}^e} \psi_i^e \, ds + \beta_{23}^e T_\infty^{23} \int_0^{h_{23}^e} \psi_i^e \, ds + \beta_{31}^e T_\infty^{31} \int_0^{h_{31}^e} \psi_i^e \, ds
\end{aligned}
\tag{8.5.7}
$$

where β_{ij}^e is the film coefficient (assumed to be constant) for the side connecting nodes i and j of element Ω_e, T_∞^{ij} is the ambient temperature on the side, and h_{ij}^e is the length of the side. For a rectangular element, expressions in (8.5.7) must be modified to account for four line integrals on four sides of the element.

Only those line integrals that have a convection boundary condition need to be evaluated. The boundary integrals are line integrals involving the interpolation functions. The local coordinate s is taken along the side, with its origin at the first node of the side (see Fig. 8.5.1). As noted earlier, the interpolation functions on any given side are the one-dimensional interpolation functions. Therefore, the evaluation of integrals is made easy. Indeed, the integrals

$$
\int_0^{h_{ij}^e} \psi_i^e \psi_j^e \, ds, \quad \int_0^{h_{ij}^e} \psi_i^e \, ds
$$

have been evaluated in Chapter 3 in connection with mass matrix coefficients and source vector coefficients for linear and quadratic elements. We summarize the results here.

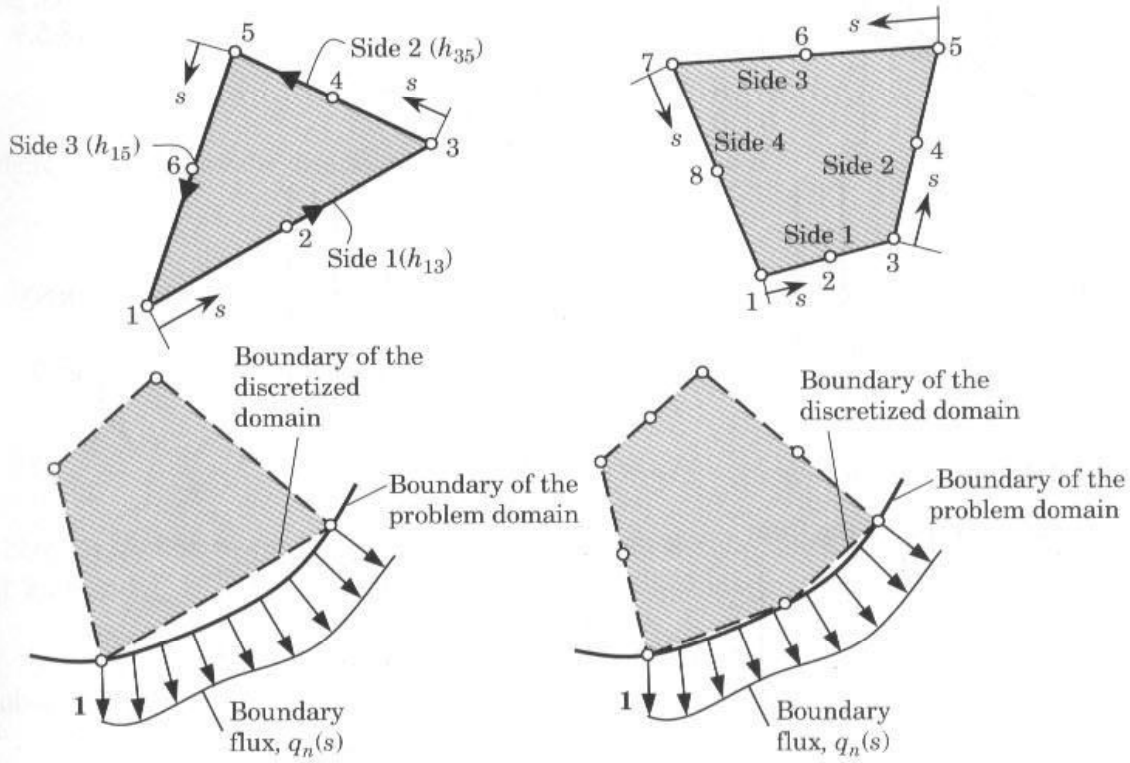

Figure 8.5.1 Triangular and quadrilateral elements, with node numbers and local coordinates for the evaluation of the boundary integrals. Also shown are the boundary approximation and flux representation using linear and quadratic elements.

Linear Triangular Element

The matrices $[H^e]$ and $\{P^e\}$ are given by

$$[H^e] = \frac{\beta_{12}^e h_{12}^e}{6}\begin{bmatrix}2 & 1 & 0\\ 1 & 2 & 0\\ 0 & 0 & 0\end{bmatrix} + \frac{\beta_{23}^e h_{23}^e}{6}\begin{bmatrix}0 & 0 & 0\\ 0 & 2 & 1\\ 0 & 1 & 2\end{bmatrix} + \frac{\beta_{31}^e h_{31}^e}{6}\begin{bmatrix}2 & 0 & 1\\ 0 & 0 & 0\\ 1 & 0 & 2\end{bmatrix} \tag{8.5.8a}$$

$$\{P^e\} = \frac{\beta_{12}^e T_\infty^{12} h_{12}^e}{2}\begin{Bmatrix}1\\ 1\\ 0\end{Bmatrix} + \frac{\beta_{23}^e T_\infty^{23} h_{23}^e}{2}\begin{Bmatrix}0\\ 1\\ 1\end{Bmatrix} + \frac{\beta_{31}^e T_\infty^{31} h_{31}^e}{2}\begin{Bmatrix}1\\ 0\\ 1\end{Bmatrix} \tag{8.5.8b}$$

Quadratic Triangular Element

$$[H^e] = \frac{\beta_{13}^e h_{13}^e}{30}\begin{bmatrix}4 & 2 & -1 & 0 & 0 & 0\\ 2 & 16 & 2 & 0 & 0 & 0\\ -1 & 2 & 4 & 0 & 0 & 0\\ 0 & 0 & 0 & 0 & 0 & 0\\ 0 & 0 & 0 & 0 & 0 & 0\\ 0 & 0 & 0 & 0 & 0 & 0\end{bmatrix} + \frac{\beta_{35}^e h_{35}^e}{30}\begin{bmatrix}0 & 0 & 0 & 0 & 0 & 0\\ 0 & 0 & 0 & 0 & 0 & 0\\ 0 & 0 & 4 & 2 & -1 & 0\\ 0 & 0 & 2 & 16 & 2 & 0\\ 0 & 0 & -1 & 2 & 4 & 0\\ 0 & 0 & 0 & 0 & 0 & 0\end{bmatrix}$$

$$+ \frac{\beta_{51} h_{51}^e}{30}\begin{bmatrix}4 & 0 & 0 & 0 & -1 & 2\\ 0 & 0 & 0 & 0 & 0 & 0\\ 0 & 0 & 0 & 0 & 0 & 0\\ 0 & 0 & 0 & 0 & 0 & 0\\ -1 & 0 & 0 & 0 & 4 & 2\\ 2 & 0 & 0 & 0 & 2 & 16\end{bmatrix} \tag{8.5.9a}$$

$$\{P^e\} = \frac{\beta_{13}^e T_\infty^{13} h_{13}^e}{6}\begin{Bmatrix}1\\ 4\\ 1\\ 0\\ 0\\ 0\end{Bmatrix} + \frac{\beta_{35}^e T_\infty^{35} h_{35}^e}{6}\begin{Bmatrix}0\\ 0\\ 1\\ 4\\ 1\\ 0\end{Bmatrix} + \frac{\beta_{51}^e T_\infty^{51} h_{51}^e}{6}\begin{Bmatrix}1\\ 0\\ 0\\ 0\\ 1\\ 4\end{Bmatrix} \tag{8.5.9b}$$

Linear Rectangular Element

The matrix $[H^e]$ is of the form

$$[H^e] = \frac{\beta_{12}^e h_{12}^e}{6}\begin{bmatrix}2 & 1 & 0 & 0\\ 1 & 2 & 0 & 0\\ 0 & 0 & 0 & 0\\ 0 & 0 & 0 & 0\end{bmatrix} + \frac{\beta_{23}^e h_{23}^e}{6}\begin{bmatrix}0 & 0 & 0 & 0\\ 0 & 2 & 1 & 0\\ 0 & 1 & 2 & 0\\ 0 & 0 & 0 & 0\end{bmatrix}$$

$$+ \frac{\beta_{34}^e h_{34}^e}{6}\begin{bmatrix}0 & 0 & 0 & 0\\ 0 & 0 & 0 & 0\\ 0 & 0 & 2 & 1\\ 0 & 0 & 1 & 2\end{bmatrix} + \frac{\beta_{41}^e h_{41}^e}{6}\begin{bmatrix}2 & 0 & 0 & 1\\ 0 & 0 & 0 & 0\\ 0 & 0 & 0 & 0\\ 1 & 0 & 0 & 2\end{bmatrix} \tag{8.5.10a}$$

and $\{P^e\}$ is given by

$$\{P^e\} = \frac{\beta_{12}^e T_\infty^{12} h_{12}^e}{2} \begin{Bmatrix} 1 \\ 1 \\ 0 \\ 0 \end{Bmatrix} + \frac{\beta_{23}^e T_\infty^{23} h_{23}^e}{2} \begin{Bmatrix} 0 \\ 1 \\ 1 \\ 0 \end{Bmatrix} + \frac{\beta_{34}^e T_\infty^{34} h_{34}^e}{2} \begin{Bmatrix} 0 \\ 0 \\ 1 \\ 1 \end{Bmatrix} + \frac{\beta_{41}^e T_\infty^{41} h_{41}^e}{2} \begin{Bmatrix} 1 \\ 0 \\ 0 \\ 1 \end{Bmatrix} \tag{8.5.10b}$$

Similar expressions hold for a quadratic rectangular element.

Axisymmetric Systems

For symmetric heat transfer about the z axis (i.e., independent of the circumferential coordinate), the governing equation is given by

$$-\left[\frac{1}{r}\frac{\partial}{\partial r}\left(rk_r\frac{\partial T}{\partial r}\right) + \frac{\partial}{\partial z}\left(k_z\frac{\partial T}{\partial z}\right)\right] = f(r, z) \tag{8.5.11}$$

where r is the radial coordinate and z is the axial coordinate. We define the flux vector (i.e., negative of heat flux) by

$$\mathbf{q} = \left(k_r\frac{\partial T}{\partial r}\hat{\mathbf{i}} + k_z\frac{\partial T}{\partial z}\hat{\mathbf{j}}\right)$$

and its normal component across the surface is

$$q_n = \left(k_r\frac{\partial T}{\partial r}n_r + k_z\frac{\partial T}{\partial z}n_z\right) \tag{8.5.12}$$

where n_r and n_z are the direction cosines of the unit normal $\hat{\mathbf{n}}$

$$\hat{\mathbf{n}} = n_r\hat{\mathbf{i}} + n_z\hat{\mathbf{j}}$$

The weak form of (8.5.11) is given by

$$\begin{aligned} 0 &= 2\pi\int_{\Omega_e} w\left\{-\left[\frac{1}{r}\frac{\partial}{\partial r}\left(k_r r\frac{\partial T}{\partial r}\right) + \frac{\partial}{\partial z}\left(k_z\frac{\partial T}{\partial z}\right)\right] - f\right\} r\,dr\,dz \\ &= 2\pi\int_{\Omega_e}\left(k_r\frac{\partial w}{\partial r}\frac{\partial T}{\partial r} + k_z\frac{\partial w}{\partial z}\frac{\partial T}{\partial z} - wf\right) r\,dr\,dz - 2\pi\oint_{\Gamma_e} wq_n\,ds \end{aligned} \tag{8.5.13a}$$

where 2π is due to the integration with respect to the circumferential coordinate over $(0, 2\pi)$, and q_n is given by (8.5.12). The convection boundary condition is of the form

$$q_n + \beta(T - T_\infty) = \hat{q}_n \tag{8.5.13b}$$

Substituting for $q_n = -\beta(T - T_\infty) + \hat{q}_n$ into (8.5.13a), we obtain

$$\begin{aligned} 0 = 2\pi\int_{\Omega_e}\left(k_r\frac{\partial w}{\partial r}\frac{\partial T}{\partial r} + k_z\frac{\partial w}{\partial z}\frac{\partial T}{\partial z} - wf\right) r\,dr\,dz \\ -2\pi\oint_{\Gamma_e} w\left[-\beta(T - T_\infty) + \hat{q}_n\right] ds \end{aligned} \tag{8.5.14}$$

The finite element model of (8.5.11) with convective boundary condition (8.5.13*b*) is

$$[K^e + H^e]\{T^e\} = \{f^e\} + \{P^e\} + \{Q^e\} \tag{8.5.15a}$$

where

$$K_{ij}^e = 2\pi \int_{\Omega_e} \left(k_r \frac{\partial \psi_i^e}{\partial r} \frac{\partial \psi_j^e}{\partial r} + k_z \frac{\partial \psi_i^e}{\partial z} \frac{\partial \psi_j^e}{\partial z} \right) r \, dr \, dz$$

$$H_{ij}^e = 2\pi \oint_{\Gamma_e} \beta^e \psi_i^e \psi_j^e \, ds, \quad f_i^e = 2\pi \int_{\Omega_e} \psi_i^e f(r) \, r \, dr \, dz \tag{8.5.15b}$$

$$Q_i^e = 2\pi \oint_{\Gamma_e} \hat{q}_n \psi_i^e \, ds, \quad P_i^e = 2\pi \oint_{\Gamma_e} \beta^e T_\infty^e \psi_i^e \, ds$$

Evaluation of the integrals in $[K^e]$, $[H^e]$, $\{F^e\}$, and $\{P^e\}$ follows from the discussion of Section 8.2.6.

Clearly, the finite element models in (8.5.6*a*) and (8.5.15*a*) are valid for Newton's type (i.e., convective heat transfer) boundary conditions. Radiative heat transfer boundary conditions are nonlinear and therefore are not considered here. For problems with no convective boundary conditions, the convective contributions $[H^e]$ and $\{P^e\}$ to the element coefficients are omitted. In addition, the convective heat transfer contributions have to be included only for those elements whose sides fall on the problem boundary with convection heat transfer specified. For example, if side 2–3 of a linear triangular element Ω_e is on the boundary with convection boundary conditions, then the only contribution to $[H^e]$ and $\{P^e\}$ comes from the second integral of respective expressions in (8.5.7).

Example 8.5.1

Consider steady-state heat conduction in an isotropic rectangular region of dimensions $3a \times 2a$ [see Fig. 8.5.2(*a*)]. The origin of the x and y coordinates is taken at the lower left corner such that x is parallel to the side $3a$ and y is parallel to side $2a$. The boundaries $x = 0$ and $y = 0$ are insulated, the boundary $x = 3a$ is maintained at zero temperature, and the boundary $y = 2a$ is maintained at a temperature $T = T_0 \cos(\pi x/6a)$. We wish to determine the temperature distribution using the finite element method in the region and the heat required at boundary $x = 3a$ to maintain it at zero temperature.

To analyze the problem, first we note that the problem is governed by (8.5.2) with zero internal heat generation, $f = 0$, and no convection boundary conditions:

$$-k\nabla^2 T = 0 \tag{8.5.16}$$

Hence, the finite element model of the problem is given by

$$[K^e]\{T^e\} = \{Q^e\}$$

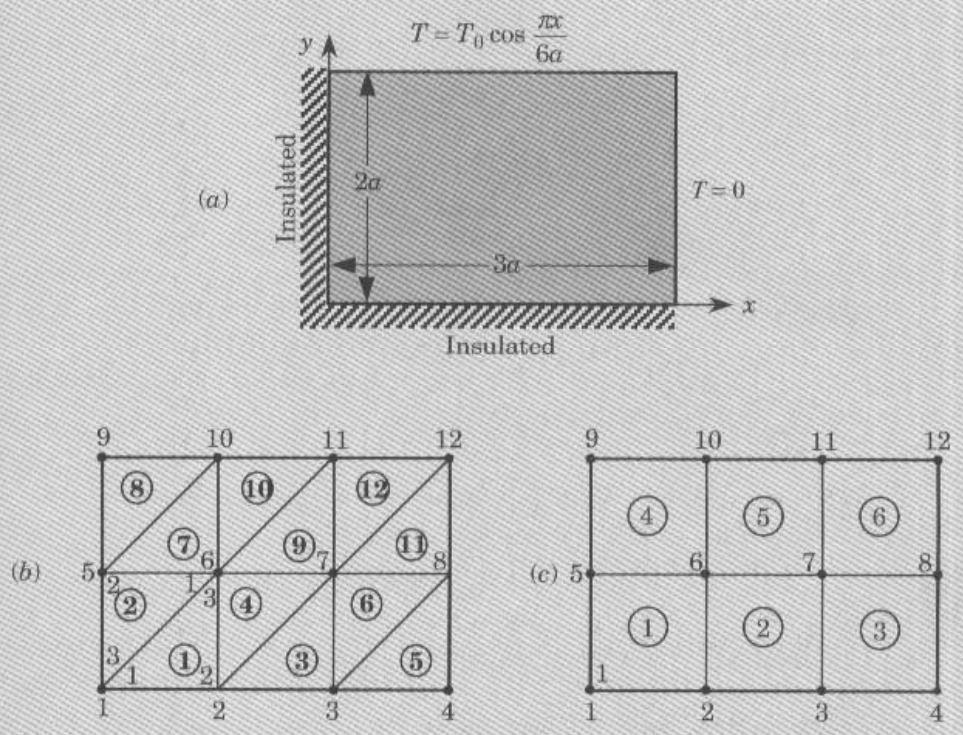

Figure 8.5.2 Finite element analysis of a heat conduction problem over a rectangular domain: (*a*) domain; (*b*) mesh of linear triangular elements; and (*c*) mesh of linear rectangular elements.

where T_i^e is the temperature at node i of element Ω_e, and

$$K_{ij}^e = \int_{\Omega_e} k \left(\frac{\partial \psi_i}{\partial x} \frac{\partial \psi_j}{\partial x} + \frac{\partial \psi_i}{\partial y} \frac{\partial \psi_j}{\partial y} \right) dx\, dy, \quad Q_i^e = \oint_{\Gamma_e} q_n \psi_i \, ds$$

Suppose that we use a 3×2 mesh (i.e., 3 subdivisions along the x axis and 2 subdivisions along the y axis) of linear triangular elements and then with a 3×2 mesh of linear rectangular elements, as shown in Fig. 3.5.2(*b*) and 3.5.2(*c*). Both meshes have the same number of global nodes (12) but differing numbers of elements.

Triangular Element Mesh (12 Elements)

The global node numbers, element numbers, and element node numbers used are shown in Fig. 8.5.2(*b*). Of course, the global node numbering and element numbering is arbitrary (does not have to follow any particular pattern), although the global node numbering dictates the size of the half bandwidth of the assembled equations, which in turn affects the computational time of Gauss elimination methods used in the solution of algebraic equations in a computer. The element node numbering scheme should be the one that is used in the development of element interpolation functions. In the present study a counterclockwise numbering system was adopted (see Figs. 8.2.4 and 8.2.8). By a suitable numbering of the element nodes, all similar elements can be made to have the same element coefficient matrix. Such considerations are important only when hand calculations are carried out.

For a typical element of the mesh of triangles in Fig. 8.5.2(*b*), the element coefficient matrix is given by [see Eqs. (8.3.4) and (8.3.5)],

$$[K^e] = \frac{k}{2}\begin{bmatrix} 1 & -1 & 0 \\ -1 & 2 & -1 \\ 0 & -1 & 1 \end{bmatrix} \tag{8.5.17}$$

where k is the conductivity of the medium. Note that the element matrix is independent of the size of the element, as long as the element is a right-angle triangle with its base equal to its height.

The assembly of the elements (in a computer) follows the logic discussed earlier. For example, we have

$$K_{11} = K_{11}^1 + K_{33}^2 = \frac{k}{2}(1+1), \quad K_{12} = K_{12}^1 = \frac{k}{2}(-1), \quad K_{13} = 0$$

$$K_{15} = K_{32}^2 = \frac{k}{2}(-1), \quad K_{16} = K_{13}^1 + K_{31}^2 = 0 + 0, \quad \text{etc.}$$

$$F_1 = Q_1^1 + Q_3^2, \quad F_6 = Q_3^1 + Q_1^2 + Q_2^4 + Q_2^7 + Q_1^9 + Q_3^{10}, \quad \text{etc.}$$

The boundary conditions require that (U_i denotes the temperature at global node i)

$$\begin{gathered} U_4 = U_8 = U_{12} = 0, \quad U_9 = T_0, \quad U_{10} = \frac{\sqrt{3}}{2}T_0, \quad U_{11} = \frac{T_0}{2} \\ F_1 = F_2 = F_3 = F_5 = 0 \quad \text{(zero heat flow due to insulated boundary)} \end{gathered} \tag{8.5.18}$$

and the balance of internal heat flow requires that

$$F_6 = F_7 = 0 \tag{8.5.19}$$

Thus, the unknown primary variables and secondary variables of the problem are:

$$\begin{gathered} U_1, \quad U_2, \quad U_3, \quad U_5, \quad U_6, \quad U_7 \\ F_4, \quad F_8, \quad F_9, \quad F_{10}, \quad F_{11}, \quad F_{12} \end{gathered}$$

We first write the six finite element equations for the six unknown primary variables. These equations come from rows 1, 2, 3, 5, 6, and 7 (corresponding to the same global nodes):

$$\begin{gathered} K_{11}U_1 + K_{12}U_2 + \cdots + K_{1(12)}U_{12} = F_1 = (Q_1^1 + Q_3^2) = 0 \\ K_{21}U_1 + K_{22}U_2 + \cdots + K_{2(12)}U_{12} = F_2 = (Q_2^1 + Q_1^3 + Q_3^4) = 0 \\ \vdots \\ K_{71}U_1 + K_{72}U_2 + \cdots + K_{7(12)}U_{12} = F_7 = (Q_3^3 + Q_1^4 + Q_2^6 + Q_2^9 + Q_1^{11} + Q_3^{12}) = 0 \end{gathered} \tag{8.5.20}$$

Using the boundary conditions and the values of K_{IJ}, we obtain

$$k\left(U_1 - \frac{1}{2}U_2 - \frac{1}{2}U_5\right) = 0$$

$$k\left(-\frac{1}{2}U_1 + 2U_2 - \frac{1}{2}U_3 - U_6\right) = 0$$

$$k\left(-\frac{1}{2}U_2 + 2U_3 - U_7\right) = 0$$

$$k\left(-\frac{1}{2}U_1 + 2U_5 - U_6 - \frac{1}{2}U_9\right) = 0 \quad (U_9 = T_0)$$

$$k(-U_2 - U_5 + 4U_6 - U_7 - U_{10}) = 0 \quad \left(U_{10} = \frac{\sqrt{3}}{2}T_0\right)$$

$$k(-U_3 - U_6 + 4U_7 - U_{11}) = 0 \quad \left(U_{11} = \frac{1}{2}T_0\right)$$

In matrix form we have

$$\frac{k}{2}\begin{bmatrix} 2 & -1 & 0 & -1 & 0 & 0 \\ -1 & 4 & -1 & 0 & -2 & 0 \\ 0 & -1 & 4 & 0 & 0 & -2 \\ -1 & 0 & 0 & 4 & -2 & 0 \\ 0 & -2 & 0 & -2 & 8 & -2 \\ 0 & 0 & -2 & 0 & -2 & 8 \end{bmatrix} \begin{Bmatrix} U_1 \\ U_2 \\ U_3 \\ U_5 \\ U_6 \\ U_7 \end{Bmatrix} = \frac{k}{2}\begin{Bmatrix} 0 \\ 0 \\ 0 \\ T_0 \\ \sqrt{3}T_0 \\ T_0 \end{Bmatrix} \tag{8.5.21}$$

The solution of these equations is (in °C)

$$\begin{aligned} U_1 &= 0.6362T_0, \quad U_2 = 0.5510T_0, \quad U_3 = 0.3181T_0 \\ U_5 &= 0.7214T_0, \quad U_6 = 0.6248T_0, \quad U_7 = 0.3607T_0 \end{aligned} \tag{8.5.22}$$

The exact solution of (8.5.16) for the boundary conditions shown in Fig. 8.5.2(*a*) is,

$$T(x, y) = T_0 \frac{\cosh(\pi y/6a)\cos(\pi x/6a)}{\cosh(\pi/3)} \tag{8.5.23}$$

Evaluating the exact solution at the nodes, we have (in °C)

$$\begin{aligned} T_1 &= 0.6249T_0, \quad T_2 = 0.5412T_0, \quad T_3 = 0.3124T_0 \\ T_5 &= 0.7125T_0, \quad T_6 = 0.6171T_0, \quad T_7 = 0.3563T_0 \end{aligned} \tag{8.5.24}$$

The heat at node 4, for example, can be computed from the fourth finite element equation

$$\begin{aligned} F_4 = Q_2^5 = K_{41}U_1 + K_{42}U_2 + K_{43}U_3 + K_{44}U_4 + K_{45}U_5 \\ + K_{46}U_6 + K_{47}U_7 + K_{48}U_8 + \cdots \end{aligned} \tag{8.5.25}$$

Noting that $K_{41} = K_{42} = K_{45} = \cdots = K_{4(12)} = 0$ and $U_4 = U_8 = 0$, we obtain

$$Q_2^5 = -\frac{1}{2}kU_3 = -0.1591kT_0 \text{ (in W)} \tag{8.5.26}$$

Rectangular Element Mesh (6 Elements)

For a 3×2 mesh of linear rectangular elements [see Fig. 8.5.2(*c*)], the element coefficient matrix is given by (8.2.55)

$$[K^e] = \frac{k}{6}\begin{bmatrix} 4 & -1 & -2 & -1 \\ -1 & 4 & -1 & -2 \\ -2 & -1 & 4 & -1 \\ -1 & -2 & -1 & 4 \end{bmatrix}, \quad \{f^e\} = \{0\} \tag{8.5.27}$$

The present mesh of rectangular elements is nodewise equivalent to the triangular element mesh considered in Fig. 8.5.2(*b*). Hence the boundary conditions in (8.5.18) and (8.5.19) are valid for the present case. The six finite element equations for the unknowns U_1, U_2, U_3, U_5, U_6, and U_7 again have the same form as those in (8.5.20), with

$$\begin{aligned} &K_{11} = K_{11}^1, \quad K_{12} = K_{12}^1, \quad K_{15} = K_{14}^1 \\ &K_{16} = K_{13}^1, \quad K_{22} = K_{22}^1 + K_{11}^2, \quad K_{23} = K_{12}^2, \quad K_{25} = K_{24}^1 \\ &K_{26} = K_{23}^1 + K_{14}^2, \quad K_{27} = K_{13}^2, \quad \text{etc.} \\ &F_1 = Q_1^1, \quad F_2 = Q_2^1 + Q_1^2, \quad F_3 = Q_2^2 + Q_1^3, \quad F_4 = Q_2^3, \quad \text{etc.} \end{aligned}$$

The equations for the unknown temperatures (i.e., condensed equations for the unknown primary variables) are

$$\frac{k}{6}\begin{bmatrix} 4 & -1 & 0 & -1 & -2 & 0 \\ -1 & 8 & -1 & -2 & -2 & -2 \\ 0 & -1 & 8 & 0 & -2 & -2 \\ -1 & -2 & 0 & 8 & -2 & 0 \\ -2 & -2 & -2 & -2 & 16 & -2 \\ 0 & -2 & -2 & 0 & -2 & 16 \end{bmatrix}\begin{Bmatrix} U_1 \\ U_2 \\ U_3 \\ U_5 \\ U_6 \\ U_7 \end{Bmatrix} = \frac{k}{6}\begin{Bmatrix} 0 \\ 0 \\ 0 \\ T_0 + \sqrt{3}T_0 \\ 2T_0 + \sqrt{3}T_0 + T_0 \\ \sqrt{3}T_0 + T_0 \end{Bmatrix} \tag{8.5.28}$$

Table 8.5.1 Comparison of the nodal temperatures $T(x, y)/T_0$, obtained using various finite element meshes[†] with the analytical solution (Example 8.5.1).

		Triangles		Rectangles		Analytical solution
x	y	3×2	6×4	3×2	6×4	
0.0	0.0	0.6362	0.6278	0.6128	0.6219	0.6249
0.5	0.0	—	0.6064	—	0.6007	0.6036
1.0	0.0	0.5510	0.5437	0.5307	0.5386	0.5412
1.5	0.0	—	0.4439	—	0.4398	0.4419
2.0	0.0	0.3181	0.3139	0.3064	0.3110	0.3124
2.5	0.0	—	0.1625	—	0.1610	0.1617
0.0	1.0	0.7214	0.7148	0.7030	0.7102	0.7125
0.5	1.0	—	0.6904	—	0.6860	0.6882
1.0	1.0	0.6248	0.6190	0.6088	0.6150	0.6171
1.5	1.0	—	0.5054	—	0.5022	0.5038
2.0	1.0	0.3607	0.3574	0.3515	0.3551	0.3563
2.5	1.0	—	0.1850	—	0.1838	0.1844

[†]See Fig. 8.5.2 for the geometry and meshes.

The solution of these equations is (in °C)

$$\begin{aligned} U_1 &= 0.6128T_0, \quad U_2 = 0.5307T_0, \quad U_3 = 0.3064T_0 \\ U_5 &= 0.7030T_0, \quad U_6 = 0.6088T_0, \quad U_7 = 0.3515T_0 \end{aligned} \tag{8.5.29}$$

The value of the heat at node 4 is given by

$$Q_2^3 = K_{43}U_3 + K_{47}U_7 = -\frac{k}{6}U_3 - \frac{2k}{6}U_7 = -0.1682kT_0 \text{ (in W)} \tag{8.5.30}$$

We note that the results obtained using the 3×2 mesh of rectangular elements is not as accurate as that obtained with the 3×2 mesh of triangular elements. This is due to the fact that there are only half as many elements in the former case when compared to the latter. Table 8.5.1 contains a comparison of the finite element solutions with the analytical solution (8.5.23) for two different meshes of linear triangular and rectangular elements.

Example 8.5.2

Consider heat transfer in a rectangular region of dimensions a by b, subjected to the boundary conditions shown in Fig. 8.5.3. We wish to write the finite element algebraic equations for the unknown nodal temperatures and heats. For illustrative purposes a 4×2 mesh of rectangular elements is chosen. We assume that the medium is orthotropic, with conductivities k_x and k_y in the x and y directions, respectively. No internal heat generation is assumed.

The heat transfer in the region is governed by the energy equation

$$-\frac{\partial}{\partial x}\left(k_x \frac{\partial T}{\partial x}\right) - \frac{\partial}{\partial y}\left(k_y \frac{\partial T}{\partial y}\right) = 0 \text{ in } \Omega$$

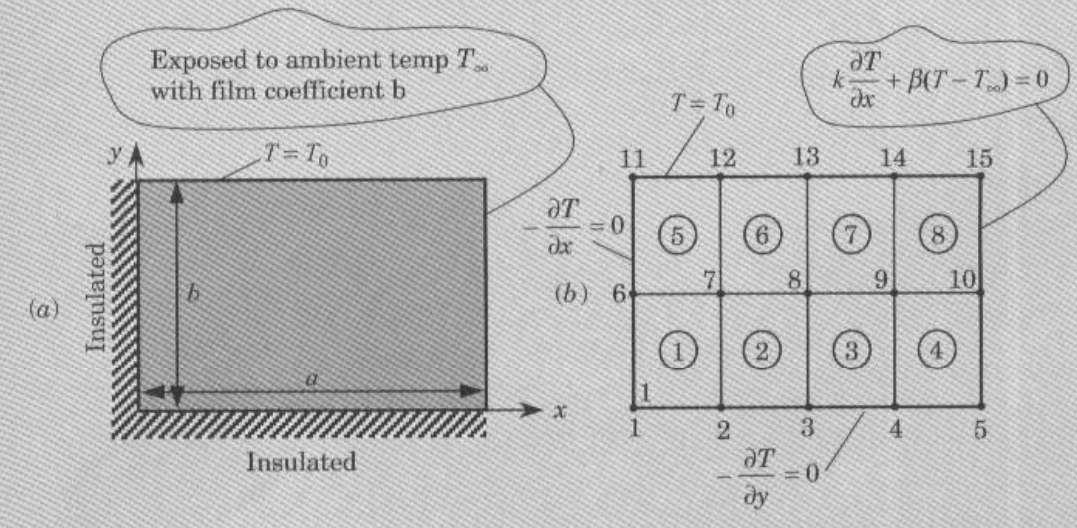

Figure 8.5.3 Domain and boundary conditions for convective heat transfer in a rectangular domain. A mesh of linear rectangular elements is also shown (Example 8.5.2).

The finite element model of the equation is given by

$$[K^e + H^e]\{T^e\} = \{Q^e\} + \{P^e\} \quad (\{f^e\} = \{0\}) \tag{8.5.31}$$

where T_i^e denotes the temperature at node i of element Ω_e, and

$$\begin{aligned} K_{ij}^e &= \int_{\Omega_e} \left(k_x \frac{\partial \psi_i}{\partial x}\frac{\partial \psi_j}{\partial x} + k_y \frac{\partial \psi_i}{\partial y}\frac{\partial \psi_j}{\partial y} \right) dx\, dy \\ H_{ij}^e &= \oint_{\Gamma_e} \beta^e \psi_i \psi_j \, ds \\ Q_i^e &= \oint_{\Gamma_e} q_n \psi_i \, ds, \quad P_i^e = \oint_{\Gamma_e} \beta^e T_\infty^e \psi_i \, ds \end{aligned} \tag{8.5.32}$$

We note that $[H^e]$ and $\{P^e\}$ must be calculated only for elements 4 and 8, which have convective boundaries.

The element matrices for the problem at hand are given by [see Eq. (8.2.53)]

$$[K^e] = \frac{k_x \mu}{6}\begin{bmatrix} 2 & -2 & -1 & 1 \\ -2 & 2 & 1 & -1 \\ -1 & 1 & 2 & -2 \\ 1 & -1 & -2 & 2 \end{bmatrix} + \frac{k_y}{6\mu}\begin{bmatrix} 2 & 1 & -1 & -2 \\ 1 & 2 & -2 & -1 \\ -1 & -2 & 2 & 1 \\ -2 & -1 & 1 & 2 \end{bmatrix} \quad (e = 1, 2, \ldots, 8)$$

$$[H^e] = \frac{\beta_{23}^e h_{23}^e}{6}\begin{bmatrix} 0 & 0 & 0 & 0 \\ 0 & 2 & 1 & 0 \\ 0 & 1 & 2 & 0 \\ 0 & 0 & 0 & 0 \end{bmatrix}, \quad \{P^e\} = \frac{\beta_{23}^e T_\infty^{23} h_{23}^e}{2}\begin{Bmatrix} 0 \\ 1 \\ 1 \\ 0 \end{Bmatrix} \quad (\text{for } e = 4, 8)$$

where μ is the aspect ratio

$$\mu = \frac{1}{2}b \Big/ \frac{1}{4}a = 2b/a$$

There are ten nodal temperatures that are to be determined, and heats at all nodes except nodes 1, 2, 3, 4 and 6 are to be computed. To illustrate the procedure, we write algebraic equations for only representative temperatures and heats.

Node 1 (for Temperatures)

$$K_{11}^1 U_1 + K_{12}^1 U_2 + K_{14}^1 U_6 + K_{13}^1 U_7 = Q_1^1 = 0$$

Node 2 (for Temperatures)

$$K_{21}^1 U_1 + (K_{22}^1 + K_{11}^2) U_2 + K_{12}^2 U_3 + K_{24}^1 U_6 + (K_{23}^1 + K_{14}^2) U_7 + K_{13}^2 U_8 = Q_2^1 + Q_1^2 = 0$$

Node 5 (for Temperatures)

$$K_{21}^4 U_4 + (K_{22}^4 + H_{22}^4) U_5 + K_{24}^4 U_9 + (K_{23}^4 + H_{23}^4) U_{10} = Q_2^4 + P_2^4 = P_2^4 \quad \text{(known)}$$

Node 10 (for Temperatures)

$$K_{31}^4 U_4 + (K_{32}^4 + H_{32}^4)U_5 + (K_{34}^4 + K_{21}^8)U_9 + (K_{33}^4 + H_{33}^4 + K_{22}^8 + H_{22}^8)U_{10} + K_{24}^8 U_{14} + (K_{23}^8 + H_{23}^8)U_{15} = (Q_3^4 + P_3^4) + (Q_2^8 + P_2^8) = P_3^4 + P_2^8 \text{ (known)}$$

Node 14 (for Heat Q_{14})

$$Q_{14} \equiv Q_3^7 + Q_4^8 = K_{31}^7 U_8 + (K_{32}^7 + K_{41}^8)U_9 + K_{42}^8 U_{10} + K_{34}^7 U_{13} + (K_{33}^7 + K_{44}^8)U_{14} + K_{43}^8 U_{15}$$

From the boundary conditions, we know temperatures at nodes 11 through 15 (i.e., U_{11}, $U_{12}, \ldots, U_{15}$ are known values). Substituting the values of K_{ij}^e, H_{ij}^e, and P_i^e, we obtain explicit form of the algebraic equations. For example, the algebraic equation corresponding to node 10 is

$$-\frac{1}{6}\left(k_x\mu + \frac{k_y}{\mu}\right)U_4 + \left[\frac{1}{6}\left(k_x\mu - \frac{2k_y}{\mu}\right) + \frac{1}{12}\beta b\right]U_5 + \frac{1}{6}\left[\left(-2k_x\mu + \frac{2k_y}{\mu}\right) + \left(-2k_x\mu + \frac{k_y}{\mu}\right)\right]U_9 + \frac{2}{3}\left[\left(k_x\mu + \frac{k_y}{\mu}\right) + \frac{\beta b}{2}\right]U_{10} + \frac{1}{6}\left(k_x\mu - \frac{2k_y}{\mu}\right)U_{14} + \frac{1}{6}\left[k_x\mu - \frac{2k_y}{\mu} + \frac{\beta b}{2}\right]U_{15} = \frac{1}{2}\beta b T_\infty$$

This completes the example.

Example 8.5.3

Consider heat transfer in a homogeneous, isotropic medium. The governing equation, in nondimensional form, is given by

$$-\nabla^2 u = f_0 \text{ in } \Omega$$

over the domain shown in Fig. 8.5.4.

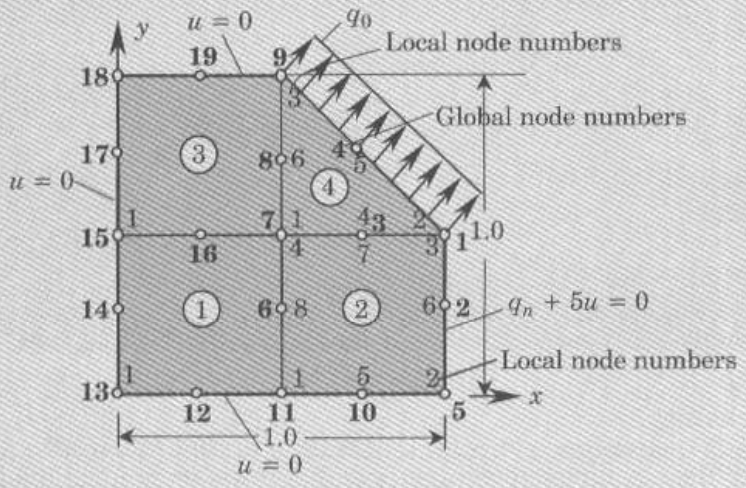

Figure 8.5.4 Domain with finite element mesh and boundary conditions for a heat transfer problem discussed in Example 8.5.3.

We wish to

(*a*) write the finite element equation associated with global node 1 in terms of element coefficients,

(*b*) compute the contribution of the flux q_0 to global nodes 1 and 4, and

(*c*) compute the contribution of the boundary condition $q_n + 5u = 0$ to the finite element equations.

(*a*) The finite element equation associated with global node 1 is

$$K_{11}U_1 + K_{12}U_2 + K_{13}U_3 + K_{14}U_4 + K_{16}U_6 + K_{17}U_7 + K_{18}U_8 = F_1$$

Writing the global coefficients in terms of the element coefficients, we obtain

$$\begin{aligned}&\left(K_{33}^{(2)} + K_{22}^{(4)} + H_{33}^{(2)} + H_{22}^{(4)}\right)U_1 + \left(K_{36}^{(2)} + H_{36}^{(2)}\right)U_2 + \left(K_{37}^{(2)} + K_{24}^{(4)}\right)U_3 \\ &\quad + K_{25}^{(4)}U_4 + K_{38}^{(2)}U_6 + \left(K_{34}^{(2)} + K_{21}^{(4)}\right)U_7 + K_{26}^{(4)}U_8 = F_3^{(2)} + P_3^{(2)} + F_2^{(4)}\end{aligned}$$

Explicit form of H_{ij}^e ($P_i^e = 0$ because $u_\infty = 0$) will be given in Part (*c*).

(*b*) The contributions of uniform flux q_0 to global nodes 1, 4, and 9 are readily known from one-dimensional quadratic element [see Eq. (3.2.37*b*)]. It can be calculated as follows:

$$\begin{aligned}Q_2^4 &= \int_0^L q_0 \psi_2^4(s)\, ds = q_0 \int_0^L \left(1 - \frac{s}{L}\right)\left(1 - \frac{2s}{L}\right) ds \\ &= q_0 \int_0^L \left(1 - 3\frac{s}{L} + \frac{2s^2}{L^2}\right) ds = q_0\left(L - 3\frac{L}{2} + \frac{2L}{3}\right) = \frac{q_0 L}{6} = Q_3^4\end{aligned}$$

where $L = 1/\sqrt{2} = 0.7071$. Similarly, contribution to global node 4 is

$$\begin{aligned}Q_5^4 &= \int_0^L q_0 \psi_5^4(s)\, ds = q_0 \int_0^L 4\frac{s}{L}\left(1 - \frac{s}{L}\right) ds \\ &= 4q_0 \int_0^L \left(\frac{s}{L} - \frac{s^2}{L^2}\right) ds = 4q_0\left(\frac{L}{2} - \frac{L}{3}\right) = \frac{4q_0 L}{6}\end{aligned}$$

(*c*) The contribution of the boundary condition $q_n + 5u = 0$ to the finite element equation associated with node 1 is

$$\begin{aligned}Q_3^2 &= \int_0^{0.5} q_n \psi_3^{(2)}(s)\, ds = -5 \int_0^{0.5} \left(u_2^{(2)}\psi_2^{(2)} + u_6^{(2)}\psi_6^{(2)} + u_3^{(2)}\psi_3^{(2)}\right)\psi_3^{(2)}\, ds \\ &= -5\left(\frac{0.5}{30}\right)(4 \times U_1 + 2 \times U_2 - 1 \times U_5) = -\frac{1}{3}U_1 - \frac{1}{6}U_2\end{aligned}$$

8.5.2 Fluid Mechanics

Here, we consider the equations governing potential flows of an ideal fluid. An *ideal fluid* is one that has zero viscosity and is incompressible. A fluid is said to be *incompressible* if the volume change is zero, (i.e., ρ is constant)

$$\nabla \cdot \mathbf{v} = 0 \tag{8.5.33}$$

where $\mathbf{v}$ is the velocity vector. A fluid is termed *inviscid* if the viscosity is zero, $\mu = 0$. A flow with negligible angular velocity is called *irrotational* if

$$\nabla \times \mathbf{v} = 0 \tag{8.5.34}$$

The irrotational flow of an ideal fluid (i.e., $\rho =$ constant and $\mu = 0$) is called a *potential flow*.

For an ideal fluid, the continuity and the momentum equations can be written as [see Schlichting (1969)]

$$\nabla \cdot \mathbf{v} = 0 \tag{8.5.35a}$$

$$\frac{1}{2}\rho \nabla(\mathbf{v} \cdot \mathbf{v}) - \rho[\mathbf{v} \times (\nabla \times \mathbf{v})] = -\nabla \hat{P} \tag{8.5.35b}$$

where $\nabla \hat{P} = \nabla P - \mathbf{f}$. For irrotational flow the velocity field $\mathbf{v}$ satisfies (8.5.34). For two-dimensional irrotational flows, these equations have the form

$$\frac{\partial v_x}{\partial x} + \frac{\partial v_y}{\partial y} = 0 \tag{8.5.35c}$$

$$\frac{1}{2}\rho\left(v_x^2 + v_y^2\right) + \hat{P} = \text{constant} \tag{8.5.35d}$$

$$\frac{\partial v_x}{\partial y} - \frac{\partial v_y}{\partial x} = 0 \tag{8.5.35e}$$

These three equations are used to determine v_x, v_y, and $\hat{P}$.

The problem of determining v_x, v_y, and $\hat{P}$ is simplified by introducing a function $\psi(x, y)$ such that the continuity equation is identically satisfied:

$$v_x = \frac{\partial \psi}{\partial y}, \quad v_y = -\frac{\partial \psi}{\partial x} \tag{8.5.36}$$

Then the irrotational flow condition in terms of ψ takes the form,

$$\frac{\partial^2 \psi}{\partial y^2} + \frac{\partial^2 \psi}{\partial x^2} \equiv \nabla^2 \psi = 0 \tag{8.5.37}$$

Equation (8.5.37) is used to determine ψ; then velocities v_x and v_y are determined from (8.5.36) and $\hat{P}$ from (8.5.35*d*). The function ψ has the physical significance that lines of constant ψ are lines across which there is no flow, i.e., they are streamlines of the flow. Hence, $\psi(x, y)$ is called the *stream function*.

In the cylindrical coordinates, the continuity equation (8.5.35*a*) takes the form

$$\frac{\partial v_r}{\partial r} + \frac{1}{r}\frac{\partial v_\theta}{\partial \theta} = 0 \tag{8.5.38}$$

where v_r and v_θ are the radial and circumferential velocity components. The stream function $\psi(r, \theta)$ is defined as

$$v_r = \frac{1}{r}\frac{\partial \psi}{\partial \theta}, \quad v_\theta = -\frac{\partial \psi}{\partial r} \tag{8.5.39}$$

and (8.5.37) takes the form

$$\nabla^2\psi \equiv \frac{\partial^2\psi}{\partial r^2} + \frac{1}{r}\frac{\partial\psi}{\partial r} + \frac{1}{r^2}\frac{\partial^2\psi}{\partial\theta^2} = 0 \tag{8.5.40}$$

There exists an alternative formulation of the potential flow equations (8.5.35*a*) and (8.5.35*b*). We can introduce a function $\phi(x, y)$, called the *velocity potential*, such that the condition of irrotational flow, Eq. (8.5.35*e*) is identically satisfied:

$$v_x = -\frac{\partial\phi}{\partial x}, \quad v_y = -\frac{\partial\phi}{\partial y} \tag{8.5.41}$$

Then the continuity equation (8.5.35*c*) takes the form,

$$-\nabla^2\phi = 0 \tag{8.5.42}$$

Comparing (8.5.39) with (8.5.41), we note that

$$-\frac{\partial\phi}{\partial x} = \frac{\partial\psi}{\partial y}, \quad -\frac{\partial\phi}{\partial y} = -\frac{\partial\psi}{\partial x} \tag{8.5.43}$$

The velocity potential has the physical significance that lines of constant ϕ are lines along which there is no change in velocity. The equipotential lines and streamlines intersect at right angles.

Although both ψ and ϕ are governed by the Laplace equation, the boundary conditions on them are different in a flow problem, as should be evident by the definitions (8.5.39) and (8.5.41). In this section, we consider applications of the finite element method to potential flows, i.e., the solution of (8.5.36) and (8.5.43).

We consider two examples of fluid flow. The first one deals with a groundwater flow problem and the second with the flow around a cylindrical body. In discussing these problems, emphasis is placed on certain modeling aspects, data generation, and postprocessing of solutions. Evaluation of element matrices and assembly are amply illustrated in previous examples and will not be discussed as it takes substantial space to write the assembled equations even for the crude meshes used in these examples.

Example 8.5.4 (Groundwater Flow or Seepage)

The governing differential equation for a homogeneous (i.e., material properties do not vary with position) acquifer of unit depth, with flow in the xy plane, is given by

$$-\frac{\partial}{\partial x}\left(a_{11}\frac{\partial\phi}{\partial x}\right) - \frac{\partial}{\partial y}\left(a_{22}\frac{\partial\phi}{\partial y}\right) = f \text{ in } \Omega \tag{8.5.44}$$

where a_{11} and a_{22} are the coefficients of permeability (in $m^3/day/m^2$) along the x and y directions, respectively, ϕ is the piezometric head or velocity potential (in m), measured from a reference level (usually the bottom of the aquifer), and f is the rate of pumping (in $m^3/day/m^3$). We know from the previous discussions that the natural and essential boundary conditions associated with (8.5.44) are as follows:

Natural

$$a_{11}\frac{\partial\phi}{\partial x}n_x + a_{22}\frac{\partial\phi}{\partial y}n_y = \phi_n \quad \text{on } \Gamma_2 \tag{8.5.45}$$

Essential

$$\phi = \phi_0 \quad \text{on } \Gamma_1 \tag{8.5.46}$$

where Γ_1 and Γ_2 are the portions of the boundary Γ of Ω such that $\Gamma_1 + \Gamma_2 = \Gamma$.

Here we consider the following specific problem: Find the lines of constant potential ϕ (equipotential lines) in a 3000 m × 1500 m rectangular aquifer Ω (see Fig. 8.5.5) bounded on the long sides by an impermeable material (i.e., $\partial\phi/\partial n = 0$) and on the short sides by a constant head of 200 m ($\phi_0 = 200$ m). In the way of sources, suppose that a river is passing through the aquifer, infiltrating the aquifer at a rate of $q_0 = 0.24$ m^3/day/m, and that two pumps are located at (830, 1000) and (600, 1900), pumping at a rate of $Q_1 = 1200$ m^3/day and $Q_2 = 2400$ m^3/day, respectively.

A mesh of 64 triangular elements and 45 nodes is used to model the domain [see Fig. 8.5.6(*a*)]. The river forms the interelement boundary between elements (26, 28, 30, 32) and (33, 35, 37, 39). In the mesh selected, neither pump is located at a node. This is done intentionally for the purpose of illustrating the calculation of the generalized forces due to a point source within an element. If the pumps are located at a node, then the rate of pumping Q_0 is input as the specified secondary variable of the node. When a source (or sink) is located at a point other than a node, we must calculate its contribution to the nodes. Similarly, the source components due to the distributed line source (i.e., the river) should be computed.

First, consider the line source. We can view the river as a line source of constant intensity, $q_0 = 0.24$ m^3/day/m. Since the length of the river is equally divided by nodes 21 through 25 (into four parts), we can compute the contribution of the infiltration of the river at each of the nodes 21 through 25 by evaluating the integrals [see Fig. 8.5.6(*b*)]:

$$\text{node 25:} \quad \int_0^h (0.24)\psi_1^1 \, ds$$

$$\text{node 24:} \quad \int_0^h (0.24)\psi_2^1 \, ds + \int_0^h (0.24)\psi_1^2 \, ds$$

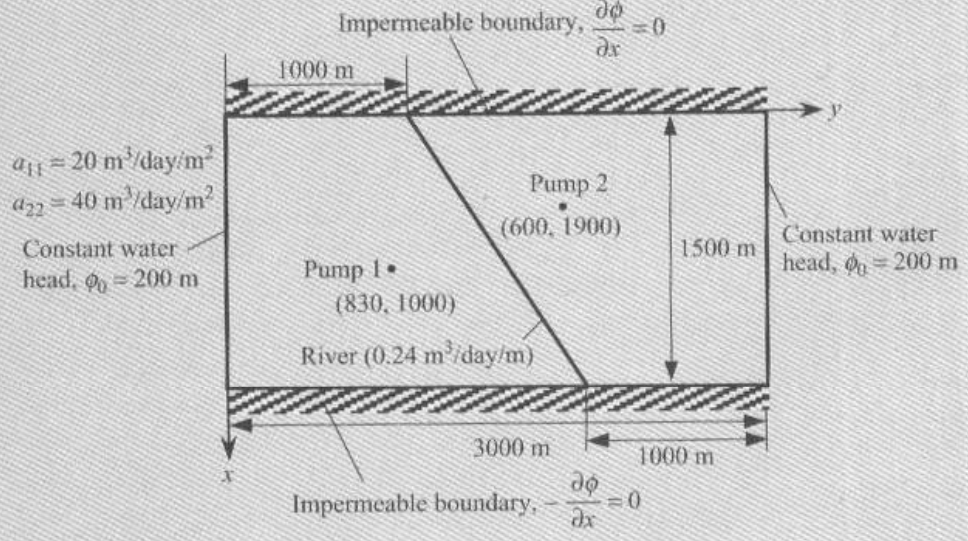

Figure 8.5.5 Geometry and boundary conditions for the groundwater flow problem of Example 8.5.4.

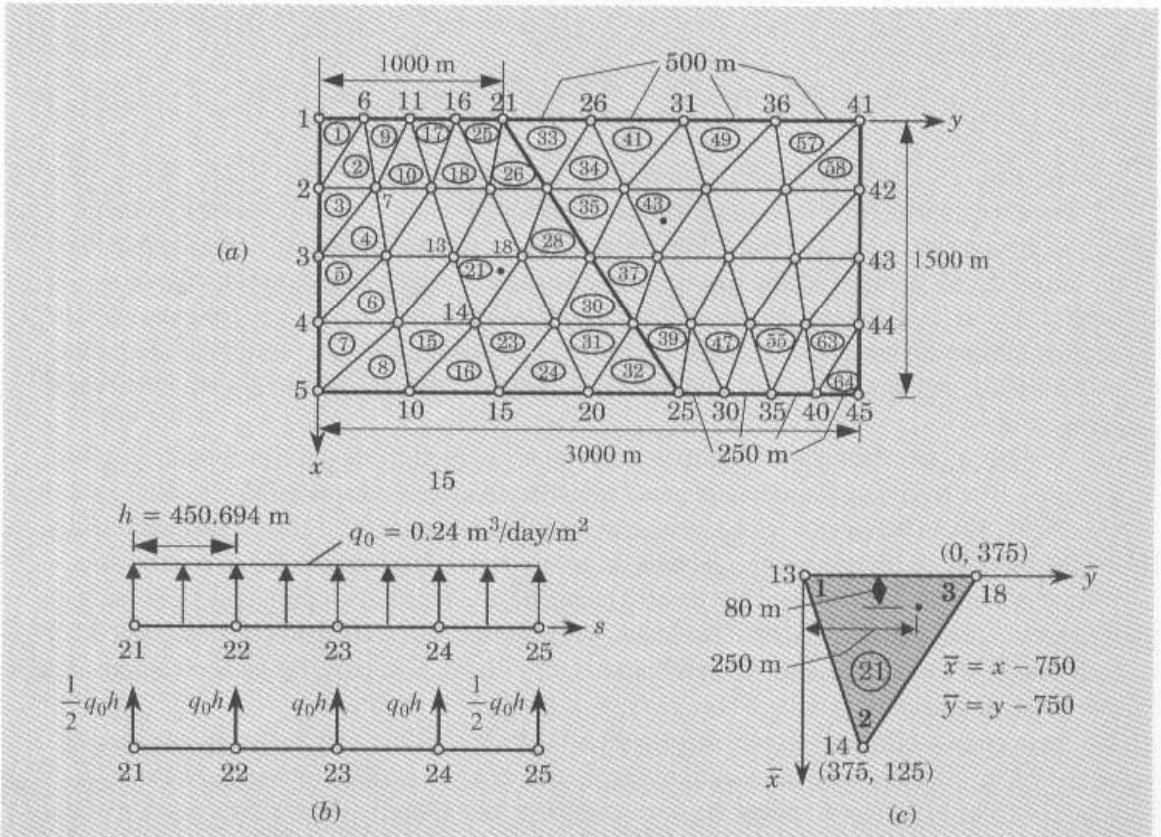

Figure 8.5.6 (*a*) Finite element mesh of triangular elements (45 nodes and 64 elements), (*b*) computation of global forces due to the infiltration of the river, and (*c*) computation of global forces for pump 1 located inside element 21 for the groundwater flow problem of Example 8.5.4.

$$\text{node 23:} \quad \int_0^h (0.24)\psi_2^2\, ds + \int_0^h (0.24)\psi_1^3\, ds$$

$$\text{node 22:} \quad \int_0^h (0.24)\psi_2^3\, ds + \int_0^h (0.24)\psi_1^4\, ds$$

$$\text{node 21:} \quad \int_0^h (0.24)\psi_2^4\, ds$$

For constant intensity q_0 and the linear interpolation functions $\psi_1^e(s) = 1 - s/h$ and $\psi_2^e(s) = s/h$, the contribution of these integrals is well known:

$$\int_0^h q_0 \psi_i^e\, ds = \frac{1}{2} q_0 h, \quad h = \frac{1}{4}[(1000)^2 + (1500)^2]^{\frac{1}{2}}, \quad q_0 = 0.24$$

Hence, we have

$$F_{21} = \frac{1}{2} q_0 h, \quad F_{22} = F_{23} = F_{24} = q_0 h, \quad F_{25} = q_0 h \frac{1}{2}$$

Next, we consider the contribution of the point sources. Since the point sources are located inside an element, we distribute the source to the nodes of the element by interpolation [see Fig. 8.5.6(*c*)]:

$$f_i^e = \int_{\Omega_e} Q_0 \delta(x - x_0, y - y_0) \psi_i^e(x, y)\, dx\, dy = Q_0 \psi_i^e(x_0, y_0)$$

For example, the source at pump 1 (located at $x_0 = 830$ m, $y_0 = 1000$ m) can be expressed as (pumping is considered to be a negative point source)

$$Q_1(x, y) = -1200\, \delta(x - 830, y - 1000) \quad \text{or} \quad Q_1(\bar{x}, \bar{y}) = -1200\, \delta(\bar{x} - 80, \bar{y} - 250)$$

where $\delta(\cdot)$ is the Dirac delta function [see Eq. (3.3.3)]. The interpolation functions ψ_i^e for element 21 are [in terms of the local coordinates $\bar{x}$ and $\bar{y}$; see Fig. 8.5.6(*c*)]

$$\psi_i(\bar{x}, \bar{y}) = \frac{1}{2A}(\alpha_i + \beta_i \bar{x} + \gamma_i \bar{y}), \quad (i = 1, 2, 3)$$

$$2A = (375)^2, \quad \alpha_1 = (375)^2, \quad \alpha_2 = 0, \quad \alpha_3 = 0$$

$$\beta_1 = -250, \quad \beta_2 = 375, \quad \beta_3 = -125, \quad \gamma_1 = -375, \quad \gamma_2 = 0, \quad \gamma_3 = 375$$

Therefore, we have

$$\psi_1(80, 250) = 0.1911, \quad \psi_2(80, 250) = 0.5956, \quad \psi_3(80, 250) = 0.2133$$

Similar computations can be done for pump 2 (see Problem 8.8).

In summary, primary variables and nonzero secondary variables are:

$$U_1 = U_2 = U_3 = U_4 = U_5 = U_{41} = U_{42} = U_{43} = U_{44} = U_{45} = 200.0$$

$$F_{21} = 54.0833, \quad F_{22} = F_{23} = F_{24} = 108.1666, \quad F_{25} = 54.0833$$

$$F_{13} = -229.33, \quad F_{14} = -256.0, \quad F_{18} = -714.67, \quad F_{27} = -411.429$$

$$F_{28} = -1440.0, \quad F_{32} = -548.571$$

The secondary variables at nodes 6–12, 15–17, 19, 20, 26, 29–31, and 33–40 are zero. This completes the data generation for the problem.

The assembled equations are solved after imposing the specified boundary conditions for the values of ϕ at the nodes. The equipotential lines can be determined using (8.3.27). The lines of constant ϕ are shown in Fig. 8.5.7(*a*).

The velocity components are determined in the postcomputation using the definition (8.5.41)

$$v_x = -\frac{\partial \phi}{\partial x}, \quad v_y = -\frac{\partial \phi}{\partial y}$$

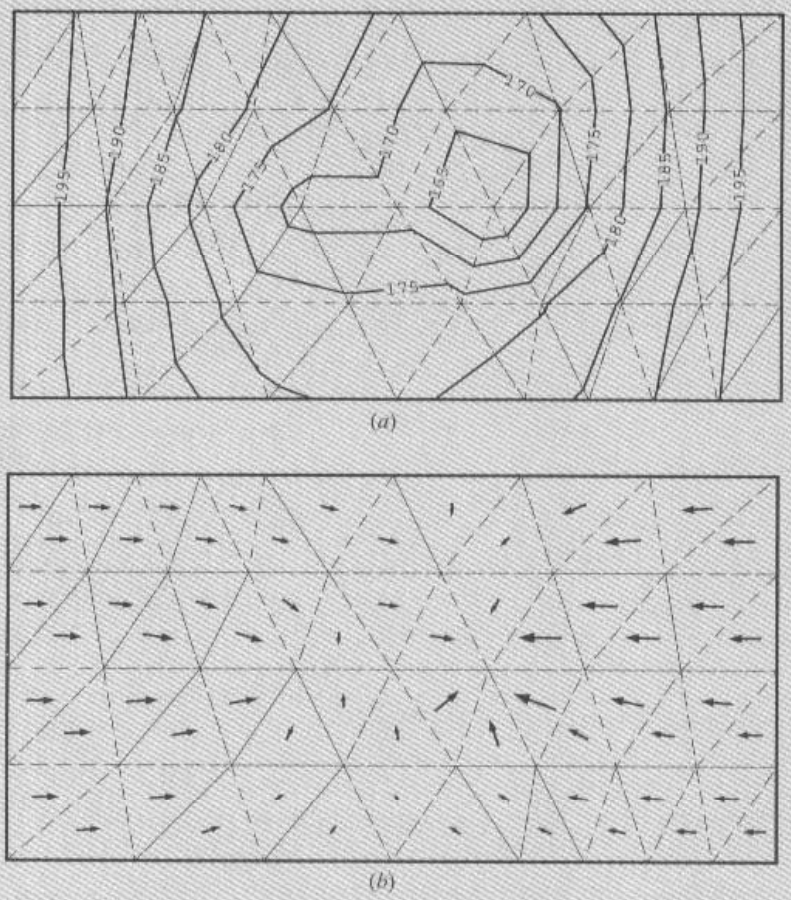

Figure 8.5.7 Plots of constant piezometric head and velocity vector for the groundwater flow: (*a*) lines of constant ϕ; and (*b*) plot of velocity vectors (Example 8.5.4).

and the velocity vector is given by

$$\mathbf{v} = v_x \hat{\mathbf{i}} + v_y \hat{\mathbf{j}}, \quad |\mathbf{v}| = \sqrt{v_x^2 + v_y^2}, \quad \theta = \tan^{-1} \frac{v_y}{v_x}$$

where θ is the angle, measured in counterclockwise direction, of the velocity vector form along the +ve x axis. The velocity vectors for the problem at hand are shown in Fig. 8.5.7(*b*). The greatest drawdown of water occurs at node 28, which has the largest portion of discharge from pump 2. This completes the discussion of the groundwater flow problem.

Next, we consider an example of irrotational flows of an ideal fluid (i.e., a nonviscous fluid). Examples of physical problems that can be approximated by such flows are provided by flow around bodies such as weirs, airfoils, buildings, and so on, and by flow of water through the earth and dams. Laplace equations (8.5.37) and (8.5.42) governing these flows are a special case of (8.2.1) and therefore, we can use the finite element equations developed earlier to model these problems.

Example 8.5.5 (Confined Flow around a Circular Cylinder)

The irrotational flow of an ideal fluid about a circular cylinder, placed with its axis perpendicular to the plane of the flow between two *long* horizontal walls (see Fig. 8.5.8) is to be analyzed using the finite element method. The equation governing the flow is given by

$$-\nabla^2 u = 0 \quad \text{in } \Omega$$

where u is either (a) the stream function or (b) the velocity potential. If u is the stream function ψ, the velocity components $\mathbf{v} = (v_x, v_y)$ of the flow field are given by

$$v_x = \frac{\partial \psi}{\partial y}, \quad v_y = -\frac{\partial \psi}{\partial x}$$

If u is the velocity potential, ϕ, the velocity components can be computed from

$$v_x = -\frac{\partial \phi}{\partial x}, \quad v_y = -\frac{\partial \phi}{\partial y}$$

In either case, the velocity field is not affected by a constant term in the solution u. We analyze the problem using both formulations. For both formulations, symmetry exists about the horizontal and vertical center lines, therefore, only a quadrant of the flow region is used as the computational domain. To determine the constant state of the solution, which does not affect the velocity field, we arbitrarily set the functions ψ and ϕ to zero (or a constant) on appropriate boundary lines.

Stream Function Formulation

The boundary conditions on the stream function ψ can be determined as follows. Streamlines have the property that flow perpendicular to a streamline is zero. Therefore, the fixed walls correspond to streamlines. Note that for inviscid flows, fluid does not stick to rigid walls. Due to the biaxial symmetry about the horizontal and vertical centerlines, only a quadrant (say, ABCDE in Fig. 8.5.9) of the domain need be used in the analysis. The fact that the velocity component perpendicular to the horizontal line of symmetry is equal to zero allows us to use that line as a streamline. Since the velocity field depends on the relative difference of two

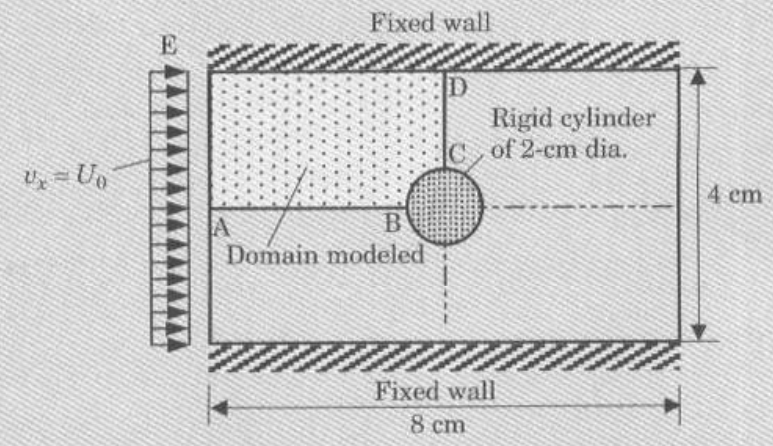

Figure 8.5.8 Domain and boundary conditions for the stream function and velocity potential formulations of irrotational flow about a cylinder (Example 8.5.5).

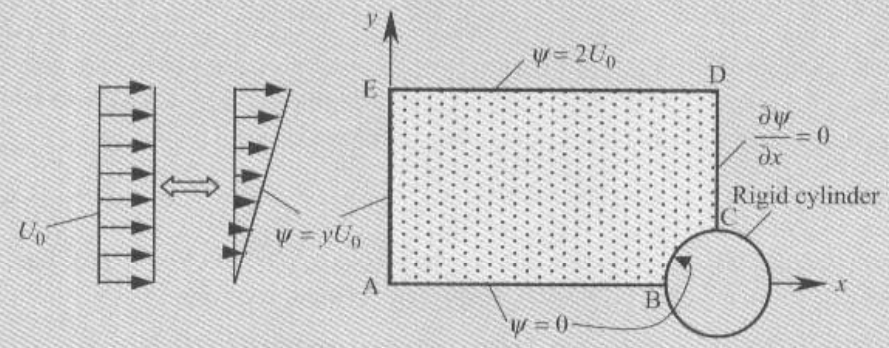

Figure 8.5.9 Computational domain and boundary conditions for the stream function formulation of inviscid flow around a cylinder (see Fig. 8.5.8).

streamlines, we take the value of the stream function that coincides with the horizontal axis of symmetry (i.e., on ABC) to be zero and then determine the value of ψ on the upper wall from the condition

$$\frac{\partial \psi}{\partial y} = U_0$$

where U_0 is the inlet horizontal velocity of the field. We determine the value of the stream function on the boundary $x = 0$ by integrating the above equation with respect to y

$$\int_0^y \frac{d\psi}{dy}\, dy = \int_0^y U_0\, dy + \psi_A = U_0 y + 0 \tag{8.5.47}$$

because $\psi_A = 0$ by the previous discussion. This gives the boundary condition on AE. Since the line ED is a streamline and its value at point E is $2U_0$, it follows that $\psi = 2U_0$ on line ED. Lastly, on CD we assume the vertical velocity is zero (i.e., $v_x = 0$); hence, $\partial\psi/\partial x = 0$ on CD. The boundary conditions are shown on the computational domain in Fig. 8.5.9.

In selecting a mesh, we should note that the velocity field is uniform (i.e., streamlines are horizontal) at the inlet and that it takes a parabolic profile at the exit (along CD). Therefore, the mesh at the inlet should be uniform, and the mesh close to the cylinder should be relatively more refined to be able to model the curved boundary and capture the rapid change in ψ. Two coarse finite element meshes are used to discuss the boundary conditions, and results for refined meshes will be discussed subsequently. Mesh T1 consists of 32 triangular elements and mesh Q1 consists of 16 quadrilateral elements. Both meshes contain 25 nodes (see Fig. 8.5.10). The mesh with solid lines in Fig. 8.5.10 corresponds to mesh Q1, and the mesh with solid and dashed lines in Fig. 8.5.10 correspond to mesh T1. It should be noted that the discretization error is not zero for this case.

The specified primary degrees of freedom (i.e., nodal values of ψ) for mesh T1 and mesh Q1 are:

$$\begin{gathered} U_1 = U_2 = \cdots = U_6 = U_{12} = U_{18} = U_{24} = U_{30} = U_{36} = U_{42} = 0.0 \\ U_7 = 1.333, \quad U_{13} = 0.667, \quad U_{19} = U_{25} = U_{31} = U_{37} = 2.0 \end{gathered} \tag{8.5.48}$$

There are no nonzero specified secondary variables; the secondary variables are specified to be zero at the nodes on line CD:

$$F_{38} = F_{39} = F_{40} = F_{41} = 0$$

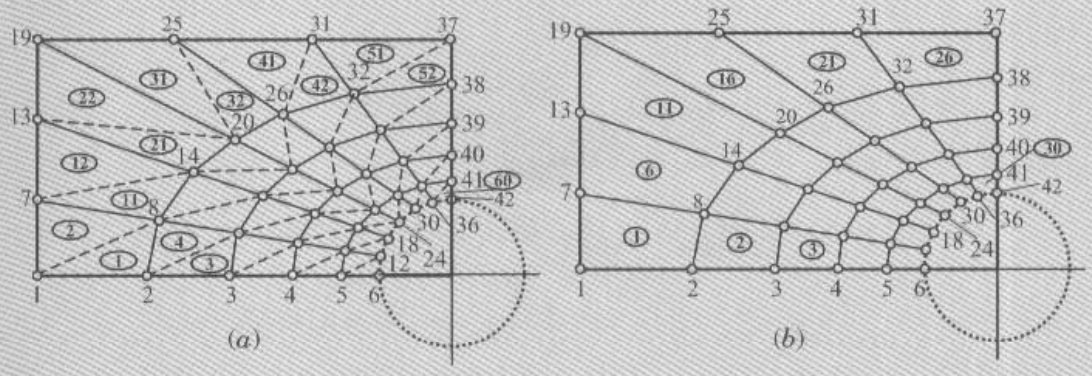

Figure 8.5.10 Meshes used for inviscid flow around a cylinder. (*a*) Mesh of linear triangles. (*b*) Mesh of linear quadrilaterals.

Although the secondary variable is specified to be zero at nodes 37 and 42, where the primary variable is also specified, we choose to impose the boundary conditions on the primary variable over the secondary variables.

Velocity Potential Formulation (PF)

The boundary conditions on the velocity potential ϕ can be derived as follows (see Fig. 8.5.11). The fact that $v_y = -\partial\phi/\partial y = 0$ (no penetration) on the upper wall as well as on the horizontal line of symmetry gives the boundary conditions there. Along AE the velocity $v_x = -\partial\phi/\partial x$ is specified to be U_0. On the surface of the cylinder the normal velocity, $v_n = -\partial\phi/\partial n$, is zero. Thus, all boundary conditions, so far, are of the flux type. On the boundary CD we must know either ϕ or $\partial\phi/\partial n = \partial\phi/\partial x$. It is clear that $-\partial\phi/\partial x = v_x$ is not known on CD. Therefore, we assume that ϕ is known, and we set it equal to $\phi_0 =$ constant. The constant ϕ_0 is arbitrary, and it does not contribute to the velocity field (because $-\partial\phi/\partial x = v_x$ and $-\partial\phi/\partial y = v_y$ are independent of the constant ϕ_0). It should be noted that determining the constant part in the solution for ϕ (i.e., eliminating the rigid body motion) requires knowledge of ϕ at one or more points of the mesh. We take $\phi = \phi_0 = 0$ on CD.

The mathematical boundary conditions of the problem must be translated into finite element data. The boundary conditions on the primary variables come from the boundary CD. We have

$$U_{37} = U_{38} = U_{39} = U_{40} = U_{41} = U_{42} = 0.0$$

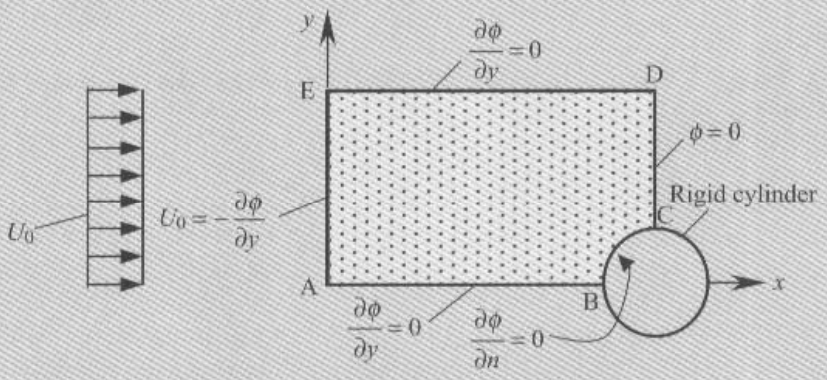

Figure 8.5.11 Computational domain and boundary conditions for the velocity potential formulation of inviscid flow around a cylinder (see Fig. 8.5.8).

The only nonzero boundary conditions on the secondary variables come from the boundary AE. There, we must evaluate the boundary integral

$$\int_{\Gamma_e} \frac{\partial \phi}{\partial n} \psi_i \, ds = U_0 \int_{AE} \psi_i(y) \, dy$$

for each node i on AE. We obtain ($h = 2/3 = 0.66667$)

$$Q_1 = U_0 \int_0^h \left(1 - \frac{\bar{y}}{h}\right) d\bar{y} = 0.33333 U_0$$

$$Q_7 = U_0 \int_0^h \frac{\bar{y}}{h} d\bar{y} + U_0 \int_0^h \left(1 - \frac{\bar{y}}{h}\right) d\bar{y} = 0.66667 U_0$$

$$Q_{13} = U_0 \int_0^h \frac{\bar{y}}{h} d\bar{y} + U_0 \int_0^h \left(1 - \frac{\bar{y}}{h}\right) d\bar{y} = 0.66667 U_0$$

$$Q_{19} = U_0 \int_0^h \frac{\bar{y}}{h} d\bar{y} = \frac{h U_0}{2} = 0.3333 U_0$$

Numerical Results

Table 8.5.2 contains the values of the stream function and its derivative $(\partial \psi / \partial y)(= v_x)$ at selected *points/elements* of the meshes. The finite element program **FEM2D** (see Chapter 13 for details) is used in the analysis. The stream function values obtained with mesh T1 and mesh Q1 are very close to each other. Recall that the derivative $\partial \psi / \partial y$ is constant in a linear triangular element, whereas it varies linearly with x in a linear rectangular element. Therefore, mesh T1 and mesh Q1 results will not be the same. The velocities included in Table 8.5.2 correspond to elements closest to the symmetry line (i.e., $y = 0$ line) and surface of the cylinder.

The tangential velocity v_t on the cylinder surface can be computed from the relation,

$$v_t(\theta) = v_x \sin\theta + v_y \cos\theta = \frac{\partial \psi}{\partial y} \sin\theta - \frac{\partial \psi}{\partial x} \cos\theta \tag{8.5.49}$$

Contour plots of streamlines, velocity potential, and horizontal velocity $v_x = \partial \psi / \partial y$ obtained with mesh Q1 are shown in Fig. 8.5.12. Note that there is a difference between the

Table 8.5.2 Finite element results from the stream function formulation of inviscid flow around a cylinder (Example 8.5.5).

		Stream function		Velocity $v_x = \partial\psi/\partial y$		Velocity $v_x = -\partial\phi/\partial x$	
x	y	Mesh T1	Mesh Q1	Mesh T1	Mesh Q1	Mesh T1	Mesh Q1
1.3183	0.7354	0.7092	0.7095	0.9643(1)[†]	0.9852(1)	0.9922(1)	0.9989(1)
2.2705	0.5444	0.4372	0.4379	0.8032(3)	0.9005(2)	0.9371(3)	0.9408(2)
2.8564	0.4268	0.1667	0.1650	0.3906(5)	0.6432(3)	0.7047(5)	0.7018(3)
1.4112	1.4459	1.4241	1.4270	0.0000(7)	0.2679(4)	0.2999(7)	0.3197(4)
2.4305	1.0457	0.8730	0.8823	0.4469(15)	0.8746(8)	0.6469(15)	0.8364(8)
3.0577	0.7995	0.3357	0.3384	1.636(24)	1.586(12)	1.873(24)	1.453(12)
2.6931	1.5388	1.3758	1.4010	2.544(32)	2.4551(16)	2.163(32)	2.075(16)
3.1937	1.2057	0.7706	0.7980				
3.5018	1.0007	0.2520	0.2658				
4.0000	1.5714	1.2395	1.2065				
4.0000	1.2619	0.6191	0.5796				
4.0000	1.0714	0.1817	0.1588				

[†]The numbers in parentheses denote element number; the derivatives of ψ and ϕ are evaluated at the center of this element.

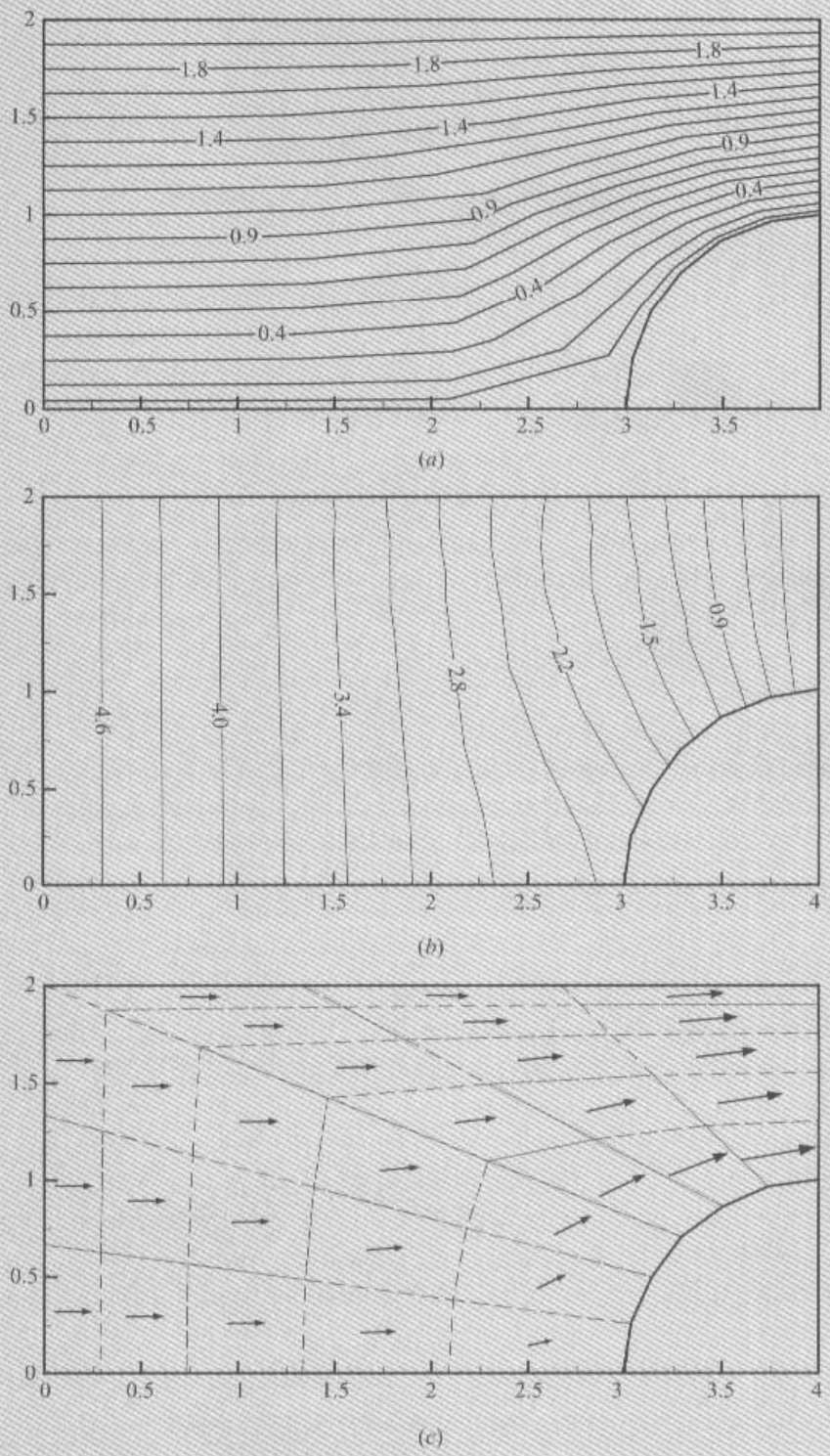

Figure 8.5.12 Contours of (*a*) stream function, (*b*) velocity potential, and (*c*) x component of velocity (with the velocity potential formulation), as obtained using mesh Q1.

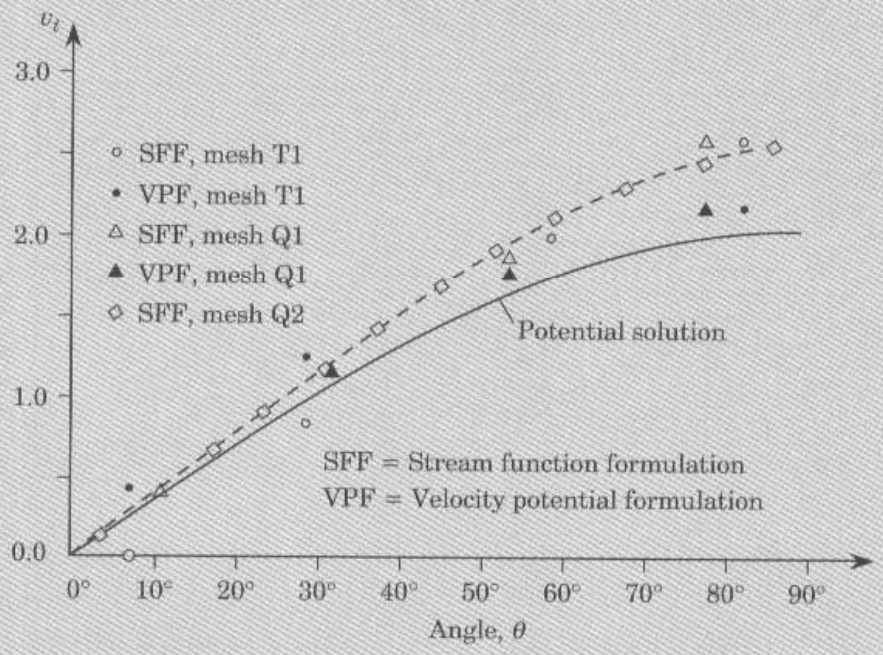

Figure 8.5.13 Variation of the tangential velocity along the cylinder surface: comparison of the finite element results with the potential theory solution (mesh Q2 contains 96 elements and 117 nodes).

velocities obtained with the two formulations (for either mesh). This is primarily due to the nature of the boundary value problems in the two formulations. In the stream function formulation, there are more boundary conditions on the primary variable than in the velocity potential formulation.

A plot of the variation of the tangential velocity with the angular distance along the cylinder surface is shown in Fig. 8.5.13 along with the analytical potential solution

$$v_t = U_0(1 + R^2/r^2)\sin\theta \tag{8.5.50a}$$

valid on the cylinder surface. The finite element solution of a refined mesh, mesh Q2, is also included in the figure. The angle θ, radial distance r, and tangential velocity v_t can be computed from the relations

$$\theta = \tan^{-1}\left(\frac{y}{4-x}\right), \quad r = \sqrt{(4-x)^2 + y^2}, \quad v_t = v_x \sin\theta + v_y \cos\theta \tag{8.5.50b}$$

The finite element solution is in general agreement with the potential solution of the problem. However, the finite element solution is not expected to agree closely because v_t is evaluated at a radial distance $r > R$, whereas the potential solution is evaluated at $r = R$ only.

This completes the section on fluid mechanics problems that are cast in terms of a single dependent unknown, such as the stream function or velocity potential. We return to fluid

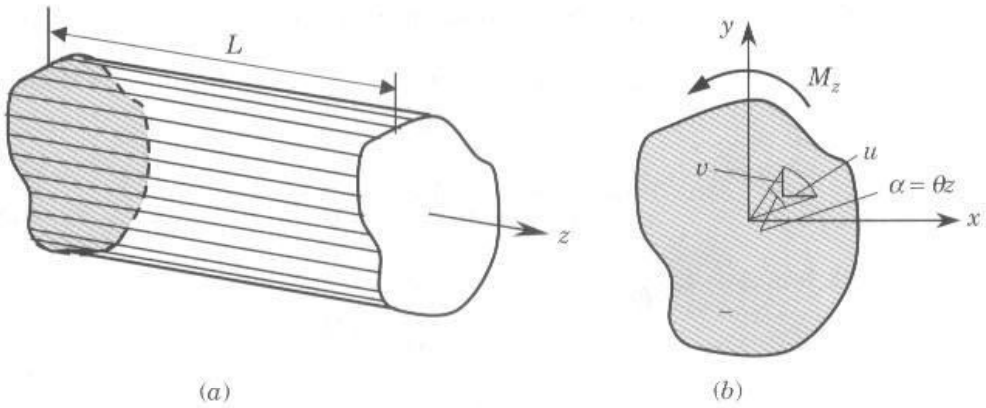

Figure 8.5.14 Torsion of cylindrical members: (*a*) a cylindrical member and (*b*) domain of analysis.

mechanics later in Chapter 10 to consider two-dimensional flows of viscous, incompressible fluids. The governing equations of such problems consist of several dependent variables and as many differential equations.

8.5.3 Solid Mechanics

In this section we consider two-dimensional boundary value problems of solid mechanics that are cast in terms of a single dependent unknown. These problems include torsion of cylindrical members and transverse deflection of membranes. This study is restricted to small deformations.

Torsion of Cylindrical Members

Consider a cylindrical bar (i.e., a long, uniform cross-sectional member), fixed at one end and twisted by a couple (i.e., torque) of magnitude M_z that is directed along the axis (z) of the bar, as shown in Fig. 8.5.14(*a*). We wish to determine the amount of twist and the associated stress field in the bar. To this end, we first derive the governing equations and then analyze the equation using the finite element method.

In general, a noncircular cross-sectional member subjected to torsional moment experiences warping at any section. We assume that all cross sections warp in the same way (which holds true for small twisting moments and deformation). This assumption allows us to assume that the displacements (u, v, w) along the coordinates (x, y, z) are of the form [see Fig. 8.5.14(*b*)]

$$u = -\theta z y, \quad v = \theta z x, \quad w = \theta \phi(x, y) \tag{8.5.51}$$

where $\phi(x, y)$ is a function to be determined and θ is the angle of twist per unit length of the bar.

The displacement field in (8.5.51) can be used to compute the strains, and stresses are computed using an assumed constitutive law. The stresses thus computed must satisfy the

three-dimensional equations of stress equilibrium in Eq. (2.3.52):

$$\begin{aligned}
\frac{\partial \sigma_{xx}}{\partial x}+\frac{\partial \sigma_{xy}}{\partial y}+\frac{\partial \sigma_{xz}}{\partial z}&=0\\
\frac{\partial \sigma_{xy}}{\partial x}+\frac{\partial \sigma_{yy}}{\partial y}+\frac{\partial \sigma_{yz}}{\partial z}&=0\\
\frac{\partial \sigma_{xz}}{\partial x}+\frac{\partial \sigma_{yz}}{\partial y}+\frac{\partial \sigma_{zz}}{\partial z}&=0
\end{aligned} \tag{8.5.52}$$

and the stress boundary conditions on the lateral surface and at the end of the cylindrical bar. Calculation of strains and then stresses using the generalized Hooke's law gives the expressions,

$$\sigma_{xz}=G\theta\left(\frac{\partial \phi}{\partial x}-y\right), \quad \sigma_{yz}=G\theta\left(\frac{\partial \phi}{\partial y}+x\right) \tag{8.5.53}$$

and all other stresses are identically zero. Here G denotes the shear modulus of the material of the bar. Substitution of these stresses into (8.5.52) yields [the first two equations in (8.5.52) are identically satisfied and the third one leads to the following equation]:

$$\frac{\partial}{\partial x}\left(G\theta\frac{\partial \phi}{\partial x}\right)+\frac{\partial}{\partial y}\left(G\theta\frac{\partial \phi}{\partial y}\right)=0 \tag{8.5.54}$$

throughout the cross section Ω of the cylinder. The boundary conditions on the lateral surfaces Γ require that $\sigma_{xz}n_x+\sigma_{yz}n_y=0$:

$$\left(\frac{\partial \phi}{\partial x}-y\right)n_x+\left(\frac{\partial \phi}{\partial y}+x\right)n_y=0 \Rightarrow \frac{\partial \phi}{\partial n}=yn_x-xn_y \tag{8.5.55}$$

Here (n_x, n_y) denote the direction cosines of the unit normal at a point on Γ.

In summary, the torsion of a cylindrical bar is governed by the equations (8.5.54) and (8.5.55). The function $\phi(x, y)$ is called the *torsion function* or *warping function*. Since the boundary condition in (8.5.55) is of the flux type, the function can be determined within an additive constant. The stresses in (8.5.53), however, are independent of this constant. The additive constant has the meaning of rigid body movement of the cylinder as a whole in the z-direction. For additional discussion of the topic the reader is referred to Timoshenko and Goodier (1970).

The Laplace equation (8.5.54) and the Neumann boundary condition (8.5.55) governing ϕ are not convenient in the analysis because of the nature and form of the boundary condition, especially for irregular cross-sectional members. The theory of analytic functions can be used to rewrite these equations in terms of the *stress function* $\Psi(x, y)$, which is related to the warping function $\phi(x, y)$ by the equations

$$\frac{\partial \Psi}{\partial x}=-\frac{\partial \phi}{\partial y}-x, \quad \frac{\partial \Psi}{\partial y}=\frac{\partial \phi}{\partial x}-y \tag{8.5.56}$$

Eliminating ϕ from (8.5.54) and (8.5.55) gives, respectively, the results

$$-\left(\frac{\partial^2\Psi}{\partial x^2}+\frac{\partial^2\Psi}{\partial y^2}\right)=2 \tag{8.5.57}$$

$$\frac{\partial\Psi}{\partial y}n_x-\frac{\partial\Psi}{\partial x}n_y=0 \tag{8.5.58}$$

The left side of (8.5.58) denotes the tangential derivative $d\Psi/ds$, and $d\Psi/ds=0$ implies that

$$\Psi=\text{constant} \quad \text{on } \Gamma$$

Since the constant part of Ψ does not contribute to the stress field

$$\sigma_{xz}=G\theta\frac{\partial\Psi}{\partial y}, \quad \sigma_{yz}=-G\theta\frac{\partial\Psi}{\partial x} \tag{8.5.59}$$

we can take $\Psi=0$ on the boundary.

In summary, the torsion problem can now be stated as one of determining the stress function Ψ such that

$$\begin{aligned} -\nabla^2\Psi &= 2 \quad \text{in } \Omega \\ \Psi &= 0 \quad \text{on } \Gamma \end{aligned} \tag{8.5.60}$$

Once Ψ is determined, the stresses can be computed from (8.5.59) for a given angle of twist per unit length (θ) and shear modulus (G).

The finite element model of (8.5.60) follows immediately from that of Eq. (8.2.1):

$$[K^e]\{u^e\}=\{f^e\}+\{Q^e\} \tag{8.5.61a}$$

where u_i^e is the value of Ψ at the ith node of Ω_e and

$$\begin{aligned} K_{ij}^e &= \int_{\Omega_e}\left(\frac{\partial\psi_i}{\partial x}\frac{\partial\psi_j}{\partial x}+\frac{\partial\psi_i}{\partial y}\frac{\partial\psi_j}{\partial y}\right)dx\,dy \\ f_i^e &= \int_{\Omega_e}2\psi_i\,dx\,dy \quad Q_i^e=\oint_{\Gamma_e}\frac{\partial\Psi}{\partial n}\psi_i\,ds \end{aligned} \tag{8.5.61b}$$

Example 8.5.6 (Torsion of a Square Cross-Sectional Bar)

Here we consider torsion of a square ($a\times a$) cross-section bar. Note that the problem is antisymmetric as far as the loading and stress distribution are concerned; however, the stress function, being a scalar function governed by the Poisson equation (8.5.60), is symmetric about the x and y axes as well as the diagonal lines. When using rectangular elements, one quadrant of the bar cross section can be used in the finite element analysis. The biaxial symmetry about the x and y axes requires imposition of the following boundary conditions on Ψ (see Example 8.3.1):

$$\frac{\partial\Psi}{\partial x}=0 \quad \text{on the line } x=0, \qquad \frac{\partial\Psi}{\partial y}=0 \quad \text{on the line } y=0$$

In addition, on the actual boundary we have the condition $\Psi=0$ on lines $x=a$ and $y=b=a$.

Table 8.5.3 Convergence of the finite element solutions for Ψ using linear and quadratic rectangular elements (four-node and nine-node elements) in Example 8.5.6.

		Linear elements			Quadratic elements†		
x	y	2×2	4×4	8×8	1×1	2×2	4×4
0.0000	0.0000	0.15536	0.14920	0.14780	0.14744	0.14730	0.14734
0.0625	0.0000	—	—	0.14583	—	—	0.14538
0.1250	0.0000	—	0.14120	0.13987	—	0.13941	0.13944
0.1875	0.0000	—	—	0.12972	—	—	0.12931
0.2500	0.0000	0.12054	0.11610	0.11502	0.11378	0.11463	0.11467
0.3125	0.0000	—	—	0.09534	—	—	0.09505
0.3750	0.0000	—	0.07069	0.07007	—	0.069873	0.06986
0.4375	0.0000	—	—	0.03854	—	—	0.03844
0.1250	0.2500	—	0.11031	0.10925	—	0.10887	0.10890
0.2500	0.2500	0.09643	0.09191	0.09090	0.09095	0.09056	0.09057
0.3750	0.2500	—	0.05729	0.05660	—	0.05626	0.05636

†The 4×4 mesh of nine-node quadratic elements gives a solution that coincides with the analytical solution to five significant decimal places.

The results of a convergence study are summarized in Tables 8.5.3 and 8.5.4. The analytical solution of the problem is given by [see (2.5.40)]

$$\Psi(x,y)=\frac{a^2}{4}-x^2-\frac{8a^2}{\pi^3}\sum_{n=0}^{\infty}\frac{(-1)^n}{(2n+1)^3}\frac{\cosh\,k_n y\cos\,k_n x}{\cosh(k_n b/2)} \tag{8.5.62a}$$

$$\sigma_{xz}=-\frac{8aG\theta}{\pi^2}\sum_{n=0}^{\infty}\frac{(-1)^n}{(2n+1)^2}\frac{\sinh\,k_n y\cos\,k_n x}{\cosh(k_n b/2)} \tag{8.5.62b}$$

$$\sigma_{yz}=G\theta\left[2x-\frac{8a}{\pi^2}\sum_{n=0}^{\infty}\frac{(-1)^n}{(2n+1)^2}\frac{\cosh\,k_n y\sin\,k_n x}{\cosh(k_n b/2)}\right] \tag{8.5.62c}$$

Table 8.5.4 Comparison of finite element solutions for the shear stress $\bar{\sigma}_{yz}(x,y)\,[=-\bar{\sigma}_{xz}(y,x)]$, computed using various meshes, with the analytical solution (Example 8.5.6).

		Mesh			Analytical
x	y	2×2	4×4	8×8	solution
0.03125	0.03125	—	—	0.0312	0.0312
0.09375	0.03125	—	—	0.0946	0.0946
0.15625	0.03125	—	—	0.1612	0.1611
0.21875	0.03125	—	—	0.2332	0.2331
0.28125	0.03125	—	—	0.03127	0.3124
0.34375	0.03125	—	—	0.4015	0.4011
0.40625	0.03125	—	—	0.5013	0.5008
0.46875	0.03125	—	—	0.6135	0.6128
0.06250	0.0625	—	0.06175	—	0.0618
0.1875	0.0625	—	0.1942	—	0.1939
0.3125	0.0625	—	0.3529	—	0.3516
0.4375	0.0625	—	0.5528	—	0.5504
0.1250	0.1250	0.1179	—	—	0.1193
0.3750	0.1250	0.4339	—	—	0.4272

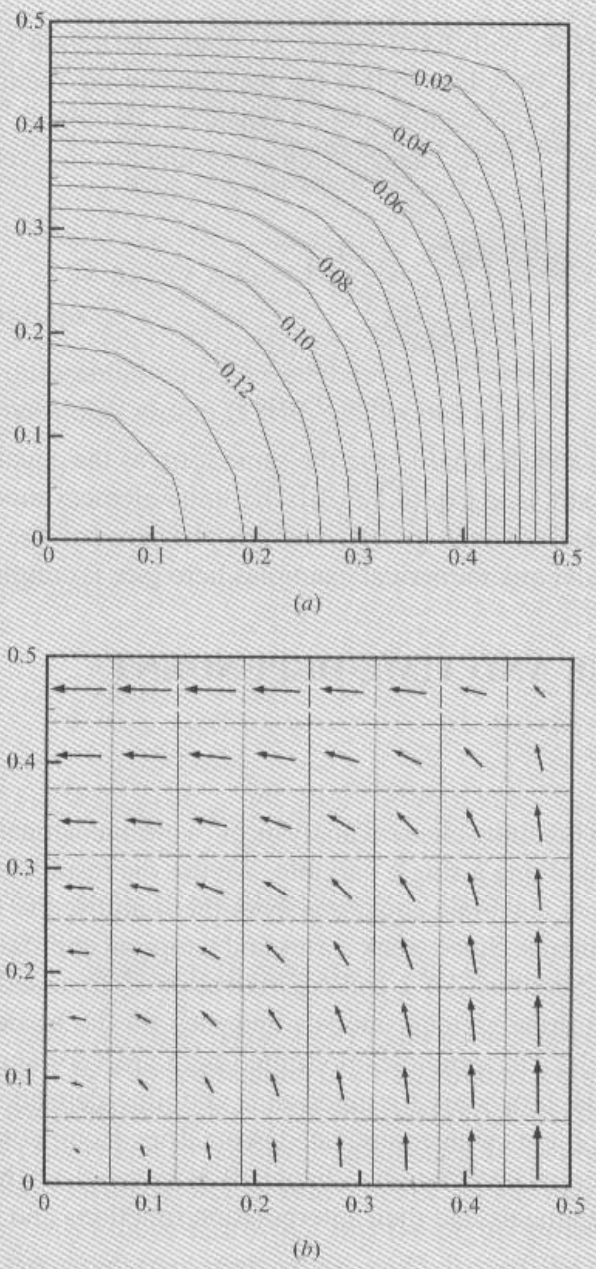

Figure 8.5.15 Contour plot of the stress function and vector plot of the shear stresses ($\mathbf{v} = \bar{\sigma}_{xz}\hat{\mathbf{i}} + \bar{\sigma}_{yz}\hat{\mathbf{j}}$) obtained using the 8×8 mesh of linear rectangular elements in a quadrant of square cross section in Example 8.5.6: (*a*) stress function and (*b*) $\mathbf{v}$.

where $k_n = (2n+1)\frac{\pi}{2}$. The problem is reanalyzed here for shear stresses σ_{xz} and σ_{yz} [see (8.5.59)]. The convergence of the finite element solutions for the stress function and stresses to the analytical solutions (8.5.62) is seen from the results presented in the tables. The contour lines of the surface $\Psi(x, y)$, and contour lines of

$$\bar{\sigma}_{xz} = \frac{\sigma_{xz}}{G\theta} = \frac{\partial \Psi}{\partial y}, \quad \bar{\sigma}_{yz} = \frac{\sigma_{yz}}{G\theta} = -\frac{\partial \Psi}{\partial x}$$

are shown in Fig. 8.5.15.

Transverse Deflections of Membranes

Suppose that a membrane, with fixed edges, occupies the region Ω in the (x, y) plane. Initially the membrane is stretched so that the tension a in the membrane is uniform and a is so large that it is not appreciably altered when the membrane is deflected by a distributed transverse force, $f(x, y)$. The equation governing the transverse deflection u of the membrane is given by

$$-a\left(\frac{\partial^2 u}{\partial x^2}+\frac{\partial^2 u}{\partial y^2}\right)=f(x, y) \quad \text{in } \Omega \tag{8.5.63a}$$

with

$$u=0 \quad \text{on } \Gamma \tag{8.5.63b}$$

Note that (8.5.63a) and (8.5.63b) have the same form as the equations used to describe torsion of cylindrical bars [see Eq. (8.5.60)]. The finite element model of the equation is obvious. In view of the close analogy between this problem and the torsion of cylindrical bars, we will not consider any numerical examples here (see Examples 8.3.1 and 8.5.6).

8.6 EIGENVALUE AND TIME-DEPENDENT PROBLEMS

8.6.1 Introduction

This section deals with the finite element analysis of two-dimensional eigenvalue and time-dependent problems involving a single variable. We use the results of Sections 2.4 and 6.2 to develop finite element algebraic equations from the semidiscrete finite element models of time-dependent problems. Since weak forms and temporal approximations were already discussed in detail in Sections 2.4.2 and 6.2, attention is focussed here on how to develop the semidiscrete finite element models and then on the associated eigenvalue and fully discretized models. The examples presented here are very simple because they are designed to illustrate the procedure for eigenvalue and time-dependent problems; solution of two-dimensional problems with complicated geometries require the use of isoparametric formulation and numerical integration. Chapter 9 is devoted to the discussion of various two-dimensional elements and their interpolation functions and numerical integration methods.

The finite element model development of eigenvalue and time-dependent problems involves, as described in Section 6.2, two main stages. The first stage, called *semidiscretization*, is to develop the weak form or weighted-residual form of the equations over an element and to seek spatial approximation of the dependent variables of the problem. The end result of this step is a set of ordinary differential equations in time among the nodal values of the dependent variables. For transient problems, the second stage consists of time approximations of the ordinary differential equations (i.e., numerical integration of the equations) by finite difference schemes. This step leads to a set of algebraic equations involving the nodal values at time t_{s+1} [$=(s+1)\Delta t$, where s is an integer and Δt is the time increment] in terms of known values from the previous time step(s). For eigenvalue problems, the second stage consists of seeking a solution of the form $u_j(t)=U_j e^{-\lambda t}$

for nodal values and determining the eigenvalues λ and eigenfunctions $U_j\psi_j(x, y)$ (no sum on j). The two-stage procedure was clearly illustrated for one-dimensional problems in Section 6.2. The procedure will be applied here to two-dimensional problems involving a single equation in a single variable. Since the emphasis in this section is on the time approximations, the development of the weak form and spatial finite element model will not be covered explicitly here, and the reader is referred to Sections 8.2 and 8.3 for details.

8.6.2 Parabolic Equations

Consider the partial differential equation governing the transient heat transfer and like problems in a two-dimensional region Ω with total boundary Γ,

$$c\frac{\partial u}{\partial t} - \frac{\partial}{\partial x}\left(a_{11}\frac{\partial u}{\partial x}\right) - \frac{\partial}{\partial y}\left(a_{22}\frac{\partial u}{\partial y}\right) + a_0 u = f(x, y, t) \tag{8.6.1}$$

with the boundary conditions

$$u = \hat{u} \text{ or } q_n = \hat{q}_n \quad \text{on } \Gamma \quad (t \geq 0) \tag{8.6.2a}$$

where

$$q_n = a_{11}\frac{\partial u}{\partial x}n_x + a_{22}\frac{\partial u}{\partial y}n_y \tag{8.6.2b}$$

The initial conditions (i.e., at $t = 0$) are of the form

$$u(x, y, 0) = u_0(x, y) \quad \text{in } \Omega \tag{8.6.3}$$

Here t denotes time, and c, a_{11}, a_{22}, a_0, $\hat{u}$, u_0, f, and $\hat{q}_n$ are given functions of position and/or time. Equation (8.6.1) is a modification of (8.2.1) in that it contains a time derivative term, which accounts for time variations of the physical process represented by (8.2.1).

The weak form of (8.6.1) and (8.6.2) over an element Ω_e is obtained by the standard procedure: Multiply (8.6.1) with the weight function $v(x, y)$ and integrate over the element, integrate by parts (spatially) those terms that involve higher-order derivatives using the gradient or divergence theorem, and replace the coefficient of the weight function in the boundary integral with the secondary variable [i.e., use (8.6.2*b*)]. We obtain

$$0 = \int_{\Omega_e}\left[v\left(c\frac{\partial u}{\partial t} + a_0 u - f\right) + a_{11}\frac{\partial v}{\partial x}\frac{\partial u}{\partial x} + a_{22}\frac{\partial v}{\partial y}\frac{\partial u}{\partial y}\right]dx\,dy - \oint_{\Gamma_e} q_n v\,ds \tag{8.6.4}$$

Note that the procedure to obtain the weak form for time-dependent problems is not much different from that used for steady-state problems in Section 8.2.3. The difference is that all terms of the equations may be functions of time. Also, no integration by parts with respect to time is used, and the weight function v is not a function of time.

The *semidiscrete* finite element model is obtained from (8.6.4) by substituting a finite element approximation for the dependent variable, u. In selecting the approximation

for u, once again we assume that the time dependence can be separated from the space variation,

$$u(x, y, t) \approx \sum_{j=1}^{n} u_j^e(t)\psi_j^e(x, y) \tag{8.6.5}$$

where u_j^e denotes the value of $u(x, y, t)$ at the spatial location (x_j, y_j) at time t. The ith differential equation (in time) of the finite element model is obtained by substituting $v = \psi_i^e(x, y)$ and replacing u by (8.6.5) in (8.6.4):

$$0 = \sum_{j=1}^{n} \left(M_{ij}^e \frac{du_j^e}{dt} + K_{ij}^e u_j^e \right) - f_i^e - Q_i^e \tag{8.6.6a}$$

or, in matrix form

$$[M^e]\{\dot{u}^e\} + [K^e]\{u^e\} = \{f^e\} + \{Q^e\} \tag{8.6.6b}$$

where a superposed dot on u denotes a derivative with time ($\dot{u} = \partial u/\partial t$), and

$$\begin{aligned} M_{ij}^e &= \int_{\Omega_e} c\psi_i^e \psi_j^e \, dx\, dy \\ K_{ij}^e &= \int_{\Omega_e} \left(a_{11} \frac{\partial \psi_i^e}{\partial x} \frac{\partial \psi_j^e}{\partial x} + a_{22} \frac{\partial \psi_i^e}{\partial y} \frac{\partial \psi_j^e}{\partial y} + a_0 \psi_i^e \psi_j^e \right) dx\, dy \\ f_i^e &= \int_{\Omega_e} f(x, y, t)\psi_i^e \, dx\, dy \end{aligned} \tag{8.6.6c}$$

This completes the semidiscretization step.

Eigenvalue Analysis

The problem of finding $u_j^e(t) = U_j e^{-\lambda t}$ such that (8.6.6) holds for homogeneous boundary and initial conditions and $f = 0$ is called an *eigenvalue problem*. Substituting for $u_j^e(t)$ into (8.6.6*b*), we obtain

$$(-\lambda[M^e] + [K^e])\{u^e\} = \{Q^e\} \tag{8.6.7}$$

Upon assembly of the element equations (8.6.7), the right column vector of the condensed equations is zero (because of the homogeneous boundary conditions), giving rise to the global eigenvalue problem

$$([K] - \lambda[M])\{U\} = \{0\} \tag{8.6.8}$$

The order of the matrix equations is $N \times N$, where N is the number of nodes at which the solution is not known. A nontrivial solution to (8.6.8) exists only if the determinant of the coefficient matrix is zero:

$$|[K] - \lambda[M]| = 0$$

which, when expanded, results in an Nth-degree polynomial in λ. The N roots λ_j ($j = 1, 2, \ldots, N$) of this polynomial give the first N eigenvalues of the discretized system (the continuous system, in general, has an infinite number of eigenvalues). There exist standard eigenvalue routines to solve (8.6.8), which give N eigenvalues and eigenvectors.

Transient Analysis

Note that the form of (8.6.6*b*) is the same as the parabolic equation discussed in Section 6.2 [see Eq. (6.2.21*a*)]. Whether a problem is one-dimensional, two-dimensional, or three-dimensional, the form of the semidiscrete finite element model is the same. Therefore, the time approximation schemes discussed in Section 6.2 for parabolic equations can be readily applied.

Using the α-family of approximation

$$\{u\}_{s+1} = \{u\}_s + \Delta t[(1-\alpha)\{\dot{u}\}_s + \alpha\{\dot{u}\}_{s+1}] \quad (0 \le \alpha \le 1) \tag{8.6.9}$$

we can transform the ordinary differential equations (8.6.6*b*) into a set of algebraic equations at time t_{s+1}:

$$[\hat{K}]_{s+1}\{u\}_{s+1} = \{\hat{F}\}_{s,s+1} \tag{8.6.10a}$$

where

$$[\hat{K}]_{s+1} = [M] + a_1[K]_{s+1}$$

$$\{\hat{F}\} = \Delta t(\alpha\{F\}_{s+1} + (1-\alpha)\{F\}_s) + ([M] - a_2[K]_s)\{u\}_s \tag{8.6.10b}$$

$$a_1 = \alpha\Delta t, \quad a_2 = (1-\alpha)\Delta t$$

Equation (8.6.10*a*), after assembly and imposition of boundary conditions, is solved at each time step for the nodal values u_j at time $t_{s+1} = (s+1)\Delta t$. At time $t = 0$ (i.e., $s = 0$), the right-hand side of (8.6.10*a*) is computed using the initial values $\{u\}_0$; the vector $\{F\}$, which is the sum of the source vector $\{f\}$ and internal flux vector $\{Q\}$, is always known for both times t_s and t_{s+1}, at all nodes at which the solution is unknown [because $f(x, t)$ is a *known* function of time and the sum of Q_j^e at these nodes is zero].

It should be recalled from Section 6.2 that, for different values of α, we obtain the following well-known time approximation schemes [see Eq. (6.2.20)]:

$$\alpha = \begin{cases} 0, & \text{the forward difference scheme (conditionally stable); } O(\Delta t) \\ \dfrac{1}{2}, & \text{the Crank–Nicolson scheme (unconditionally stable); } O(\Delta t)^2 \\ \dfrac{2}{3}, & \text{the Galerkin scheme (unconditionally stable); } O(\Delta t)^2 \\ 1, & \text{the backward difference scheme (unconditionally stable); } O(\Delta t) \end{cases}$$

For the forward difference scheme the stability requirement is

$$\Delta t < \Delta t_{\text{cri}} = \frac{2}{(1-2\alpha)\lambda_{\max}}, \quad \alpha < \frac{1}{2} \tag{8.6.11}$$

where $\lambda_{\max}$ is the largest eigenvalue of the finite element equations (8.6.8).

We consider examples of an eigenvalue problem and a time-dependent problem next.

Example 8.6.1 (Eigenvalue Analysis)

Consider the differential equation,

$$\frac{\partial u}{\partial t} - \left(\frac{\partial^2 u}{\partial x^2} + \frac{\partial^2 u}{\partial y^2}\right) = f \tag{8.6.12a}$$

in a unit square, subjected to the boundary conditions

$$\frac{\partial u}{\partial x}(0, y, t) = 0, \quad \frac{\partial u}{\partial y}(x, 0, t) = 0, \quad u(x, 1, t) = 0, \quad u(1, y, t) = 0 \tag{8.6.12b}$$

and initial conditions

$$u(x, y, 0) = 0 \tag{8.6.12c}$$

As a first choice we may choose a 1×1 mesh of two triangular elements. Alternatively, for the choice of triangles, we can use the diagonal symmetry and model the domain with one triangular element (see Fig. 8.3.1*c*). The element matrices for a right-angle triangle with $a = b$ are:

$$[K^e] = \frac{1}{2}\begin{bmatrix} 1 & -1 & 0 \\ -1 & 2 & -1 \\ 0 & -1 & 1 \end{bmatrix}, \quad [M^e] = \frac{a^2}{24}\begin{bmatrix} 2 & 1 & 1 \\ 1 & 2 & 1 \\ 1 & 1 & 2 \end{bmatrix}$$

The eigenvalue problem becomes ($a = 1.0$)

$$\left(-\frac{\lambda}{24}\begin{bmatrix} 2 & 1 & 1 \\ 1 & 2 & 1 \\ 1 & 1 & 2 \end{bmatrix} + \frac{1}{2}\begin{bmatrix} 1 & -1 & 0 \\ -1 & 2 & -1 \\ 0 & -1 & 1 \end{bmatrix}\right)\begin{Bmatrix} U_1 \\ U_2 \\ U_3 \end{Bmatrix} = \begin{Bmatrix} Q_1^1 \\ Q_2^1 \\ Q_3^1 \end{Bmatrix}$$

The boundary conditions require $U_2 = U_3 = 0$ and $Q_1^1 = 0$. Hence, we have

$$\left(-\frac{\lambda}{12} + \frac{1}{2}\right)U_1 = 0 \quad \text{or} \quad \lambda = 6$$

The eigenfunction becomes

$$U(x, y) = \psi_1(x, y) = 1 - x$$

which is defined over the octant of the domain. For a quadrant of the domain, by symmetry, the eigenfunction becomes $U(x, y) = (1 - x)(1 - y)$.

For a mesh of single rectangular element with $a = b$ (see Fig. 8.3.1*b*), we have

$$[K^e] = \frac{1}{6}\begin{bmatrix} 4 & -1 & -2 & -1 \\ -1 & 4 & -1 & 2 \\ -2 & -1 & 4 & -1 \\ -1 & -2 & -1 & 4 \end{bmatrix}, \quad [M^e] = \frac{a^2}{36}\begin{bmatrix} 4 & 2 & 1 & 2 \\ 2 & 4 & 2 & 1 \\ 1 & 2 & 4 & 2 \\ 2 & 1 & 2 & 4 \end{bmatrix}$$

and

$$\left(-\frac{\lambda}{36}\begin{bmatrix} 4 & 2 & 1 & 2 \\ 2 & 4 & 2 & 1 \\ 1 & 2 & 4 & 2 \\ 2 & 1 & 2 & 4 \end{bmatrix} + \frac{1}{6}\begin{bmatrix} 4 & -1 & -2 & -1 \\ -1 & 4 & -1 & 2 \\ -2 & -1 & 4 & -1 \\ -1 & -2 & -1 & 4 \end{bmatrix}\right)\begin{Bmatrix} U_1 \\ U_2 \\ U_3 \\ U_4 \end{Bmatrix} = \begin{Bmatrix} Q_1^1 \\ Q_2^1 \\ Q_3^1 \\ Q_4^1 \end{Bmatrix}$$

Table 8.6.1 Comparison of finite element solutions for eigenvalues, obtained using various meshes, with the analytical solution (Example 8.6.1).

	Triangles				Rectangles				Analytical solution†
λ	1×1	2×2	4×4	8×8	1×1	2×2	4×4	8×8	
$\lambda_1(\lambda_{11})$	6.000	5.415	5.068	4.969	6.000	5.193	4.999	4.951	4.935
$\lambda_2(\lambda_{13})$	—	32.000	27.250	25.340	—	34.290	27.370	25.330	24.674
$\lambda_3(\lambda_{31})$	—	38.200	28.920	25.730	—	34.290	27.370	25.330	24.674
$\lambda_4(\lambda_{33})$	—	76.390	58.220	48.080	—	63.380	49.740	45.710	44.413
$\lambda_4(\lambda_{15})$	—	—	85.350	69.780	—	—	84.570	69.260	64.152
$\lambda_5(\lambda_{51})$	—	—	86.790	69.830	—	—	84.570	69.260	64.152

†The analytical solution is $\lambda_{mn}=\frac{1}{4}\pi^2(m^2+n^2)$ $(m,n=1,3,5,\ldots)$.

Using the boundary conditions $U_2=U_3=U_4=0$ and $Q_1^1=0$, we obtain

$$\left(-\frac{\lambda}{36}\times4+\frac{4}{6}\right)U_1=0, \quad \text{or } \lambda=6$$

The eigenfunction over the quadrant of the domain is given by

$$U(x,y)=\psi_1(x,y)=(1-x)(1-y)$$

For this problem, the one-element mesh of triangles in an octant of the domain gives the same solution as the one-element mesh of rectangular elements in a quadrant of the domain.

Table 8.6.1 contains eigenvalues obtained with various meshes of triangular and rectangular elements, along with the analytical solution of the problem. It is clear that the convergence of the minimum eigenvalue obtained with the finite element method to the analytical value is rapid compared to the convergence of the higher eigenvalues, i.e., error in the higher eigenvalues is always larger than that in the minimum eigenvalue. Also, the minimum eigenvalue converges faster with mesh refinements.

Example 8.6.2 (Transient Analysis)

We wish to solve the transient heat conduction equation

$$\frac{\partial T}{\partial t}-\left(\frac{\partial^2 T}{\partial x^2}+\frac{\partial^2 T}{\partial y^2}\right)=1 \tag{8.6.13a}$$

subject to the boundary conditions (see Fig. 8.6.1*a*), for $t\geq0$,

$$\begin{aligned}&\frac{\partial T}{\partial x}(0,y,t)=0, \quad \frac{\partial T}{\partial y}(x,0,t)=0\\ &T(1,y,t)=0, \quad T(x,1,t)=0\end{aligned} \tag{8.6.13b}$$

and the initial conditions

$$T(x,y,0)=0 \quad \text{for all } (x,y) \text{ in } \Omega \tag{8.6.13c}$$

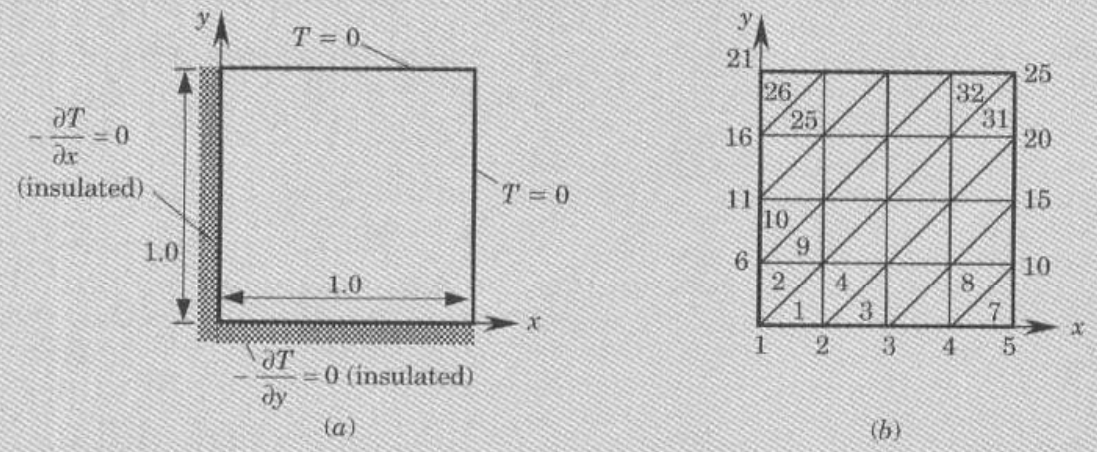

Figure 8.6.1 (a) Domain, boundary conditions and (b) finite element mesh for the transient heat conduction problem of Example 8.6.2.

We choose a 4×4 mesh of linear triangular elements (see Fig. 8.6.1b) to model the domain, and investigate the stability and accuracy of the Crank–Nicolson method (i.e., $\alpha = 0.5$) and the forward difference scheme ($\alpha = 0.0$) for the temporal approximation. Since the Crank–Nicolson method is unconditionally stable, we can choose any value of Δt. However, for large values of Δt the solution may not be accurate. The forward difference scheme is conditionally stable; it is stable if $\Delta t < \Delta t_{\text{cri}}$, where

$$\Delta t_{\text{cri}} = \frac{2}{\lambda_{\max}} = \frac{2}{386.4} = 0.00518$$

where the maximum eigenvalue of (8.6.13a) for the 4×4 mesh of triangles is 386.4.

The element equations are given by (8.6.6b), with $[M^e]$, $[K^e]$, and $\{f^e\}$ defined by (8.6.6c), wherein $c = 1$, $a_{11} = 1$, $a_{22} = 1$, $a_0 = 0$, and $f = 1$. The boundary conditions of the problem for the 4×4 mesh are given by

$$U_5 = U_{10} = U_{15} = U_{20} = U_{21} = U_{22} = U_{23} = U_{24} = U_{25} = 0.0$$

Beginning with the initial conditions $U_i = 0$ ($i = 1, 2, \ldots, 25$), we solve the assembled set of equations associated with (8.6.10).

The forward difference scheme would be unstable for $\Delta t > 0.00518$. To illustrate this point, the equations are solved using $\alpha = 0$, $\Delta t = 0.01$ and $\alpha = 0.5$, $\Delta t = 0.01$. The Crank–Nicolson method gives stable and accurate solution, while the forward difference scheme yields unstable solution (i.e., the solution error grows unboundedly with time), as can be seen from Fig. 8.6.2. For $\Delta t = 0.005$, the forward difference scheme yields stable solution.

The Crank–Nicolson method gives a stable and accurate solution for even $\Delta t = 0.05$. The temperature $T(x, 0, t)$ versus x for various values of time are shown in Fig. 8.6.3(a). The steady state is reached at time $t = 1.0$. The temperature $T(0, 0, t)$ versus time, predicted by the Crank–Nicolson method, is shown in Fig. 8.6.3(b), which indicates the evolution of the temperature from zero to the steady state. A comparison of the transient solution at $t = 1.0$ is given in Table 8.6.2 with the steady-state finite element, the finite difference, and the analytical solutions. Table 8.6.3 contains the finite element solutions for temperature predicted by 4×4 meshes of triangles and rectangles and various values of Δt and $\alpha = 0.5$.

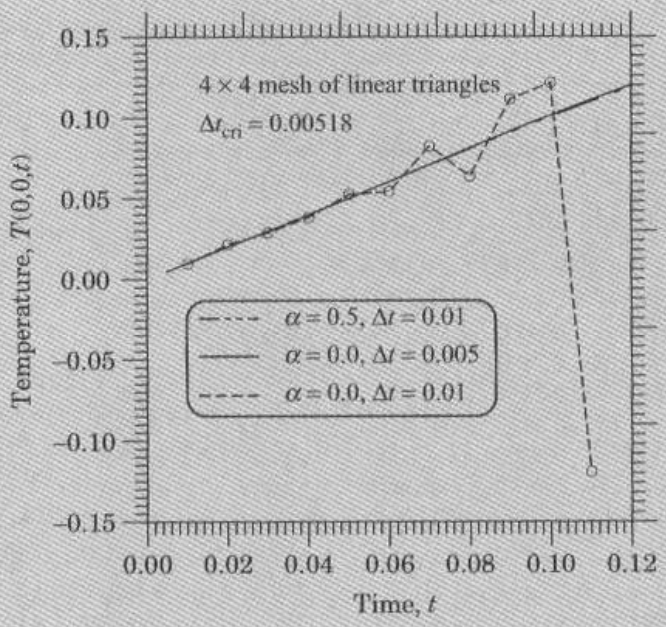

Figure 8.6.2 Stability of the transient solutions of the heat conduction problem in Example 8.6.2 analyzed using a 4 × 4 mesh of linear triangular elements and the Crank–Nicolson ($\alpha = 0.5$) and forward difference ($\alpha = 0.0$) time integration schemes.

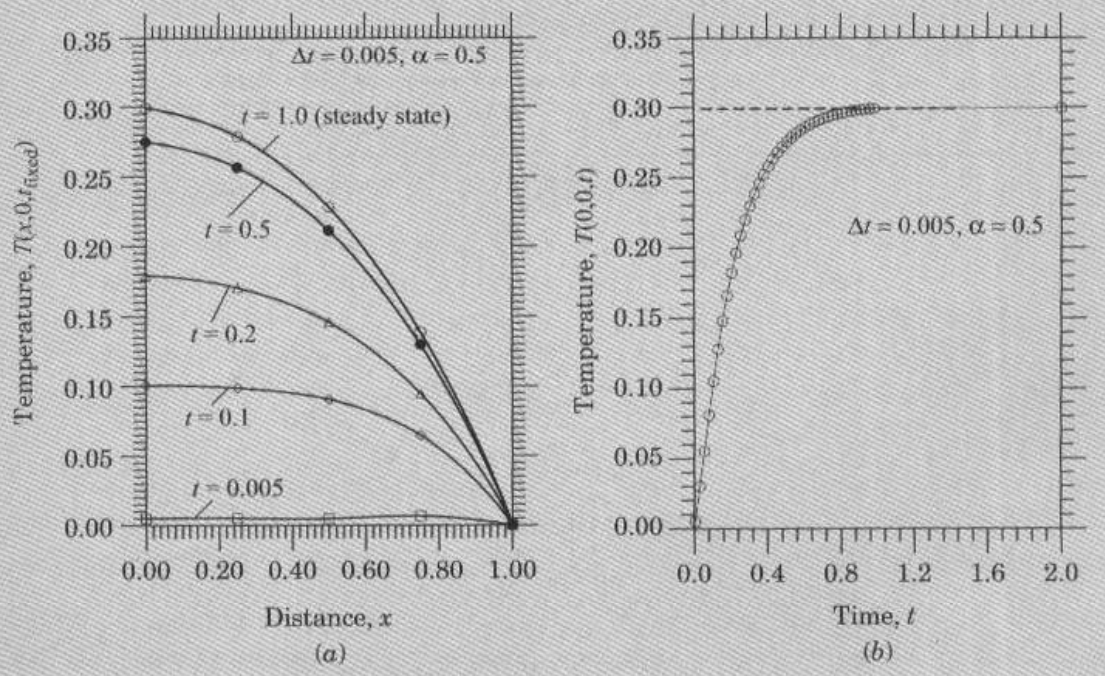

Figure 8.6.3 Variation of the temperature as a function of position x and time t for the transient heat conduction problem of Example 8.6.2 (4 × 4 mesh of linear triangles).

Table 8.6.2 Comparison of finite difference method (FDM) and finite element method (FEM) solutions with the exact solution of the heat conduction problem in Example 8.6.2.

Node	Exact (steady)	FDM (steady)	Error	FEM (steady)	Error	(FEM) at $t = 1.0$[†]
1	0.2947	0.2911	0.0036	0.3013	−0.0066	0.2993
2	0.2789	0.2755	0.0034	0.2805	−0.0016	0.2786
3	0.2293	0.2266	0.0027	0.2292	0.0001	0.2278
4	0.1397	0.1381	0.0016	0.1392	0.0005	0.1385
5	0.0000	0.0000	0.0000	0.0000	0.0000	0.0000
7	0.2642	0.2609	0.0033	0.2645	−0.0003	0.2628
8	0.2178	0.2151	0.0027	0.2172	0.0006	0.2159
9	0.1333	0.1317	0.0016	0.1327	0.0006	0.1320
10	0.0000	0.0000	0.0000	0.0000	0.0000	0.0000
13	0.1811	0.1787	0.0024	0.1801	0.0010	0.1791
14	0.1127	0.1110	0.0017	0.1117	0.0010	0.1111
15	0.0000	0.0000	0.0000	0.0000	0.0000	0.0000
19	0.0728	0.0711	0.0017	0.0715	0.0013	0.0712
20	0.0000	0.0000	0.0000	0.0000	0.0000	0.0000
25	0.0000	0.0000	0.0000	0.0000	0.0000	0.0000

[†]Obtained with the Crank–Nicolson scheme with $\Delta t = 0.005$

Table 8.6.3 Comparison of transient solutions of (8.6.13*a*) and (8.6.13*b*) obtained using meshes of triangular and rectangular elements.

Time t	Element[†]	Temperature along the line $y = 0$: $T(x, 0, t) \times 10$			
		$x = 0.0$	$x = 0.25$	$x = 0.5$	$x = 0.75$
0.1	T1	0.9758	0.9610	0.9063	0.7104
	R1	0.9684	0.9556	0.8956	0.6887
	T2	0.9928	0.9798	0.9168	0.6415
	R2	0.9841	0.9718	0.9020	0.6323
0.2	T1	1.8003	1.7238	1.4891	0.9321
	R1	1.7723	1.7216	1.4829	0.9367
	T2	1.7979	1.7060	1.4644	0.9462
	R2	1.7681	1.6990	1.4626	0.9469
0.3	T1	2.3130	2.1671	1.7961	1.1466
	R1	2.2747	2.1650	1.8084	1.1499
	T2	2.2829	2.1448	1.7943	1.1249
	R2	2.2479	2.1432	1.8018	1.1319
1.0	T1	2.9960	2.7871	2.2804	1.3843
	R1	2.9648	2.8053	2.3090	1.4059
	T2	2.9925	2.7862	2.2776	1.3849
	R2	2.9621	2.8037	2.3065	1.4053

[†]T1, triangular element mesh with $\Delta t = 0.1$; T2, triangular element mesh with $\Delta t = 0.05$; R1, rectangular element mesh with $\Delta t = 0.1$; R2, rectangular element mesh with $\Delta t = 0.05$. In all cases, $\alpha = 0.5$.

8.6.3 Hyperbolic Equations

The transverse motion of a membrane, for example, is governed by the partial differential equation of the form,

$$c\frac{\partial^2 u}{\partial t^2} - \frac{\partial}{\partial x}\left(a_{11}\frac{\partial u}{\partial x}\right) - \frac{\partial}{\partial y}\left(a_{22}\frac{\partial u}{\partial y}\right) + a_0 u = f(x, y, t) \tag{8.6.14a}$$

where $u(x, y, t)$ denotes the transverse deflection, c the material density of the membrane, a_{11} and a_{22} are the tensions in the x and y directions of the membrane, a_0 is the modulus of elastic foundation on which the membrane is stretched (often $a_0 = 0$, i.e., there is no foundation), and $f(x, y, t)$ is the transversely distributed force. Equation (8.6.14a) is known as the *wave equation* and is classified mathematically as an hyperbolic equation. The function u must be determined such that it satisfies (8.6.14a) in a region Ω and the following boundary and initial conditions:

$$u = \hat{u} \quad \text{on } \Gamma \quad \text{or} \quad q_n = \hat{q}_n \quad \text{on } \Gamma \quad (t \geq 0) \tag{8.6.14b}$$

$$u(x, y, 0) = u_0(x, y), \qquad \frac{\partial u}{\partial t}(x, y, 0) = v_0(x, y) \tag{8.6.14c}$$

where $\hat{u}$ and $\hat{q}_n$ are specified boundary values of u and q_n [see (8.6.2b)], and u_0 and v_0 are specified initial values of u and its time derivative, respectively.

The weak form of (8.6.14a) and (8.6.14b) over a typical element Ω_e is similar to that of (8.6.1) [see Eq. (8.6.4)], except that here we have the second time derivative of u:

$$0 = \int_{\Omega_e} \left[v\left(c\frac{\partial^2 u}{\partial t^2} + a_0 u - f\right) + a_{11}\frac{\partial v}{\partial x}\frac{\partial u}{\partial x} + a_{22}\frac{\partial v}{\partial y}\frac{\partial u}{\partial y}\right] dx\, dy - \oint_{\Gamma_e} q_n v\, ds \tag{8.6.15}$$

where $v = v(x, y)$ is the weight function.

The semidiscrete finite element model is obtained by substituting the finite element approximation (8.6.5) for u and $v = \psi_i$ into (8.6.15):

$$0 = \sum_{j=1}^{n}\left(M_{ij}^e \frac{d^2 u_j^e}{dt^2} + K_{ij}^e u_j^e\right) - f_i^e - Q_i^e \tag{8.6.16a}$$

or, in matrix form, we have

$$[M^e]\{\ddot{u}^e\} + [K^e]\{u^e\} = \{f^e\} + \{Q^e\} \tag{8.6.16b}$$

The coefficients M_{ij}^e, K_{ij}^e, and f_i^e are the same as those in (8.6.6c).

Eigenvalue Analysis

The problem of finding $u_j(t) = U_j e^{-i\omega t}$ $(i = \sqrt{-1})$ such that (8.6.16a) and (8.6.16b) hold for homogeneous boundary and initial conditions and $f = 0$ is called an eigenvalue problem associated with (8.6.14a). We obtain,

$$(-\omega^2[M^e] + [K^e])\{u^e\} = \{Q^e\} \tag{8.6.17}$$

The eigenvalues ω^2 and eigenfunctions $\sum_j^n U_j \psi_j(x, y)$ are determined from the assembled equations associated with (8.6.17), after imposing the homogeneous boundary conditions.

For a membrane problem, ω denotes the frequency of natural vibration. The number of eigenvalues of the discrete system (8.6.17) of the problem is equal to the number of unknown nodal values of U in the mesh.

Example 8.6.3 (Natural Vibration Analysis)

Consider the free vibrations of a homogeneous-material rectangular membrane of dimension a by b (in ft.), material density ρ (in slugs/ft.^{2}), and fixed on all its edges, i.e., $u = 0$ on Γ. Although the problem has symmetry about the center horizontal line and center vertical lines of the domain (see Fig. 8.6.4), use of any symmetry in the finite element analysis will eliminate the unsymmetric modes of vibration of the membrane. For example, if we consider a quadrant of the domain in the finite element analysis, the frequencies ω_{mn} $(m, n \neq 1, 3, 5, \ldots)$ and associated eigenfunctions will be missed in the results [i.e., we can only obtain ω_{mn} $(m, n = 1, 3, 5, \ldots)$]. By considering the full domain, the first N frequencies allowed by the mesh can be computed, where N is the number of unknown nodal values in the mesh.

If only the first eigenvalue ω_{11} is of interest or only symmetric frequencies are required, we can use a quadrant of the domain in the analysis. Indeed, results of Example 8.6.1 are applicable here, with $\lambda_{mn} = \omega_{mn}^2$. The results presented in Table 8.6.1 can be interpreted as the squares of the symmetric natural frequencies of a square $a = b = 2$ membrane with $\rho = 1$ and $a_{11} = a_{22} \equiv T = 1$. The exact natural frequencies of a rectangular membrane of dimension a by b, with tensions $a_{11} = a_{22} = T$ and density ρ are:

$$\omega_{mn} = \pi \sqrt{\frac{T}{\rho}} \sqrt{\frac{m^2}{a^2} + \frac{n^2}{b^2}} \quad (m, n = 1, 2, \ldots)$$

To obtain all the frequencies, the full domain must be modeled.

Table 8.6.4 contains the first nine frequencies of a rectangular membrane of 4 ft. by 2 ft., tension $T = 12.5$ lb/ft., and density $\rho = 2.5$ slugs/ft.^{2}, as computed using various meshes of linear triangular and rectangular elements in the total domain. The convergence of the finite element results to the analytical solution is clear. The accuracy of frequencies associated with the symmetric modes is the same when $(n/2) \times (n/2)$ mesh used in a quadrant as when $n \times n$ mesh is used the total domain. The mesh of linear rectangular element yields more accurate results compared with the mesh of linear triangular elements.

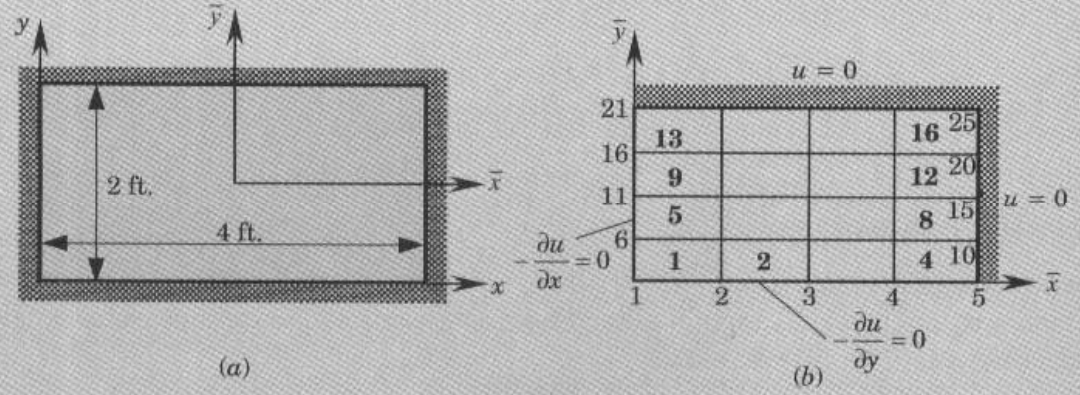

Figure 8.6.4 Analysis of a rectangular membrane: (*a*) actual geometry and (*b*) computational domain with finite element mesh of rectangular elements and boundary conditions (4 × 4 mesh of linear elements or 2 × 2 mesh of nine-node quadratic elements).

Table 8.6.4 Comparison of natural frequencies computed using various meshes of linear triangular and rectangular elements with the analytical solution of a rectangular membrane fixed on all its sides ($a_{11} = a_{22} = 12.5$, $\rho = T = 2.5$).

	Triangular (linear)			Rectangular (linear)			
ω_{mn}	2×2	4×4	8×8	2×2	4×4	8×8	Analytical
ω_{11}	5.0000	4.2266	4.0025	4.3303	4.0285	3.9522	3.9270
ω_{21}	—	5.9083	5.2068	—	5.2899	5.0478	4.9673
ω_{31}	—	8.2392	6.8788	—	7.2522	6.6020	6.3321
ω_{12}	—	8.3578	7.5271	—	7.9527	7.4200	7.2410
ω_{22}	—	10.0618	8.4565	—	8.6603	8.0571	7.8540
ω_{41}	—	12.1021	8.8856	—	9.9805	8.5145	7.8540
ω_{32}	—	13.2011	9.9280	—	12.7157	9.1117	8.7810
ω_{51}	—	14.6942	11.1193	—	13.1700	10.5797	9.4574
ω_{42}	—	15.8117	11.4425	—	14.0734	10.7280	9.9346

Transient Analysis

The hyperbolic equation (8.6.16*b*) can be reduced to a system of algebraic equations by approximating the second-order time derivative. As discussed in Section 6.2, the Newmark time integration schemes are the most commonly used ones in structural dynamics. Since Eq. (8.6.16*b*) is a special case (with $[C] = [0]$) of Eq. (6.2.28*a*), the results in Eqs. (6.2.38)–(6.2.40) hold with $[C] = [0]$. For ready reference, the main results are summarized here.

Newmark's Scheme

$$\begin{aligned} \{u\}_{s+1} &= \{u\}_s + \Delta t\{\dot{u}\}_s + \frac{(\Delta t)^2}{2}\{\ddot{u}\}_{s+\gamma} \\ \{\dot{u}\}_{s+1} &= \{\dot{u}\}_s + \Delta t\{\ddot{u}\}_{s+\alpha} \\ \{\ddot{u}\}_{s+\theta} &= (1-\theta)\{\ddot{u}\}_s + \theta\{\ddot{u}\}_{s+1} \end{aligned} \tag{8.6.18a}$$

where

$$\begin{aligned} &\alpha = \frac{1}{2},\ \gamma = \frac{1}{2}: && \text{constant-average acceleration method (stable scheme)} \\ &\alpha = \frac{1}{2},\ \gamma = \frac{1}{3}: && \text{linear acceleration method (conditionally stable)} \\ &\alpha = \frac{1}{2},\ \gamma = 0: && \text{central difference method (conditionally stable)} \end{aligned} \tag{8.6.18b}$$

Stability Criterion

$$\Delta t < \Delta t_{\text{cri}} = \left[\frac{1}{2}\omega_{\max}^2 (\alpha - \gamma)\right]^{-\frac{1}{2}}, \quad \alpha \geq \frac{1}{2}, \quad \gamma < \alpha \tag{8.6.19}$$

where $\omega^2_{\max}$ is the maximum eigenvalue of the corresponding discrete eigenvalue problem (8.6.17) (i.e., the same mesh and element type used in the transient analysis must be used in the eigenvalue analysis). Note that a more refined mesh will yield a higher maximum eigenvalue and a lower Δt_{cri}.

Time Marching Scheme

$$[\hat{K}^e]_{s+1}\{u^e\}_{s+1} = \{\hat{F}^e\}_{s,s+1} \tag{8.6.20a}$$

where (the superscript e is omitted for brevity in the following),

$$[\hat{K}]_{s+1} = [K]_{s+1} + a_3[M]_{s+1}$$

$$\{\hat{F}\}_{s,s+1} = \{F\}_{s+1} + [M]_{s+1}(a_3\{u\}_s + a_4\{\dot{u}\}_s + a_5\{\ddot{u}\}_s) \tag{8.6.20b}$$

$$a_3 = \frac{2}{\gamma(\Delta t)^2}, \quad a_4 = \Delta t a_3, \quad a_5 = \frac{1}{\gamma} - 1$$

Once $\{u\}_{s+1}$ is calculated from (8.6.20*a*), the velocities and accelerations at time $t_{s+1} = \Delta t(s+1)$ are calculated from

$$\begin{aligned} \{\ddot{u}\}_{s+1} &= a_3(\{u\}_{s+1} - \{u\}_s) - a_4\{\dot{u}\}_s - a_5\{\ddot{u}\}_s \\ \{\dot{u}\}_{s+1} &= \{\dot{u}\}_s + a_2\{\ddot{u}\}_s + a_1\{\ddot{u}\}_{s+1} \end{aligned} \tag{8.6.21}$$

$$a_1 = \alpha\Delta t, \quad a_2 = (1-\alpha)\Delta t$$

For the centered difference scheme ($\gamma = 0$), the alternative formulation of Problem 6.23 must be used.

Note that (8.6.20*a*) is valid for an element. Therefore, operations indicated in (8.6.20*b*) are carried out for an element, and $[\hat{K}^e]$ and $\{\hat{F}^e\}$ are assembled as in a static analysis. For the first time step, the initial conditions on u and $\partial u/\partial t$ are used to compute $\{u\}_0$ and $\{\dot{u}\}_0$ for each element of the entire mesh. The acceleration vector $\{\ddot{u}\}_0$ is computed from (8.6.16*b*) at $t = 0$:

$$\{\ddot{u}\}_0 = [M]^{-1}(\{F\}_0 - [K]\{u\}_0) \tag{8.6.22}$$

Often, it is assumed that $\{F\}_0 = \{0\}$. If the initial conditions are zero, $\{u\}_0 = \{0\}$, and the applied force is assumed to be zero at $t = 0$, we then take $\{\ddot{u}\}_0 = \{0\}$.

Example 8.6.4 (Transient Analysis)

Consider a homogeneous rectangular membrane of sides $a = 4$ ft. and $b = 2$ ft. fixed on all its four edges. Assume that the tension in the membrane is 12.5 lb/ft. (i.e., $a_{11} = a_{22} = 12.5$) and the density is $\rho = c = 2.5$ slugs/ft.^{2}. The initial deflection of the membrane is assumed to be

$$u_0(x, y) = 0.1(4x - x^2)(2y - y^2) \tag{8.6.23}$$

and the initial velocity is $v_0 = 0$. We wish to determine the deflection $u(x, y, t)$ of the membrane as a function of time using the finite element method. The analytical solution of this problem

is [see Kreyszig (1988), p. 684)],

$$u(x, y, t) = \frac{409.6}{\pi^6} \sum_{m,n=1,3,\ldots} \frac{1}{m^3 n^3} \cos \omega_{mn} t \sin \frac{m\pi x}{4} \sin \frac{n\pi y}{2} \tag{8.6.24a}$$

$$\omega_{mn} = \frac{\pi}{4} \sqrt{5(m^2 + 4n^2)} \tag{8.6.24b}$$

where the origin of the (x, y) coordinate system is located at the lower corner of the domain [see Fig. 8.6.4(*a*)].

In the finite element analysis, we can utilize the biaxial symmetry of the problem and model one quadrant of the domain [see Fig. 8.6.4(*b*)]. We set up a new coordinate system $(\bar{x}, \bar{y})$ for the computational domain. The initial displacement in the new coordinates is given by (8.6.23) with x and y replaced in terms of $\bar{x}$ and $\bar{y}$: $x = \bar{x} + 2$, $y = \bar{y} + 1$. The initial values of $\ddot{u}$ are calculated using (8.6.22) with $\{F\}_0 = \{0\}$ and $\{u\}_0$ as given in (8.6.23) by $u_0(x, y)$. At $\bar{x} = 2$ and $\bar{y} = 1$, all nodal values for the function u and its time derivatives are zero.

As for the critical time step, we calculate $\lambda_{\max}$ from the solution of (8.6.17) using the same mesh as that used for the transient analysis and then use (8.6.19) to compute Δt_{cri}. Of course, for $\alpha = \frac{1}{2}$ and $\gamma = \frac{1}{2}$, there is no restriction on the time step for a stable solution. For a 4×4 mesh of linear rectangular elements in a quadrant, the maximum eigenvalue is found to be $\lambda_{\max} = 1072.68$, which yields $\Delta t_{\text{cri}} = 0.1058$ for the linear acceleration scheme ($\alpha = 0.5$, $\gamma = \frac{1}{3}$).

Stability characteristics of the solutions computed using the constant-average acceleration ($\alpha = 0.5$, $\gamma = 0.5$) and linear acceleration ($\alpha = 0.5$, $\gamma = \frac{1}{3}$) schemes for $\Delta t = 0.25 > \Delta t_{\text{cri}}$ are shown in Fig. 8.6.5. Plots of the center deflection $u(0, 0, t)$ versus time t are shown in Fig. 8.6.6. The finite element solutions are in good agreement with the analytical solution (8.6.24*a*) and (8.6.24*b*).

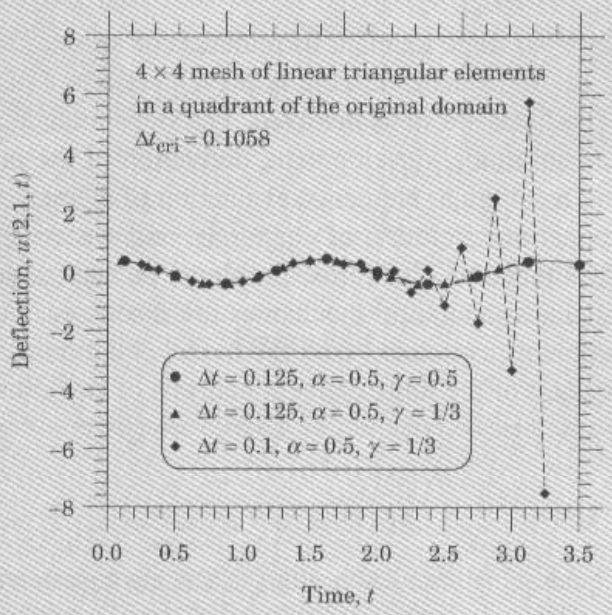

Figure 8.6.5 Stability characteristics of the constant-average acceleration and linear acceleration schemes (a 4×4 mesh of linear rectangular elements is used in a quadrant of the domain).

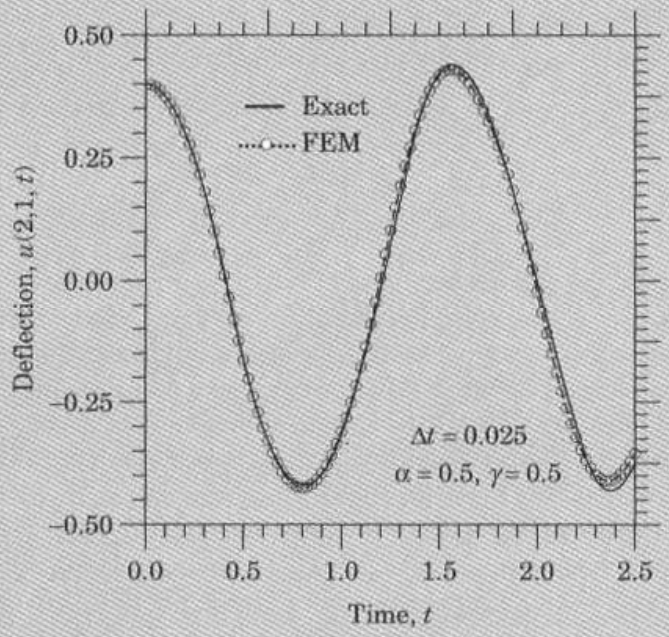

Figure 8.6.6 Comparison of the center deflection obtained using various meshes with the analytical solution of a rectangular membrane with initial deflection.

8.7 SUMMARY

A step by step procedure for finite element formulation of second-order equations in two dimensions with a single dependent variable is presented. The Poisson equation in two dimensions is used to illustrate the steps involved. The steps include: weak formulation of the equation, finite element model development, derivation of the interpolation functions for linear triangular and rectangular elements, evaluation of element matrices and vectors, assembly of element equations, solution of equations, and postcomputation of the gradient of the solution. A number of illustrative problems of heat transfer (conduction and convection), fluid mechanics, and solid mechanics are discussed. Finally, the eigenvalue and time-dependent problems associated with the model equation are also discussed. This chapter constitutes the heart of the finite element analysis of two-dimensional problems in Chapters 10–12.

PROBLEMS

Note: Most problems require some formulative effort (sketching a mesh when it is not given, calculations of element matrices and source vectors in some cases, assembling equations, identifying the boundary conditions in terms of the nodal variables, writing condensed equations, and so on). In some cases, a complete solution is required. When the problem size is large, essential steps of setting up the problem are required. Many of these problems will be solved by **FEM2D** in Chapter 13.

8.1 For a linear triangular element, show that

$$\sum_{i=1}^{3} \alpha_i^e = 2A_e, \quad \sum_{i=1}^{3} \beta_i^e = 0, \quad \sum_{i=1}^{3} \gamma_i^e = 0$$

$$\alpha_i^e + \beta_i^e \hat{x}^e + \gamma_i^e \hat{y}^e = \frac{2}{3} A_e \quad \text{for any } i$$

where

$$\hat{x}^e = \sum_{i=1}^{3} x_i^e, \quad \hat{y}^e = \sum_{i=1}^{3} y_i^e$$

and (x_i^e, y_i^e) are the coordinates of the ith node of the element ($i = 1, 2, 3$).

8.2 Consider the partial differential equation over a typical element Ω_e with boundary Γ_e

$$-\nabla^2 u + cu = 0 \quad \text{in } \Omega_e, \qquad \text{with } \frac{\partial u}{\partial n} + \beta u = q_n \quad \text{on } \Gamma_e$$

Develop the weak form and finite element model of the equation over an element Ω_e.

8.3 Assuming that c and β are constant in Problem 8.2, write the element coefficient matrix and source vector for a linear (a) rectangular element and (b) triangular element.

8.4 Calculate the linear interpolation functions for the linear triangular and rectangular elements shown in Fig. P8.4. *Answer:* (a) $\psi_1 = (12.25 - 2.5x - 1.5y)/8.25$.

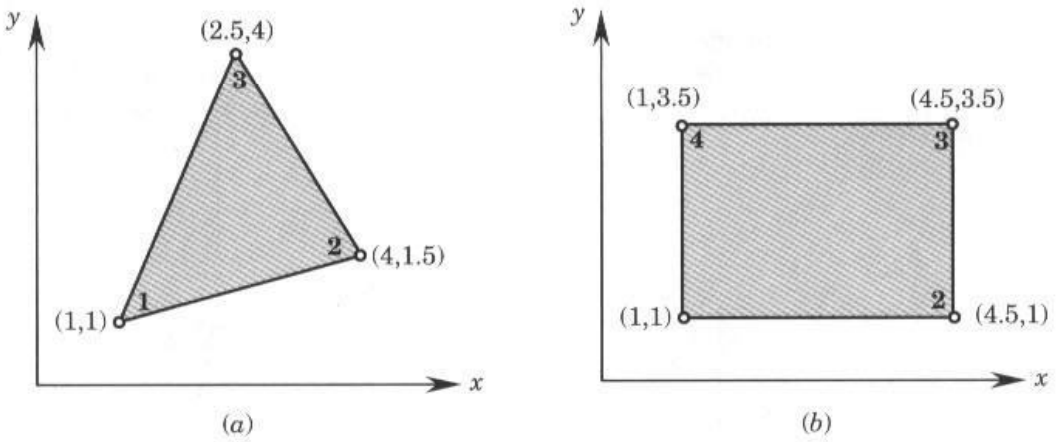

Figure P8.4

8.5 The nodal values of a triangular element in the finite element analysis of a field problem, $-\nabla^2 u = f_0$, are:

$$u_1 = 389.79, \quad u_2 = 337.19, \quad u_3 = 395.08$$

The interpolation functions of the element are given by

$$\psi_1 = \frac{1}{8.25}(12.25 - 2.5x - 1.5y), \quad \psi_2 = \frac{1}{8.25}(-1.5 + 3x - 1.5y)$$

$$\psi_3 = \frac{1}{8.25}(-2.5 - 0.5x + 3y)$$

(*a*) Find the component of the flux in the direction of the vector $4\hat{\mathbf{i}} + 3\hat{\mathbf{j}}$ at $x = 3$ and $y = 2$.

(*b*) A point source of magnitude Q_0 is located at point $(x_0, y_0) = (3, 2)$ inside the triangular element. Determine the contribution of the point source to the element source vector. Express your answer in terms of Q_0.

8.6 The nodal values of an element in the finite element analysis of a field problem $-\nabla^2 u = f_0$ are $u_1 = 389.79$, $u_2 = 337.19$, and $u_3 = 395.08$ (see Fig. P8.6). (*a*) Find the gradient of the solution, and (*b*) Determine where the 392 isoline intersects the boundary of the element in Fig. P8.6.

Answer: $\nabla u_h = 10.58\hat{\mathbf{e}}_1 - 105.2\hat{\mathbf{e}}_2$.

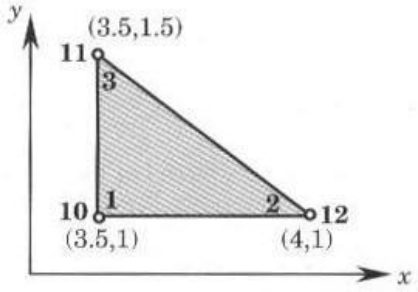

Figure P8.6

8.7 If the nodal values of the elements shown in Fig. P8.7 are $u_1 = 0.2645$, $u_2 = 0.2172$, and $u_3 = 0.1800$ for the triangular element and $u_1 = 0.2173$, $u_3 = 0.1870$, and $u_2 = u_4 = 0.2232$ for the rectangular element, compute u, $\partial u/\partial x$, and $\partial u/\partial y$ at the point $(x, y) = (0.375, 0.375)$.

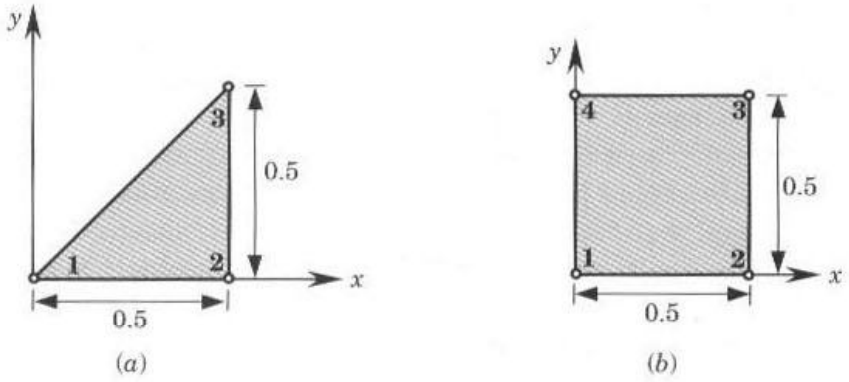

Figure P8.7

8.8 Compute the contribution of the pump 2 discharge to the nodes of element 43 in the groundwater flow problem of Example 8.5.4.

8.9 Find the coefficient matrix associated with the Laplace operator when the rectangular element in Fig. P8.9(*a*) is divided into two triangles by joining node 1 to node 3 [see Fig. P8.9(*b*)]. Compare the resulting matrix with that of the rectangular element in Eq. (8.2.54).

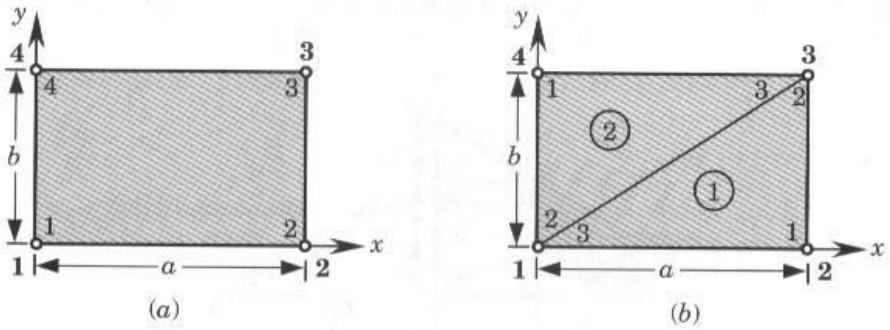

Figure P8.9

8.10 Compute the element matrices

$$S_{ij}^{01} = \int_0^a \int_0^b \psi_i \frac{d\psi_j}{dx}\, dx\, dy, \quad S_{ij}^{02} = \int_0^a \int_0^b \psi_i \frac{d\psi_j}{dy}\, dx\, dy$$

where $\psi_i(x, y)$ are the linear interpolation functions of a rectangular element with sides a and b.

8.11 Give the assembled coefficient matrix for the finite element meshes shown in Figs. P8.11(a) and P8.11(b). Assume one degree of freedom per node, and let $[K^e]$ denote the element coefficient matrix for the eth element. The answer should be in terms of element matrices K_{ij}^e.

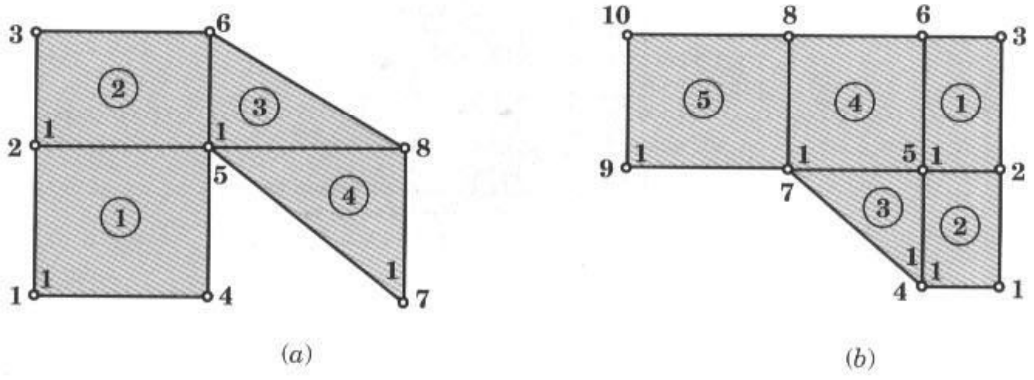

Figure P8.11

8.12 Repeat Problem 8.11 for the mesh shown in Fig. P8.12.

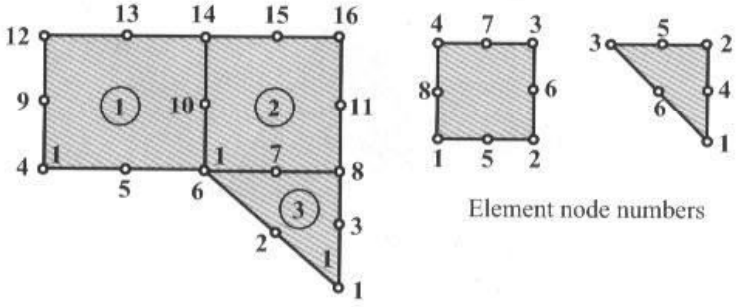

Figure P8.12

8.13 Compute the global source vector corresponding to the nonzero specified boundary flux for the finite element meshes of linear elements shown in Fig. P8.13.

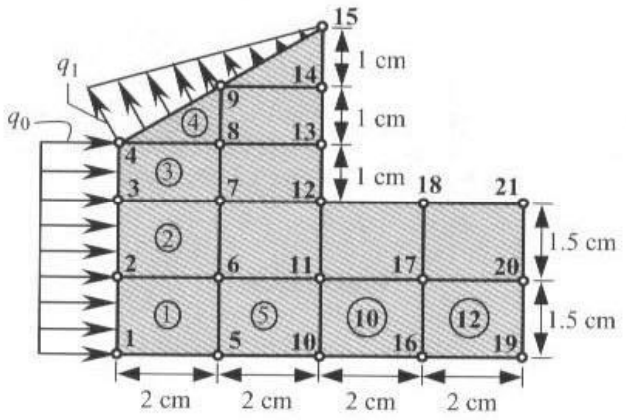

Figure P8.13

8.14 Repeat Problem 8.13 for the finite element mesh of quadratic elements shown in Fig. P8.14.

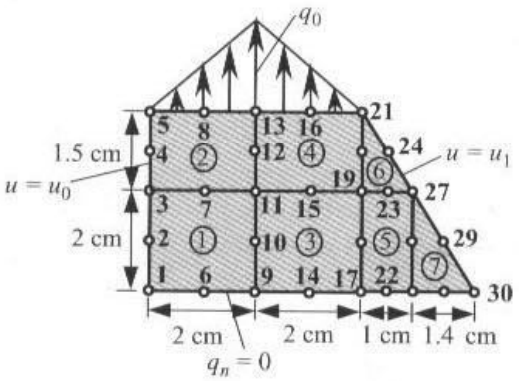

Figure P8.14

8.15 A line source of intensity q_0 is located across the triangular element shown in Fig. P8.15. Compute the element source vector.

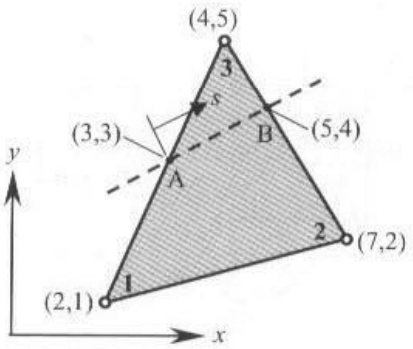

Figure P8.15

8.16 Repeat Problem 8.15 when the line source has varying source, $q(s) = q_0 s/L$, where s is the coordinate along the line source.

8.17 Consider the following partial differential equation governing the variable u:

$$c\frac{\partial u}{\partial t} - \frac{\partial}{\partial x}\left(a\frac{\partial u}{\partial x}\right) - \frac{\partial}{\partial y}\left(b\frac{\partial u}{\partial y}\right) - f_0 = 0$$

where c, a, b, and f_0 are constants. Assume an approximation of the form

$$u_h(x, y, t) = (1 - x)yu_1(t) + x(1 - y)u_2(t)$$

where u_1 and u_2 are nodal values of u at time t.

(*a*) Develop the fully discretized finite element model of the equation.

(*b*) Evaluate the element coefficient matrices and source vector for a square element of dimension 1 unit by 1 unit (so that the evaluation of the integrals is made easy).

Note: You should not be concerned with this nonconventional approximation of the dependent unknown but just use it as given to answer the question.

8.18 Solve the Laplace equation

$$-\left(\frac{\partial^2 u}{\partial x^2} + \frac{\partial^2 u}{\partial y^2}\right) = 0 \quad \text{in } \Omega$$

on a rectangle, when $u(0, y) = u(a, y) = u(x, 0) = 0$ and $u(x, b) = u_0(x)$. Use the symmetry and (*a*) a mesh of 2×2 triangular elements and (*b*) a mesh of 2×2 rectangular elements (see Fig. P8.18). Compare the finite element solution with the exact solution

$$u(x, y) = \sum_{n=1}^{\infty} A_n \sin\frac{n\pi x}{a} \sinh\frac{n\pi y}{b}$$

where

$$A_n = \frac{2}{a \sinh(n\pi b/a)} \int_0^a u_0(x) \sin\frac{n\pi x}{a} dx$$

Take $a = b = 1$, and $u_0(x) = \sin\ \pi x$ in the computations. For this case, the exact solution becomes

$$u(x, y) = \frac{\sin \pi x\ \sinh \pi y}{\sinh\ \pi}$$

Answer: For a 2×2 mesh of triangles, $U_4 = 0.23025$ and $U_5 = 0.16281$; for a 2×2 mesh of rectangles, $U_4 = 0.1520$ and $U_5 = 0.1075$.

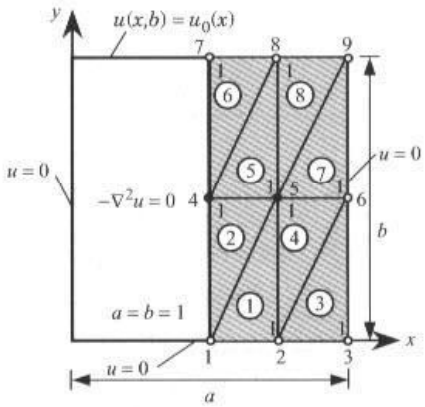

Figure P8.18

8.19 Solve Problem 8.18 when $u_0(x) = 1$. The analytical solution is given by

$$u(x, y) = \frac{4}{\pi} \sum_{n=0}^{\infty} \frac{\sin(2n+1)\pi x \, \sinh(2n+1)\pi y}{(2n+1)\sinh(2n+1)\pi}$$

Answer: (*a*) $U_4 = 0.2647$ and $U_5 = 0.2059$.

8.20 Solve Problem 8.18 when $u_0(x) = 4(x - x^2)$. *Answer:* (*a*) $U_4 = 0.2353$ and $U_5 = 0.1691$; (*b*) $U_4 = 0.1623$ and $U_5 = 0.1068$

8.21 Solve the Laplace equation for the unit square domain and boundary conditions given in Fig. P8.21. Use one rectangular element.

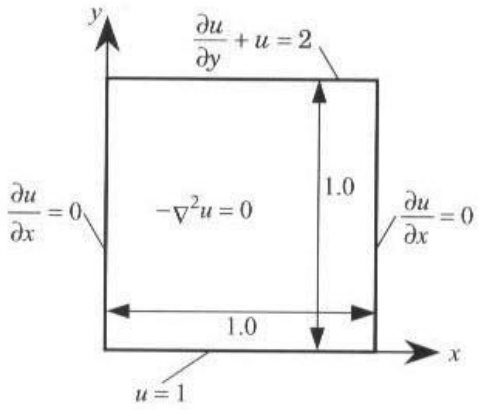

Figure P8.21

8.22 Use two triangular elements to solve the problem in Fig. P8.21. Use the mesh obtained by joining points (1,0) and (0,1).

8.23 Consider the steady-state heat transfer (or other phenomenon) in a square region shown in Fig. P8.23. The governing equation is given by

$$-\frac{\partial}{\partial x}\left(k\frac{\partial u}{\partial x}\right) - \frac{\partial}{\partial y}\left(k\frac{\partial u}{\partial y}\right) = f_0$$

The boundary conditions for the problem are:

$$u(0, y) = y^2, \quad u(x, 0) = x^2, \quad u(1, y) = 1 - y, \quad u(x, 1) = 1 - x$$

Assuming $k = 1$ and $f_0 = 2$, determine the unknown nodal value of u using the uniform 2×2 mesh of rectangular elements. *Answer:* $U_5 = 0.625$.

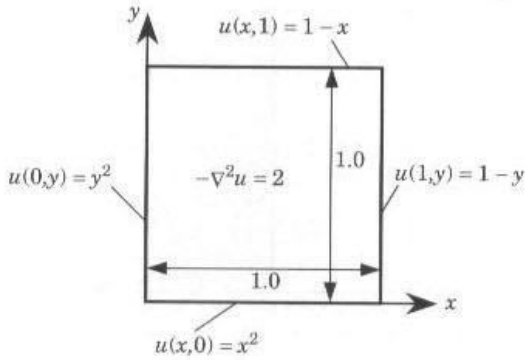

Figure P8.23

8.24 Solve Problem 8.23 using the mesh of a rectangle and two triangles, as shown in Fig. P8.24. *Answer:* $U_5 = 0.675$.

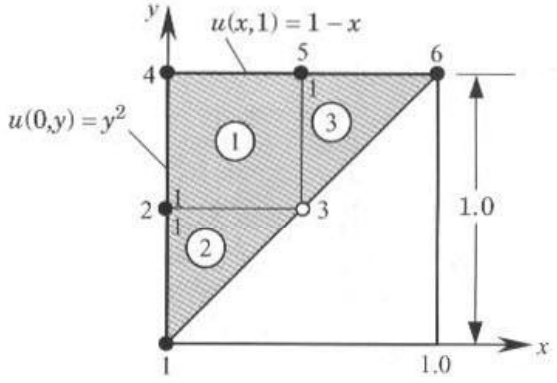

Figure P8.24

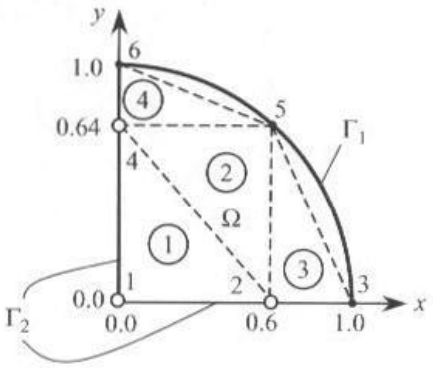

Figure P8.25

8.25 Solve the Poisson equation $-\nabla^2 u = 2$ in Ω, $u = 0$ on Γ_1, $\partial u/\partial n = 0$ on Γ_2, where Ω is the first quadrant bounded by the parabola $y = 1 - x^2$ and the coordinate axes (see Fig. P8.25), and Γ_1 and Γ_2 are the boundaries shown in Fig. P8.25.

8.26 Solve the axisymmetric field problem shown in Fig. P8.26 for the mesh shown there. Note that the problem has symmetry about any $z =$ constant line. Hence, the problem is essentially one dimensional. You are only required to determine the element matrix and source vector for element 1 and give the known boundary conditions on the primary and secondary variables.

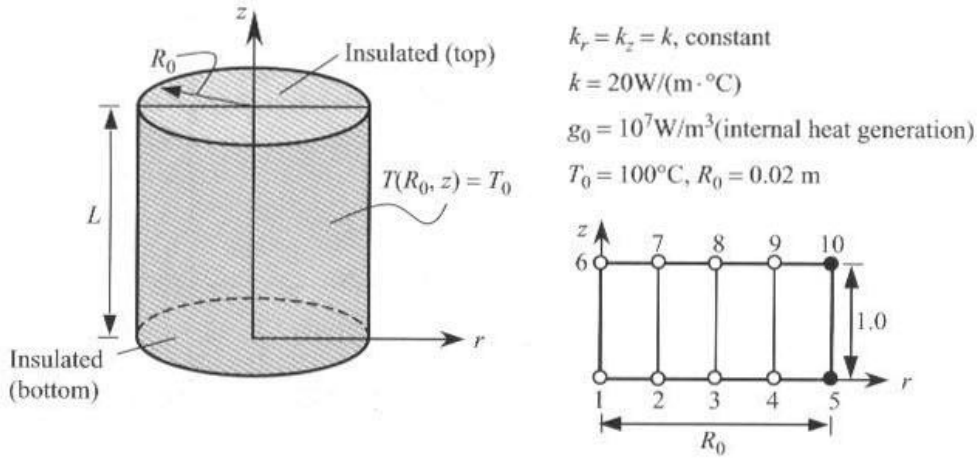

Figure P8.26

8.27 Formulate the axisymmetric field problem shown in Fig. P8.27 for the mesh shown. You are only required to give the known boundary conditions on the primary and secondary variables and compute the secondary variable at $r = R_0/2$ using equilibrium and the definition. Use the element at the left of the node.

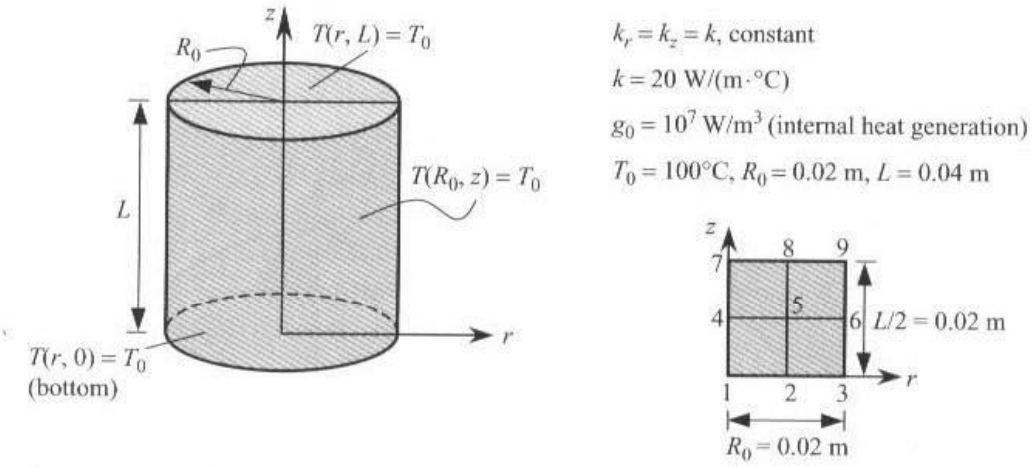

Figure P8.27

8.28 A series of heating cables have been placed in a conducting medium, as shown in Fig. P8.28. The medium has conductivities of $k_x = 10$ W/(cm · °C) and $k_y = 15$ W/(cm · °C), the upper surface is exposed to a temperature of −5°C, and the lower surface is bounded by an insulating medium. Assume that each cable is a point source of 250 W/cm. Take the convection coefficient between the medium and the upper surface to be $\beta = 5$ W/(cm^2 · K). Use a 8 × 8 mesh of linear rectangular (or triangular) elements in the computational domain (use any symmetry available in the problem), and formulate the problem (i.e., give element matrices for a typical element, give boundary conditions on primary and secondary variables, and compute convection boundary contributions).

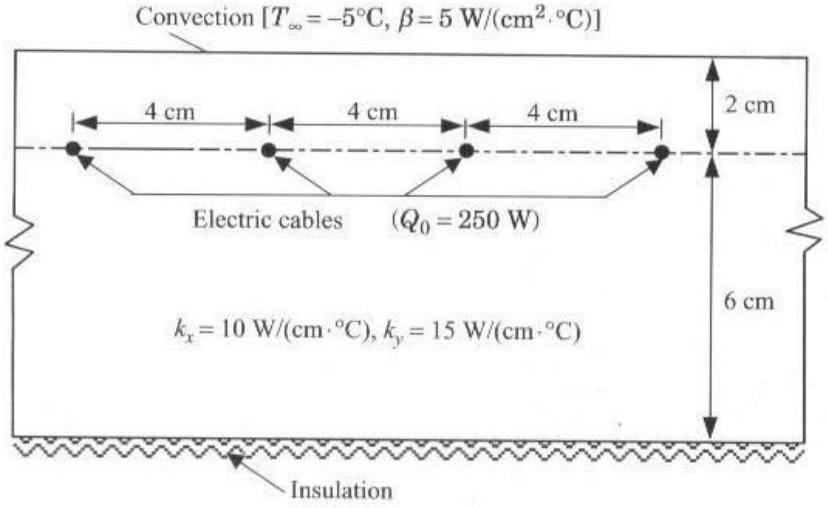

Figure P8.28

8.29 Formulate the finite element analysis information to determine the temperature distribution in the molded asbestos insulation shown in Fig. P8.29. Use the symmetry to identify a computational domain and give the specified boundary conditions at the nodes of the mesh. What is the connectivity of matrix for the mesh shown?

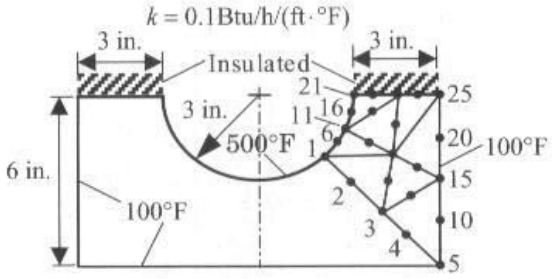

Figure P8.29

8.30 Consider steady-state heat conduction in a square region of side $2a$. Assume that the medium has conductivity of k (in W/(m·°C)) and uniform heat (energy) generation of g_0 (in W/m^3). For the boundary conditions and mesh shown in Fig. P8.30, write the finite element algebraic equations for nodes 1, 3, and 7.

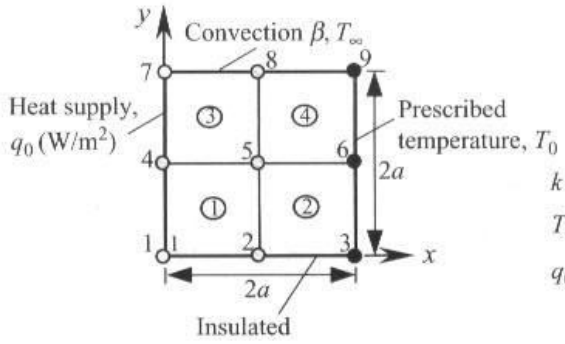

$k = 30$ W/(m·°C), $\beta = 60$ W/(m^2·°C)

$T_\infty = 0$°C, $T_0 = 100$°C, $a = 1$ cm

$q_0 = 2 \times 10^5$ W/m^2, $g_0 = 10^7$ W/m^3

Figure P8.30

8.31 For the convection heat transfer problem shown in Fig. P8.31, write the four finite element equations for the unknown temperatures. Assume that the thermal conductivity of the material is $k = 5$ W/(m·°C), the convection heat transfer coefficient on the left surface is $\beta = 28$ W/(m^2 · °C), and the internal heat generation is zero. Compute the heats at nodes 2, 4 and 9 using (*a*) element equations (i.e., equilibrium), and (*b*) definition in Eq. (8.2.19*b*) (use the temperature field of elements 1 and 2).

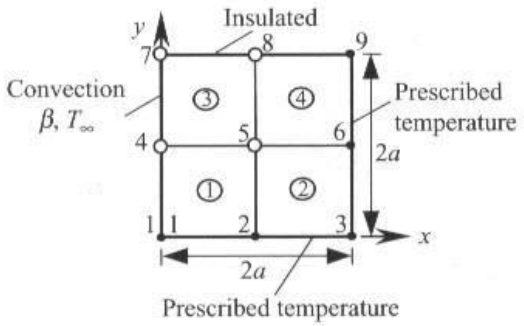

$k = 5$ W/(m·°C), $\beta = 28$ W/(m^2·°C)

$T_\infty = 0$°C, $T_3 = T_6 = T_9 = 40$°C,

$T_1 = T_2 = 10$°C, $a = 0.15$ m

Figure P8.31

8.32 Write the finite element equations for the unknown temperatures of the problem shown in Fig. P8.32.

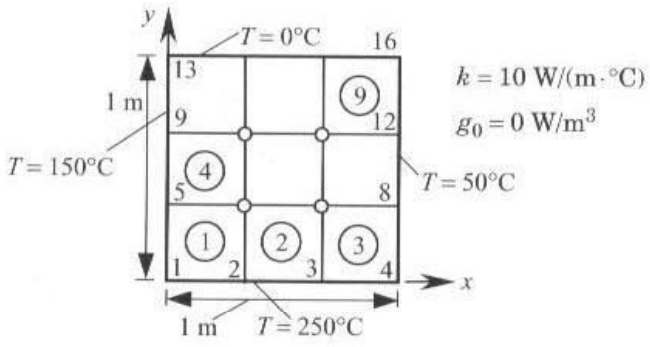

Figure P8.32

8.33 Write the finite element equations for the heats at nodes 1 and 13 of Problem 8.32. The answer should be in terms of the nodal temperatures $T_1, T_2, \ldots, T_{16}$.

8.34 Write the finite element equations associated with nodes 13, 16, and 19 for the problem shown in Fig. P8.34.

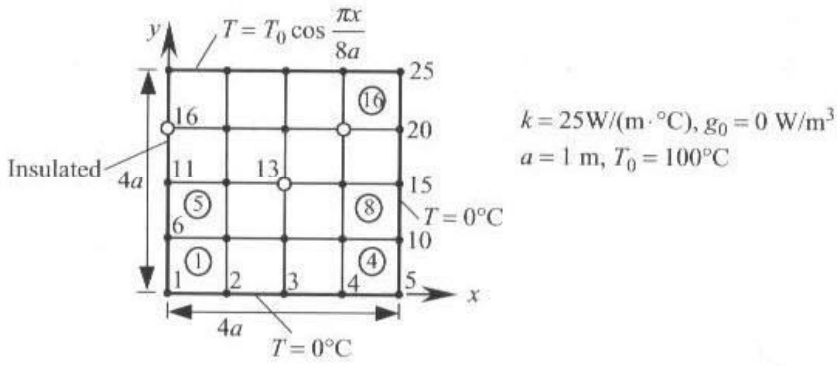

Figure P8.34

8.35 The fin shown in Fig. P8.35 has its base maintained at 300°C and exposed to convection on its remaining boundary. Write the finite element equations at nodes 7 and 10.

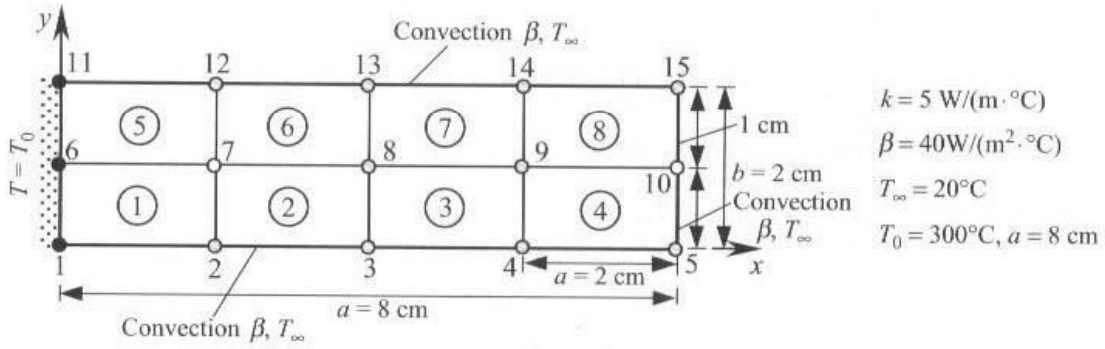

Figure P8.35

8.36 Compute the heat loss at nodes 10 and 13 of Problem 8.35.

8.37 Consider the problem of the flow of groundwater beneath a coffer dam. Solve the problem using the velocity potential formulation. The geometry and boundary conditions are shown in Fig. P8.37.

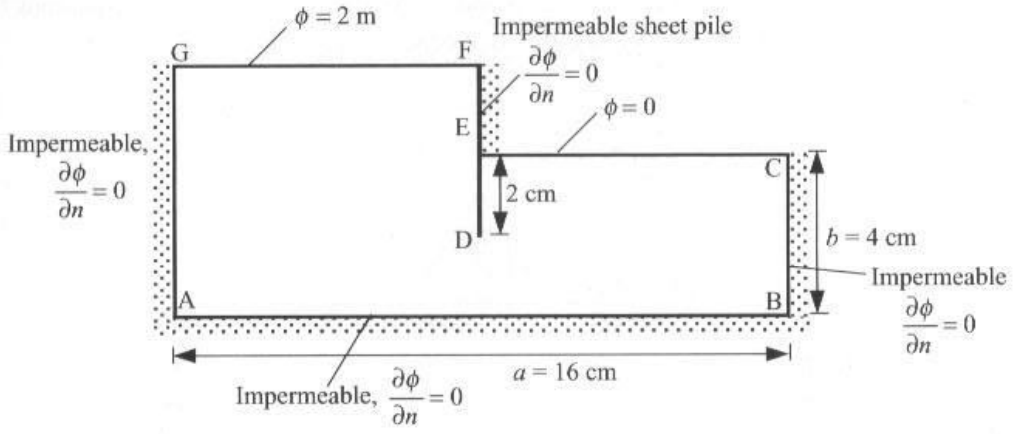

Figure P8.37

8.38 Formulate the groundwater flow problem of the domain shown in Fig. P8.38 for finite element analysis. The pump is located at $(x, y) = (787.5, 300)$ m.

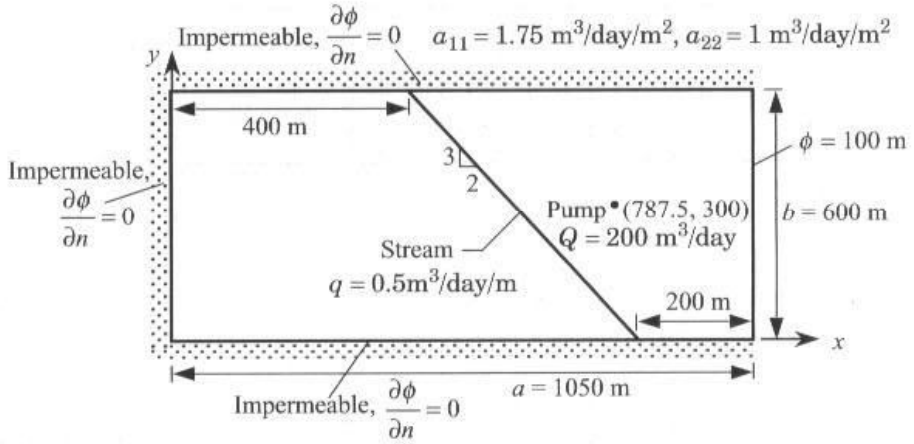

Figure P8.38

8.39 Repeat Problem 8.38 for the domain shown in Fig. P8.39.

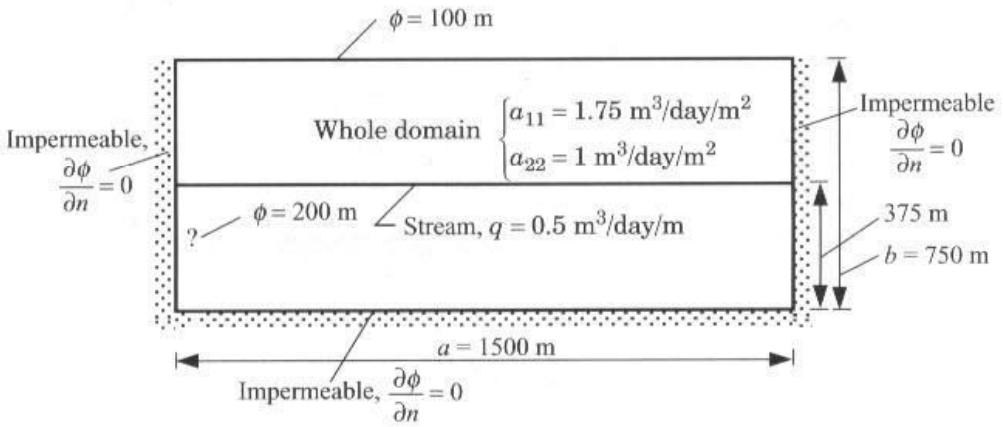

Figure P8.39

8.40 Consider the steady confined flow through the foundation soil of a dam (see Fig. P8.40). Assuming that the soil is isotropic ($k_x = k_y$), formulate the problem for finite element analysis (identify the specified primary and secondary variables and their contribution to the nodes). In particular, write the finite element equations at nodes 8 and 11. Write the finite element equations for the horizontal velocity component in 5th and 10th elements.

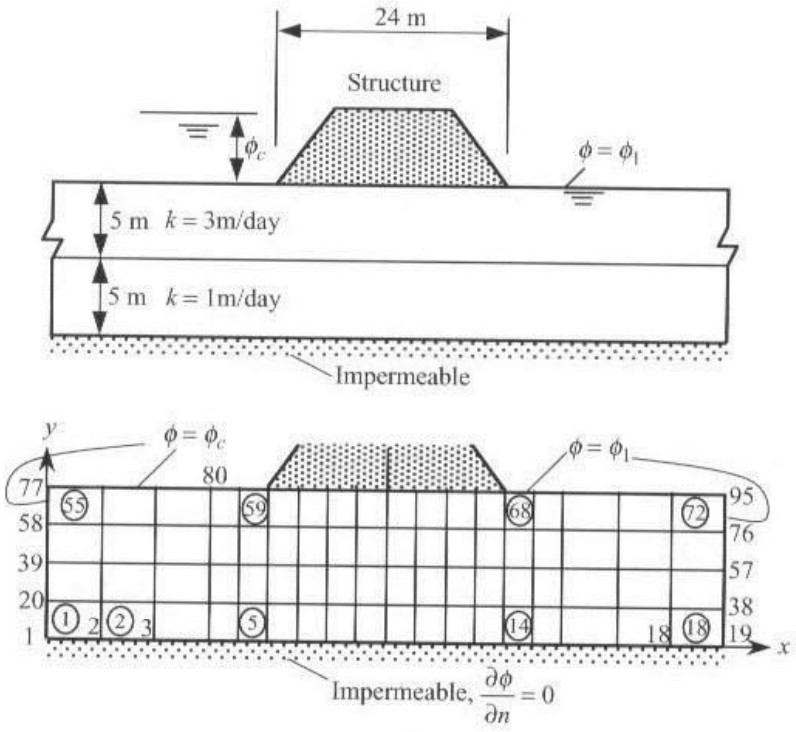

Figure P8.40

8.41 Formulate the problem of the flow about an elliptical cylinder using the (*a*) stream function and (*b*) velocity potential. The geometry and boundary conditions are shown in Fig. P8.41.

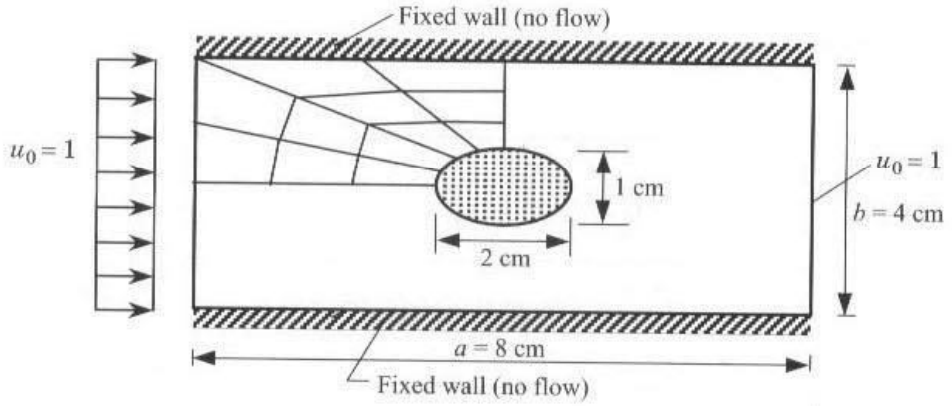

Figure P8.41

8.42 Repeat Problem 8.41 for the domain shown in Fig. P8.42.

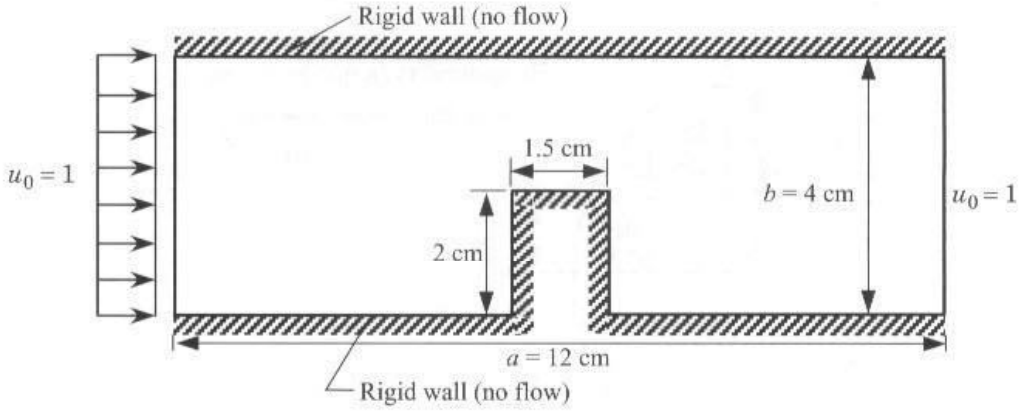

Figure P8.42

8.43 The Prandtl theory of torsion of a cylindrical member leads to

$$-\nabla^2 u = 2G\theta \quad \text{in } \Omega; \quad u = 0 \quad \text{on } \Gamma$$

where Ω is the cross section of the cylindrical member being twisted, Γ is the boundary of Ω, G is the shear modulus of the material of the member, θ is the angle of twist, and u is the stress function. Solve the equation for the case in which Ω is a circular section (see Fig. P8.43) using the mesh of linear triangular elements. Compare the finite element solution with the exact solution (valid for elliptical sections with axes a and b):

$$u = \frac{G\theta a^2 b^2}{a^2 + b^2}\left(1 - \frac{x^2}{a^2} - \frac{y^2}{b^2}\right)$$

Use $a = 1$, $b = 1$, and $f_0 = 2G\theta = 10$.

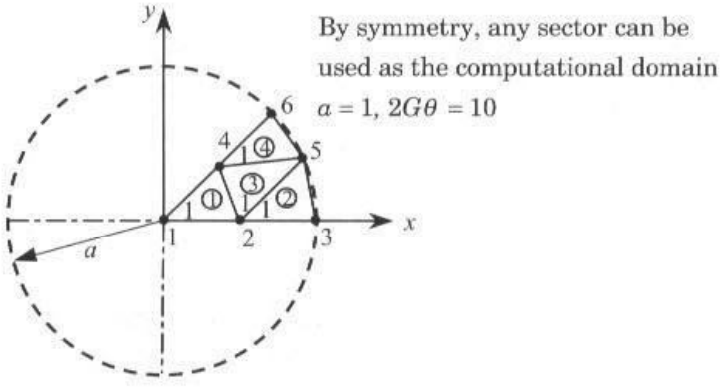

Figure P8.43

8.44 Repeat Problem 8.43 for an elliptical section member (see Fig. P8.44). Use $a = 1$ and $b = 1.5$.

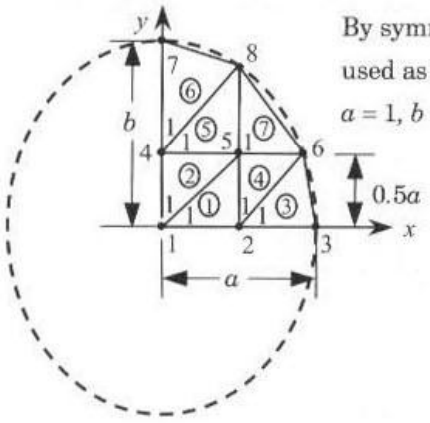

By symmetry, a quadrant can be used as the computational domain

$a = 1, b = 1.5, 2G\theta = 10$

Figure P8.44

8.45 Repeat Problem 8.43 for the case in which Ω is an equilateral triangle (see Fig. P8.45). The exact solution is given by

$$u = -G\theta\left[\frac{1}{2}(x^2 + y^2) - \frac{1}{2a}(x^3 - 3xy^2) - \frac{2}{27}a^2\right]$$

Take $a = 1$ and $f_0 = 2G\theta = 10$. Give the finite element equation for node 5.

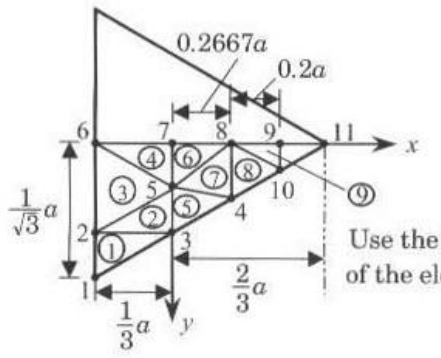

$y_5 = 0.5y_3, y_2 = y_3$

$x_8 = 0.2667a$

$x_9 = x_8 + 0.2a$

$x_{10} = x_8 + 0.4a$

Use the smallest node as the first node of the element to write the connectivity

Figure P8.45

8.46 Consider the torsion of a hollow square cross-sectional member. The stress function Ψ is required to satisfy the Poisson equation in (8.5.60) and the following boundary conditions:

$$\Psi = 0 \quad \text{on the outer boundary;} \quad \Psi = 2r^2 \quad \text{on the inner boundary}$$

where r is the ratio of the outside dimension to the inside dimension, $r = 6a/2a$. Formulate the problem for finite element analysis using the mesh shown in Fig. P8.46.

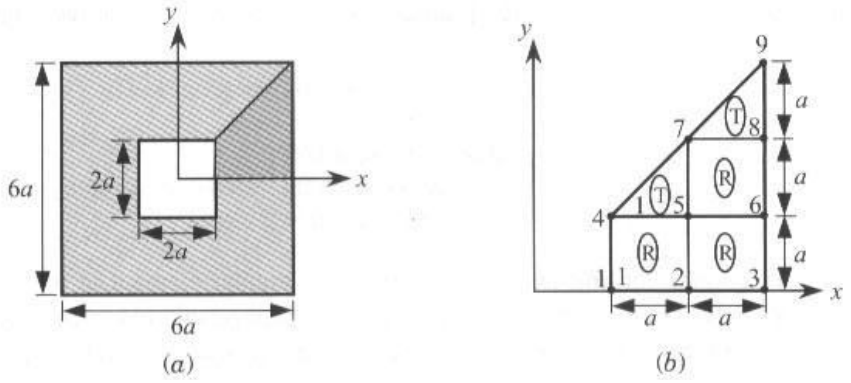

Figure P8.46

8.47 Repeat Problem 8.46 with the mesh of linear triangles [join nodes 1 and 5, 2 and 6, and 5 and 8 in Fig. P8.46(*b*)].

8.48 The membrane shown in Fig. P8.48 is subjected to uniformly distributed transverse load of intensity f_0 (in N/m^2). Write the condensed equations for the unknown displacements.

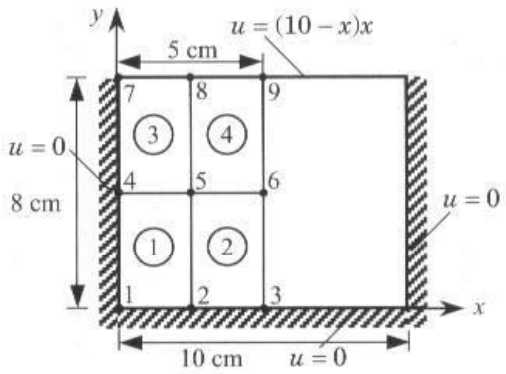

Figure P8.48

8.49 The circular membrane shown in Fig. P8.49 is subjected to uniformly distributed transverse load of intensity f_0 (in N/m^2). Write the condensed equations for the unknown displacements.

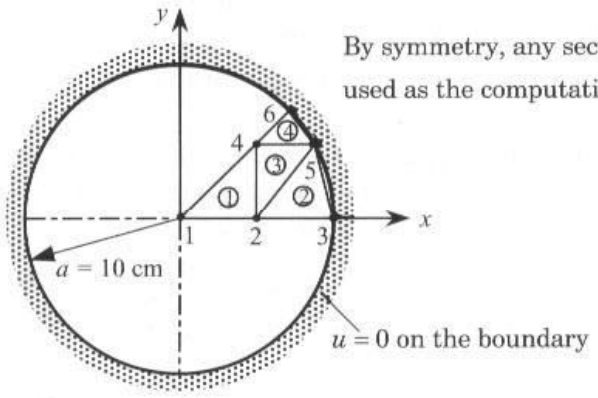

Figure P8.49

8.50 Determine the critical time step for the transient analysis (with $\alpha \leq \frac{1}{2}$) of the problem

$$\frac{\partial u}{\partial t} - \nabla^2 u = 1 \quad \text{in } \Omega; \quad u = 0 \quad \text{in } \Omega \text{ at } t = 0$$

by determining the maximum eigenvalue of the problem

$$-\nabla^2 u = \lambda u \quad \text{in } \Omega; \quad u = 0 \quad \text{on } \Gamma$$

The domain is a square of unit length. Use (*a*) one triangular element in the octant, (*b*) four linear elements in the octanta, and (*c*) a 2×2 mesh of linear rectangular elements in a quadrant (see Fig. P8.50). Determine the critical time step for the forward difference scheme. *Answer:* (*a*) $\lambda = 24$. (*b*) $\lambda_{max} = 305.549$.

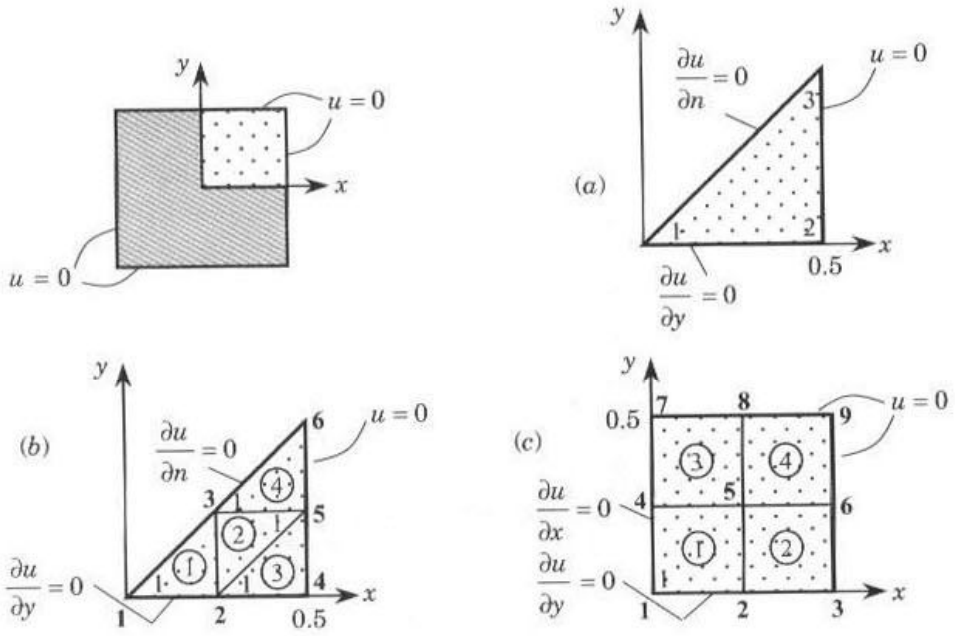

Figure P8.50

8.51 Set up the condensed equations for the transient problem in Problem 8.50 for the α-family of approximation. Use the mesh shown in Fig. P8.50(*b*).

8.52 Set up the condensed equations for the time-dependent analysis of the circular membrane in Problem 8.49.

8.53 Determine the fundamental natural frequency of the rectangular membrane in Problem 8.48.

8.54 Determine the critical time step based on the forward difference scheme for the time-dependent analysis of the circular membrane in Problem 8.49.

8.55 (*Central difference method*) Consider the following matrix differential equation in time:

$$[M]\{\ddot{U}\} + [C]\{\dot{U}\} + [K]\{U\} = \{F\}$$

where the superposed dot indicates differentiation with respect to time. Assume

$$\{\ddot{U}\}_n = \frac{1}{(\Delta t)^2}(\{U\}_{n-1} - 2\{U\}_n + \{U\}_{n+1}), \quad \{\dot{U}\}_n = \frac{1}{2(\Delta t)}(\{U\}_{n+1} - \{U\}_{n-1})$$

and derive the algebraic equations for the solution of $\{U\}_{n+1}$ in the form

$$[A]\{U\}_{n+1} = \{F\}_n - [B]\{U\}_n - [D]\{U\}_{n-1}$$

Define $[A]$, $[B]$, and $[D]$ in terms of $[M]$, $[C]$, and $[K]$.

8.56 Consider the first-order differential equation in time

$$a\frac{du}{dt} + bu = f$$

Using linear approximation, $u(t) = u_1\psi_1(t) + u_2\psi_2(t)$, $\psi_1 = 1 - t/\Delta t$, and $\psi_2 = t/\Delta t$, derive the associated algebraic equation and compare with that obtained using the α-family of approximation.

8.57 (*Space-time element*) Consider the differential equation

$$c\frac{\partial u}{\partial t} - \frac{\partial}{\partial x}\left(a\frac{\partial u}{\partial x}\right) = f \quad \text{for } 0 < x < L, \quad 0 \le t \le T$$

with

$$u(0,t) = u(L,t) = 0 \quad \text{for } 0 \le t \le T, \quad u(x,0) = u_0(x) \quad \text{for } 0 < x < L$$

where $c = c(x)$, $a = a(x)$, $f = f(x,t)$, and u_0 are given functions. Consider the rectangular domain defined by

$$\Omega = \{(x,t) : 0 < x < L, \quad 0 \le t \le T\}$$

A finite element discretization of Ω by rectangles is a time-space rectangular element (with y replaced by t). Give a finite element formulation of the equation over a time-space element, and discuss the *mathematical/practical* limitations of such a formulation. Compute the element matrices for a linear element.

8.58 (*Space-time finite element*) Consider the time-dependent problem

$$\frac{\partial^2 u}{\partial x^2} = c\frac{\partial u}{\partial t}, \quad \text{for } 0 < x < 1, \quad t > 0$$

$$u(0,t) = 0, \quad \frac{\partial u}{\partial x}(1,t) = 1, \quad u(x,0) = x$$

Use linear rectangular elements in the (x,t)-plane to model the problem. Note that the finite element model is given by $[K^e]\{u^e\} = \{Q^e\}$, where

$$K_{ij}^e = \int_0^{\Delta t}\int_{x_a}^{x_b}\left(\frac{\partial \psi_i^e}{\partial x}\frac{\partial \psi_j^e}{\partial x} + c\psi_i^e\frac{\partial \psi_j^e}{\partial t}\right)dx\,dt$$

$$Q_1^e = \left(-\int_0^{\Delta t}\frac{\partial u}{\partial x}\,dt\right)\Bigg|_{x=x_a}, \quad Q_2^e = \left(\int_0^{\Delta t}\frac{\partial u}{\partial x}\,dt\right)\Bigg|_{x=x_b}$$

8.59 The collocation time approximation methods are defined by the following relations:

$$\{\ddot{u}\}_{n+\alpha} = (1-\alpha)\{\ddot{u}\}_n + \alpha\{\ddot{u}\}_{n+1}$$

$$\{\dot{u}\}_{n+\alpha} = \{\dot{u}\}_n + \alpha\Delta t[(1-\gamma)\{\ddot{u}\}_n + \gamma\{\ddot{u}\}_{n+\alpha}]$$

$$\{u\}_{n+\alpha} = \{u\}_n + \alpha\Delta t\{\dot{u}\}_n + \frac{\alpha(\Delta t)^2}{2}[(1-2\beta)\{\ddot{u}\}_n + 2\beta\{\ddot{u}\}_{n+\alpha}]$$

The collocation scheme contains two of the well-known schemes: $\alpha = 1$ gives the Newmark's scheme; and $\beta = \frac{1}{6}$ and $\gamma = \frac{1}{2}$ gives the Wilson scheme. The collocation scheme is unconditionally stable, second-order accurate for the following values of the parameters:

$$\alpha \geq 1, \quad \gamma = \frac{1}{2}, \quad \frac{\alpha}{2(1+\alpha)} \geq \beta \geq \frac{2\alpha^2 - 1}{4(2\alpha^3 - 1)}$$

Formulate the algebraic equations associated with the matrix differential equation

$$[M]\{\ddot{u}\} + [C]\{\dot{u}\} + [K]\{u\} = \{F\}$$

using the collocation scheme.

8.60 Consider the following pair of coupled partial differential equations:

$$-\frac{\partial}{\partial x}\left(a\frac{\partial u}{\partial x}\right) - \frac{\partial}{\partial y}\left[b\left(\frac{\partial u}{\partial y} + \frac{\partial v}{\partial x}\right)\right] + \frac{\partial u}{\partial t} - f_x = 0 \tag{i}$$

$$-\frac{\partial}{\partial x}\left[b\left(\frac{\partial u}{\partial y} + \frac{\partial v}{\partial x}\right)\right] - \frac{\partial}{\partial y}\left(c\frac{\partial v}{\partial y}\right) + \frac{\partial v}{\partial t} - f_y = 0 \tag{ii}$$

where u and v are the dependent variables (unknown functions), a, b, and c are known functions of x and y, and f_x and f_y are known functions of position (x, y) and time t.

(*a*) Use the three-step procedure on each equation with a different weight function for each equation (say, w_1 and w_2) to develop the (semidiscrete) weak form.

(*b*) Assume finite element approximation of (u, v) in the following form

$$u(x, y) = \sum_{j=1}^{n} \psi_j(x, y) U_j(t), \quad v(x, y) = \sum_{j=1}^{n} \psi_j(x, y) V_j(t) \tag{iii}$$

and develop the (semidiscrete) finite element model in the form

$$\begin{aligned} 0 &= \sum_{j=1}^{n} M_{ij}^{11} \dot{U}_j + \sum_{j=1}^{n} K_{ij}^{11} U_j + \sum_{j=1}^{n} K_{ij}^{12} V_j - F_i^1 \\ 0 &= \sum_{j=1}^{n} M_{ij}^{22} \dot{V}_j + \sum_{j=1}^{n} K_{ij}^{21} U_j + \sum_{j=1}^{n} K_{ij}^{22} V_j - F_i^2 \end{aligned} \tag{iv}$$

You must define the algebraic form of the element coefficients K_{ij}^{11}, K_{ij}^{12}, F_i^1 etc.

(*c*) Give the fully discretized finite element model of the model (in the standard form; you are not required to derive it).

REFERENCES FOR ADDITIONAL READING

1. Eskinazi, S., *Principles of Fluid Mechanics*, Allyn and Bacon, Boston, MA, 1962.
2. Holman, J. P., *Heat Transfer*, 6th ed., McGraw-Hill, New York, 1986.
3. Kohler, W. and Pittr, J., "Calculation of Transient Temperature Fields with Finite Elements in Space and Time Dimensions," *International Journal for Numerical Methods in Engineering*, **8**, 625–631, 1974.
4. Kreyszig, E., *Advanced Engineering Mathematics*, 6th ed., John Wiley, New York, 1988.
5. Mikhlin, S. G., *Variational Methods in Mathematical Physics*, (translated from the Russian by T. Boddington), Pergamon Press, Oxford, UK, 1964.

6. Mikhlin, S. G., *The Numerical Performance of Variational Methods*, (translated from the Russian by R. S. Anderssen), Wolters-Noordhoff, The Netherlands, 1971.
7. Oden, J. T. and Reddy, J. N., *Variational Methods in Theoretical Mechanics*, 2nd ed., Springer-Verlag, Berlin, 1983.
8. Özisik, M. N., *Heat Transfer A Basic Approach*, McGraw-Hill, New York, 1985.
9. Reddy, J. N., *Applied Functional Analysis and Variational Methods in Engineering*, McGraw-Hill, New York, 1986; reprinted by Krieger, Melbourne, FL, 1991.
10. Reddy, J. N., *Energy Principles and Variational Methods in Applied Mechanics*, 2nd ed., John Wiley, New York, 2002.
11. Reddy, J. N. and Rasmussen, M. L., *Advanced Engineering Analysis*, John Wiley, New York, 1982; reprinted by Krieger, Melbourne, FL, 1990.
12. Rektorys, K., *Variational Methods in Mathematics, Science and Engineering*, D. Reidel Publishing Co., Boston, MA, 1980.
13. Schlichting, H., *Boundary-Layer Theory* (translated by J. Kestin), 7th ed., McGraw-Hill, New York, 1979.
14. Sobey, R. J., "Hermitian Space-Time Finite Elements for Estuarine Mass Transport," *International Journal for Numerical Methods in Fluids*, **2**, 277–297, 1982.
15. Timoshenko, S. P. and Goodier, J. N., *Theory of Elasticity*, 3rd ed., McGraw-Hill, New York, 1970.
16. Ugural, A. C. and Fenster, S. K., *Advanced Strength and Applied Elasticity*, 4th ed., Prentice Hall, Upper Saddle River, NJ, 2003.